


April 2023

## EFFECT OF CHEMICAL IDENTITY AND MORPHOLOGY ON AMPHIPHILIC-ZWITTERIONIC BLOCK COPOLYMER MEMBRANES

*University of Massachusetts Amherst*

Follow this and additional works at: [https://scholarworks.umass.edu/dissertations\\_2](https://scholarworks.umass.edu/dissertations_2)

 Part of the [Membrane Science Commons](#), [Polymer and Organic Materials Commons](#), [Polymer Chemistry Commons](#), and the [Polymer Science Commons](#)

---

### Recommended Citation

"EFFECT OF CHEMICAL IDENTITY AND MORPHOLOGY ON AMPHIPHILIC-ZWITTERIONIC BLOCK COPOLYMER MEMBRANES" (2023). *Doctoral Dissertations*. 2745.  
<https://doi.org/10.7275/33231136> [https://scholarworks.umass.edu/dissertations\\_2/2745](https://scholarworks.umass.edu/dissertations_2/2745)

This Open Access Dissertation is brought to you for free and open access by the Dissertations and Theses at ScholarWorks@UMass Amherst. It has been accepted for inclusion in Doctoral Dissertations by an authorized administrator of ScholarWorks@UMass Amherst. For more information, please contact [scholarworks@library.umass.edu](mailto:scholarworks@library.umass.edu).

**EFFECT OF CHEMICAL IDENTITY AND MORPHOLOGY ON AMPHIPHILIC-  
ZITTERIONIC BLOCK COPOLYMER MEMBRANES**

A Dissertation Presented

by

RIA GHOSH

Submitted to the Graduate School of the  
University of Massachusetts Amherst in partial fulfillment  
of the degree requirements for the degree of

DOCTOR OF PHILOSOPHY

February 2023

Polymer Science and Engineering

© Copyright by Ria Ghosh 2023  
All Rights Reserved

**EFFECT OF CHEMICAL IDENTITY AND MORPHOLOGY ON AMPHIPHILIC-  
ZITTERIONIC BLOCK COPOLYMER MEMBRANES**

A Dissertation Presented

by

RIA GHOSH

Approved as to style and content by:

---

E. Bryan Coughlin, Chair

---

Alexander Ribbe, Member

---

Jessica Schiffman, Member

---

David A. Hoagland, Department Head  
Polymer Science and Engineering

## ACKNOWLEDGEMENTS

Foremost, I would like to thank my advisor, Professor E. Bryan Coughlin, for all his guidance and support during my Ph.D. journey. He has shaped me into the scientist that I am today. From Bryan, I have learned to constantly be curious and ask questions because you never know what scientific discovery you might stumble upon. I always appreciate Bryan utilizing my mishaps and turning them into teaching moments to further improve me for the future. Thank you for being a great mentor and my academic father for these last five years and bestowing me with wisdom that I can carry forward in my career.

I would like to thank my committee members Dr Alexander Ribbe and Dr Jessica for their insightful discussions and feedback on my work. Their thought-provoking questions challenged me to look at my work from different angles to have a better understanding overall. I also would like to show my appreciation to Dr. Todd Emrick for imparting his vast knowledge in the field of zwitterion and guiding me through all the difficulties I experienced while experimenting with different zwitterions. I greatly appreciate their vast expertise that has provided guidance for my research and encouraged me to become a better scientist with a breath of knowledge.

I also had the opportunity to work with exceptional scientists at UMass and Argonne National Laboratory throughout my graduate career. Their assistance enhanced my research projects in ways that I could not do on my own. I would especially like to thank my collaborators Rushabh Shah and Choolong Kim, for providing their expertise and guiding me through my research projects. I always enjoyed the in-person and virtual meetings to discuss science; your passion and enthusiasm for science explorations were

contagious! I would also like to thank Dr. Weiguo Hu for his help in teaching me everything NMR related and his assistance in solid-state NMR experiments and Minqui Hu for his constant assistance with SAXS.

Through the course of my time here in PSE, I was fortunate to have the Coughlin Group family support me through this journey. I would like to thank Dr. Pirl Ertem, Dr. Rohit Gupta, Dr. Joshua Enokida, Dr. Yifeng Du, Dr. Huyen Vu for being great mentors and teaching me everything in the lab as well as helping me navigate life after graduate school. I also want to thank the current group, Anne Radzanowski, Roshni Chethalen, Yuhui (Helen) Du, Juan Correa Ruiz for being my research family. I will hold dear to memories of our ventures outside of lab (when we had the chance) and our group lunches/dinners to relax and bond over food. In addition, I would like to thank the visiting Mainz students Nico Allewa, Matay Kaplan, Adrian Hauck and Tom Reimer for sharing much joy and laughter with our group during their stay.

I am also grateful to have awesome undergrad Wen Wei-Wong. It was my great pleasure to teach you and train you in synthetic chemistry. Your never ending questions and always curious mind helped me to think about several aspects of my work more critically. Working with you and Tom Reimer was my great pleasure. Both of you helped me with your skills and gave me a chance to realize my passion for teaching.

Of course, I want to thank the Class of 2017 for being there through my time here. I want to recognize Prof. Todd Emrick's research group members, especially Dr. Le Zhou for answering all my questions patiently regarding zwitterion and showing me various technique and giving me tips and idea. Along with that you always managed to cheer me up during my stressful time. I also want to thank Mingqiu Hu for helping me out with

Ganesha SAXS and answering my doubts and helping me with trouble shoot at minutes notice. I also want to say special thanks to Rushabh Shah from Prof. Jessica Schiffman lab to help me with all water transport experiments and impart his knowledge in the application side of my work.

I want to thank my partner Bidya Dash, for being there for me when I struggled with graduate school. You were willing to tolerate my experimental cooking whenever I was stressed by deadlines and milestones and taking me for ice cream. I am grateful to have you in my life and as someone for me to lean on.

Most importantly, I am especially thankful for my family. Their endless love and support allowed me to get through some of the toughest challenges I encountered. From our daily phone calls, they constantly reminded me of the big picture and how everything would work out in the end. Words cannot simply describe the sacrifices they endured for me to pursue my dream of being a scientist.

# **ABSTRACT**

## **EFFECT OF CHEMICAL IDENTITY AND MORPHOLOGY ON AMPHIPHILIC-ZWITTERIONIC BLOCK COPOLYMER MEMBRANES**

FEBRUARY 2023

RIA GHOSH, B.Sc., UNIVERSITY OF CALCUTTA

B.Tech., UNIVERSITY OF CALCUTTA

M.S., UNIVERSITY OF MASSACHUSETTS AMHERST

Ph.D., UNIVERSITY OF MASSACHUSETTS AMHERST

Directed by: Professor E. Bryan Coughlin

Amphiphilic block copolymers have gained a broad research interest attributed to their self-assembly properties over a range of pH, temperature, and ionic strength. Polyzwitterions have attracted special attention due to their hydrophilicity, charge sensitivity and coulombic attraction of the opposite charges over a range of environments making them a popular material of study in the field of stimuli responsive systems, for example in self-healing hydrogels, and water transport membranes. Combining the stimuli responsiveness and higher hydrophilicity of zwitterionic polymers with self-assembly behavior of amphiphilic block copolymers created an interest to study the effect of composition and identity of the zwitterionic block on the morphology of novel amphiphilic- zwitterionic block copolymer systems.



A novel chemistry to synthesis a series of amphiphilic-zwitterionic block copolymer was developed. As a first step, a parent block copolymer precursors of poly (dimethyl amino ethyl methacrylate)-*b*-poly (n butyl acrylate-*ran*-allyl methacrylate) (PDMAEMA-*b*- P(nBA-*ran*-AMA)) with different copolymer volume fractions were synthesized using controlled radical polymerization. The advantage of using this technique is the ability to synthesize a polymer chain with predetermined molecular weight and well-defined chemical composition while also maintaining a narrow dispersity. Variation of the zwitterionic groups; sulfobetaine, carboxybetaine or cholinephosphate were investigated through post-polymerization modification of the PDMAEMA block using nucleophilic ring-opening reactions of 1,3-propane sultone ,  $\beta$ -propiolactone or n-butyl substituted phospholane. Proton NMR spectroscopy data were analyzed to calculate degree of polymerization (DP) from the distinct peak of each repeating unit of pendent groups in parent neutral block copolymers and its modified amphiphilic-zwitterionic counterpart. These DP of the neutral block copolymer were then used to calculate the relative volume fraction of each block and aid the future calculation of post-polymerization modification on the PDMAEMA block and crosslinking chemistry on the poly allyl methacrylate (PAMA) block. Thermal stability of these zwitterionic systems was investigated by using thermogravimetric analysis (TGA) and differential scanning calorimetry (DSC).

Mechanically robust free standing amphiphilic zwitterionic copolymer poly (n butyl acrylate-*ran*-allyl methacrylate)-*b*-polybetaine methacrylate membrane were tailored using thiol-ene click chemistry on the pendent double bond of the allyl methacrylate repeating unit with a dithiol crosslinking agent under UV irradiation. The analysis of the effect of composition, and identity of the zwitterionic block on the resultant films

morphologies was probed. The systematic variations in volume fractions of each block were targeted to generate different morphologies. The impact of the copolymer composition on the morphology were analyzed using small angle X-ray scattering (SAXS). Various relative humidity sweeps and temperature variation SAXS were performed through collaboration with Argonne National Laboratory to investigate the effect of different environmental conditions of the morphologies. In addition to SAXS, transmission electron microscopy (TEM) was performed to study real space imaging of these structures. With the results from these characterization methods, it was possible to perform a structure-property relationship study of these novel Amphiphilic-Zwitterionic block copolymers.

Looking forward, results from this study have the potential to guide future applications in the field of water transport filtration membranes. The effect on morphology, zwitterionic content and block copolymer composition on water uptake and salt uptake was evaluated using gravimetric analysis, and dead-end filtration performance studies showing promising initial results.

# TABLE OF CONTENTS

	Page
ACKNOWLEDGEMENTS .....	iv
ABSTRACT.....	vii
LIST OF TABLES .....	xiv
LIST OF FIGURES .....	xv
LIST OF SCHEMES.....	xxi
LIST OF EQUATIONS .....	xxii
ABBREVIATION.....	xxiii
Chapter	
1. INTRODUCTION .....	1
1.1 Introduction to Ion-containing Polymers.....	1
1.2 Introduction to Polyzwitterion .....	2
1.3 Introduction to Amphiphilic Copolymers .....	4
1.4 Synthetic Routes and Their Advantages and Disadvantages for Amphiphilic Zwitterionic Copolymer.....	5
1.4.1 Direct Polymerization .....	5
1.4.2 Post-Polymerization Modification.....	6
1.5 Block Copolymer Microphase Separation .....	6
1.6 Advanced Material Applications for Polyzwitterions.....	12
1.6.1 Antifouling Coating.....	12

1.6.2	Hydrogel Material.....	12
1.6.3	Dispersant and Stabilizers.....	13
1.6.4	Antifreeze Material.....	14
1.6.5	Drug Delivery and Gene Therapy .....	14
1.7	Zwitterionic Amphiphilic Copolymer for Water Transport Membrane .....	15
1.8	Dissertation Overview .....	17
1.8.1	Tailoring of a Novel Amphiphilic-Zwitterionic Block Copolymer to Form Photo Crosslinked Free-Standing Films.....	17
1.8.2	Analyzing the Effect of Composition and Identity of Zwitterionic Block on Morphology.....	18
1.9	Reference .....	20
2.	MODULAR CHEMISTRY FOR DEVELOPING A LIBRARY OF NOVEL AMPHIPHILIC ZWITTERIONIC (A-Z) BLOCK COPOLYMERS .....	36
2.1	Background and Motivation .....	36
2.2	Instrumentation and Characterization .....	37
2.3	Homopolymerization of PDMAEMA.....	38
2.3.1	Kinetic Study for Synthesis of PDMAEMA.....	38
2.3.2	Synthesis of PDMAEMA with Different Molecular Weight.....	42
2.4	Chain Extension of PDMAEMA with Different Hydrophobic block .....	46
2.4.1	Chain Extension with Polyisoprene .....	46

2.4.2	Chain Extension with Poly Allyl Acrylate .....	49
2.4.3	Kinetic Study for Synthesis of Poly[(dimethyl aminoethyl methacrylate)- <i>b</i> - ( <i>n</i> -butyl acrylate- <i>ran</i> -allyl methacrylate)] .....	51
2.4.4	Synthesis of Poly[(dimethyl aminoethyl methacrylate)- <i>b</i> -( <i>n</i> -butyl acrylate- <i>ran</i> -allyl methacrylate)] with Different Volume Fraction .....	55
2.5	Post Polymerization Modification with Different Heterocyclic Rings .....	58
2.5.1	Ring-Opening of 1,3-Propane Sultone .....	58
2.5.2	Ring-Opening of <i>n</i> -Butyl Substituted Phospholane Ring .....	65
2.5.3	Ring-Opening with $\epsilon$ -propiolactone .....	73
2.6	Conclusions:.....	76
2.7	References .....	77
3.	EVALUATION OF AMPHIPHILIC ZWITTERIONIC BLOCK COPOLYMER MEMBRANES FOR WATER TRANSPORT.....	78
3.1	Introduction.....	78
3.2	Experimental Section .....	80
3.2.1	Fabricating Mechanically Robust A-Z Block Copolymer Membrane via Photo Crosslinking .....	80
3.2.2	Instrument and Characterization .....	83
3.2.3	Morphology Study via SAXS .....	84
3.2.4	Study Via TEM .....	93

3.3	Conclusions.....	93
3.4	References.....	95
4.	AMPHIPHILIC-ZWITTERIONIC POLYMER FOR WATER TRANSPORT AND SELECTIVE ION TRANSPORT MEMBRANE.....	97
4.1	Background and Motivations.....	97
4.2	Water Uptake Experiments.....	98
4.2.1	Gravimetric Analysis.....	98
4.2.2	Salt Transport Experiments.....	100
4.2.3	Water Flux Study.....	101
4.3	Conclusion.....	104
4.4	References.....	105
5.	SUMMARY AND FUTURE PERSPECTIVE.....	106
5.1	Introduction.....	106
5.2	Summary of Conclusion.....	106
5.3	Future Perspective.....	109
5.4	Outlook.....	111
5.5	References.....	112
	APPENDIX : SUPPLEMENTAL FIGURES.....	113
	BIBLIOGRAPHY.....	116

## LIST OF TABLES

Table	Page
2.1: Kinetic study data for homopolymer block .....	39
2.2: Overview of the Synthesis and Corresponding Properties of the PDMAEMA Homopolymer Series .....	44
2.3: Kinetic study of synthesis of PDMAEMA-b-P(BA-ran-AMA) .....	52
2.4: Overview of the Synthesis and Corresponding Properties of the PDMAEMA-b-P(BA-AMA) Series as Indicated by GPC .....	56
2.5: Overview of the Synthesis and Corresponding Properties of the PDMAEMA-b-P(BA-AMA) Series as Indicated by NMR .....	58
2.6: Percent quaternization as indicated by NMR .....	59
2.7: Percent quaternization as indicated by NMR .....	69
2.8: Percent quaternization as indicated by NMR .....	74

## LIST OF FIGURES

Figure	Page
1.1:Schematic representation of A. Polyanion, B. Polycation and C. Polyzwitterions .....	2
1.2:General representation of polybetaines.....	4
1.3:Microphase separation of Diblock Copolymer. (a) topological structure of the microphase (b) the theoretical phase diagram of a symmetric diblock copolymer. Image taken from ref 60.....	7
1.4:Schematic representation of polymer chain arrangement in different morphology from sphere (a) to cylindrical (b) to lamella (c), as a function of relative volume fraction. Image is taken from ref. 60.....	8
1.5:Effect of charge entropy and solubility effect on block copolyelectrolyte nanostructure. a cartoon of neutral block copolymer (top) and block copolyelectrolyte (bottom). b neutral block copolymer phase diagram. original phase boundary with the influence of ion entropy and solubility effect for block copolyelectrolyte with different charge fractions. d adjustment of the phase diagram to overlap with the uncharge phase boundary with the shifted $\chi_{\text{eff}}$ , using $C=-160.0$ . Image taken from ref 68.....	9
1.6:effect of charge cohesion on block copolyelectrolyte morphology. Electrostatic cohesion between charged block and the counterions. It is an asymmetric effect as it only affects the charged block. b shift of phase diagram based of coulombic	



interaction strength. Higher strength value results in phase separated morphology even at $\chi=0$ . Image is taken from ref 68. ....	10
1.7: Ion transport in charged system through percolating minority charged phase vs in uncharged system which is primarily bulk domain percolating around minority phase. Image is taken from ref 68. ....	11
1.8: Structure of zwitterionic polymer exhibiting self-healing properties upon stretching and cutting. Image taken from ref 76. ....	13
1.9: Catalytic stabilization of gold nanoparticle. Image taken from ref 76 .....	14
2.1:a) GPC trace of the crude aliquot at 2hr interval b) $M_n$ and $D$ plot as indicated by GPC value .....	40
2.2:a) $^1H$ -NMR spectra of the crude aliquot at different time interval b) % conversion plot as calculated from the unreacted monomer to polymer peak ration .....	41
2.3:a) DMF-GPC Trace b) $^1H$ -NMR spectra of DMAEMA homopolymer .....	45
2.4: $^1H$ -NMR of PDMAEMA-b-PI .....	47
2.5:a) $^1H$ -NMR Spectra of PSBMA-PI b) Solubility of PDMAEMA-b-PI vs PSBMA-b-PI in TFE .....	48
2.6:a) DMF-GPC Trace b) $^1H$ -NMR spectra of block copolymer .....	50

2.7:a) GPC trace of the crude aliquot at 2 h interval b) $M_n$ and $D$ plot as indicated by GPC value .....	53
2.8:a) $^1\text{H-NMR}$ spectra of the crude aliquot at different time interval b) percent conversion plot as calculated from the unreacted monomer to polymer .....	54
2.9:a) DMF-GPC Trace b) $^1\text{H-NMR}$ spectra of parent block copolymer .....	57
2.10: Representative NMR of A-Z block copolymer with 54% of quaternization .....	60
2.11: FTIR analysis of the A-Z block copolymer with different percentage quaternization as compared with the parent block copolymer .....	61
2.12: TGA analysis of the A-Z block copolymer as compared with that of the parent block copolymer .....	63
2.13: DSC analysis of the A-Z block copolymer as compared with that of the parent block copolymer .....	64
2.14: Competitive reaction pathway in the reaction of tertiary amine and alkyl substituted phospholane. Image taken from reference 2 .....	65
2.15: A) $^1\text{H-NMR}$ , B) $^{13}\text{C-NMR}$ & C) $^{31}\text{P-NMR}$ of 2-butyl-1,3,2-dioxaphospholane 2-oxide .....	67
2.16: Representative NMR of A-Z block copolymer with 20% of quaternization .....	69

2.17:FTIR analysis of the A-Z block copolymer with different percentage quaternization as compared with the parent block copolymer .....	70
2.18:TGA analysis of the A-Z block copolymer as compared with that of the parent block copolymer .....	72
2.19:DSC analysis of the A-Z block copolymer as compared with that of the parent block copolymer .....	73
2.20:Representative NMR of A-Z block copolymer with 0% of quaternization .....	75
2.21:FTIR analysis of the A-Z block copolymer with different percentage quaternization as compared with the parent block copolymer .....	75
3.1:mechanical and dimensional stability of a A-Z block copolymer membrane before and after crosslinking.....	81
3.2:With the increase in percent zwitterion in an A-Z block copolymer system with same hydrophilic volume fraction, the membranes becoming more brittle.....	82
3.3:Antipolyelectrolytic effect of zwitterion. Image taken from Ref. 9 .....	83
3.4: Morphology study of block copolymer membrane with $f=0.10$ by SAXS under controlled environment pretreated with a) pure DI water b) 0.5 M NaCl aqueous solution c) 1.0 M NaCl aqueous solution.....	86

3.5: Morphology study of block copolymer membrane with $f=0.22$ by SAXS under controlled environment pretreated with a) pure DI water b) 0.5M NaCl aqueous solution c) 1.0M NaCl aqueous solution.....	88
3.6: Morphology study of block copolymer membrane with $f=0.47$ by SAXS under controlled environment pretreated with a) pure DI water b) 0.5M NaCl aqueous solution c) 1.0M NaCl aqueous solution.....	90
3.7: Morphology study of block copolymer membrane with $f=0.66$ by SAXS under controlled environment pretreated with a) pure DI water b) 0.5M NaCl aqueous solution c) 1.0M NaCl aqueous solution.....	92
3.8: TEM images of the parent block copolymer with $f=0.10$ and its 100% zwitterionic form as compared to its SAXS images. ....	93
4.1: Mass uptake of block copolymer system with different volume fraction of the hydrophilic block and different % of zwitterion content .....	98
4.2: a) Schematic of working principle of dead end filtration system b) the actual set up of Dead End Filtration instrument build by Dr. Kerianne Dobosz. Image take from Ref. 5.....	102
4.3: Water permeability measurement of block copolymer with different volume fraction ( $f$ ) of hydrophilic block and different % zwitterion content .....	103
4.4: Water permeability of block copolymer with hydrophilic $f=0.10$ and different % zwitterion under different pressure .....	103

A1: COSY-NMR of A-Z block copolymer, 50% quaternized with 1,3-propane sultone	113
A2: COSY-NMR of A-Z block copolymer, 50% quaternized with n-butyl substituted phospholane ring .....	114
A3: TEM images of the parent block copolymer with $f=0.46$ and its 100% zwitterionic form as compared to its SAXS images. ....	115
A4: TEM images of the parent block copolymer with $f=0.67$ and its 100% zwitterionic form as compared to its SAXS images. ....	115

## LIST OF SCHEMES

Scheme	Page
2.1:Homopolymerization of PDMAEMA .....	42
2.2:Chain Extension with Isoprene .....	46
2.3:Post-polymerization Modification of PDMAEMA-b-PI by 1,3-Propane Sultone .....	48
2.4:Chain extension via random mixture of n-butyl acrylate and allyl methacrylate .....	50
2.5:Post polymerization modification of parent diblock polymer via nucleophilic ring opening of 1,3-propane sultone.....	59
2.6:Synthesis of 2-butyl-1,3,2-dioxaphospholane 2-oxide .....	66
2.7:Post polymerization modification of parent diblock polymer via nucleophilic ring opening of 2-butyl-1,3,2-dioxaphospholane 2-oxide.....	68
2.8:Post polymerization modification of parent diblock polymer via nucleophilic ring opening of $\beta$ -propiolactone .....	74
3.1:Fabrication of robust copolymer membrane via photo crosslinking .....	80

## LIST OF EQUATIONS

Equation	Page
4.1:Mass Absorbtion.....	98
4.2:Hydration Number .....	99
4.3:Weight Percent of Salt Absorbtion.....	100
4.4:Salt Diffusion.....	100
4.5:Salt Permeability Coefficient.....	101
4.6:Permeated Water Volume.....	101
4.7:Water Permeability .....	102

## ABBREVIATION

°C	degree Celsius
$\bar{D}$	Molecular Weight Dispersity, $M_w/M_n$
$\delta$	Chemical shift
$\chi$	Flory-Huggins Parameter
$\phi$	Volume Fraction
A-Z	Amphiphilic Zwitterionic
AA	Allyl Acrylate
ABCVA	4,4'-Azobis (4-cyanovaleric acid)
AMA	Allyl Methacrylate
BCPs	Block Copolymer
BCPMA	Butyl substituted choline phosphate methacrylate
CBMA	Carboxybetaine Methacrylate
CDTCPA	4-Cyano-4-[(dodecylsulfanylthiocarbonyl)sulfanyl]pentanoic acid
CTA	Chain Transfer Agent
d-spacing	Domain Spacing
DMAEMA	Dimethylamino ethyl methacrylate
DMF	N,N-Dimethylformamide
DSC	Dynamic Scanning Calorimetry
equiv.	Molar equivalent
$f$	Relative volume fraction of each block
FT-IR	Fourier Transformation Infrared Spectroscopy
GPC	Gel Permeation Chromatography



h	Hour
HyPhB	Hydrophobic
kg	Kilogram
MeOH	Methanol
MEHQ	Mono Ethyl Hydroquinone
mg	Milligram
mL	Milliliter
MMA	Methyl methacrylate
mmol	Millimole
M <sub>n</sub>	Number average molecular weight
mol	Mole
MW	(Number Average) Molecular Weight
M <sub>w</sub>	Weight Average Molecular Weight
n-BA	normal Butyl Acrylate
N	Degree of Polymerization
nm	Nanometer
NMR	Nuclear Magnetic Resonance Spectroscopy
q	Scattering Wave Factor
RAFT	Reversible Addition-Fragmentation Chain Transfer Radical Polymerization
SBMA	Sulfoxy Betaine Methacrylate
SCFT	Self-Consistent Field Theory
SAXS	Small Angle X-ray Scattering
TEM	Transmission Electron Microscopy

T <sub>g</sub>	Glass transition temperature
TGA	Thermo-Gravimetric Analysis
THF	Tetrahydrofuran
TFE	Trifluoroethanol

# CHAPTER 1

## INTRODUCTION

### 1.1 Introduction to Ion-containing Polymers

Over the past several decades, ion-containing polymers have created a broad platform for fundamental and applied research.<sup>1</sup> This growing interest is rooted in the beneficial properties exhibited by ion-containing polymers in the field of desalination and wastewater treatment,<sup>2-5</sup> ion exchange membranes for fuel cells and batteries,<sup>6,7</sup> composites,<sup>8</sup> drug carriers,<sup>9</sup> hydrogels, and self-healing materials.<sup>10-12</sup> The properties of this class of polymers, as the name indicates, result from the presence of ionic groups covalently bonded with the polymer backbone. Electrostatic forces of the charged group give rise to many complex interactions, whose combined effects give rise to their solution and bulk properties such as water solubility, ion-transport ability,<sup>6</sup> interaction with salt ions in solution, improved mechanical strength,<sup>13</sup> improved miscibility of polymer blends and surface activity.<sup>14</sup> Ion-containing polymers range from naturally occurring polypeptides and nucleotides to synthetically tailored surfactants and stabilizers.<sup>15</sup> Ion-containing polymers have been classified further into two subcategories based on the nature of the charges present along the polymer chain.

**Polyelectrolytes** are a sub class of ion-containing polymers whose repeat units contain a covalently bonded ion that is stationary, and an ionically bonded counterion, also referred to as the ionizable mobile charge. These polyelectrolytes ionize upon dissolution in a polar solvent resulting in a polymer with charged groups.<sup>9,14</sup> Depending on the charge of the stationary ion, polyelectrolytes can be categorized into polyanion (negative bonded ion) and polycations (positive bonded ion) (Figure 1.1A and 1.1B).<sup>16-19</sup> On the other hand,

**polyzwitterions** are the charges of ion- containing polymers where each repeat unit has equal numbers of both negative and positive charges covalently bonded with the polymer backbone (Figure 1.1C).<sup>15,20</sup>

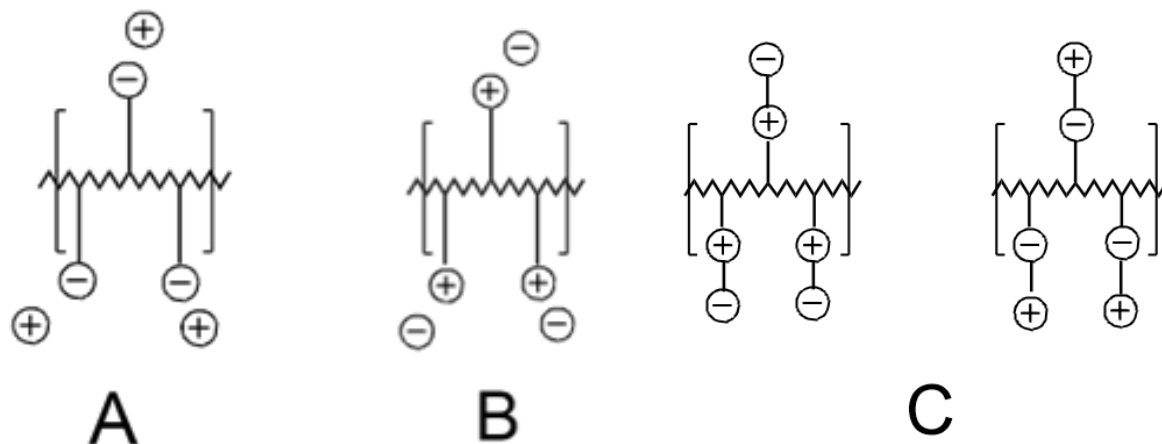


**Figure 1.1:**Schematic representation of **A. Polyanion, B. Polycation and C.**

### **Polyzwitterions**

#### **1.2 Introduction to Polyzwitterion**

Hydrophilic polyzwitterions exhibit overall charge neutrality due to equal charge stoichiometry of ions covalently bonded either directly on the polymer backbone, or on the same or different monomeric pendent groups.<sup>15,20-22</sup> The zwitterionic moieties of these polymers are responsive to environmental conditions, temperature, added salt, pH, and the combination of these factors. Neutral hydrogels comprising 2-Hydroxyethyl methacrylate (HEMA) or Poly(*N*-isopropylacrylamide) (PNIPAM) shows lower critical solution temperature behavior, whereas polyzwitterionic hydrogels exhibit upper critical solution temperature behavior based on the polymer backbone and zwitterionic component.<sup>23-25</sup> High hydrophilicity, charge sensitivity and Coulombic attraction of the opposite charges over wide range of ionic strength and environmental conditions make polyzwitterions a

compelling material for tailoring “smart” stimuli responsive systems,<sup>26,27</sup> self-healing hydrogels<sup>22</sup> and water transport membranes for wastewater management applications.<sup>20,28,29</sup> At the isoelectric points the zwitterionic polymers show net charge neutrality whereas with increase or decrease of pH, they will exhibit net negative and positive charge respectively. They also exhibit coil-globule conformation change over a wide range of pH, *e.g.*, at the isoelectric point due to strong interaction of the opposite charges, they tend to form globular structures and phase separate, whereas repulsive interactions between the like charges at extreme ends of the pH scale leads to solubilization or the coiled structure of the zwitterionic polymer. One of the interesting properties of these polymers stems from its resemblance to widespread natural zwitterionic structures like phospholipids, polypeptides *etc.*<sup>30–36</sup> Recently polyzwitterions have attracted attention due to their bio-mimicking and surface modification ability in various fields of biomaterial, biomedicine, antifouling coating.<sup>22</sup>

**Polybetaines** are a subclass of polyzwitterions having both positive and negative charge covalently bonded within the same pendent group of the monomeric unit (Figure 1.2). These attributes contribute to their defined ionic structure and dipole moment as well as mechanical and thermal stability.<sup>37</sup> Their derivatives can be tailored by controlling; i) either acrylate or acrylamide-based polymer backbone.<sup>38,39</sup> These different backbones have an influence over the polymerization conditions (free radical polymerization or living radical polymerization) and on their material properties.<sup>28</sup> Acrylamide-based polybetaines are more alkaline stable and hydrophilic than their acrylate-based analogs.<sup>40</sup> ii) Substitution group attached with the quaternary amine. The mechanical and antifouling properties depend on the substituent groups.<sup>41</sup> iii) Spacer length, the number of carbon atoms between

the cation (quaternary ammonium) and the anion. The spacer length is directly proportional to the hydrophilicity of the polybetaines,<sup>39</sup> but inversely proportional to resisting protein adsorption.<sup>42,43</sup> iv) Anionic moiety. By changing the anionic group attached, the hydrophilic character of the zwitterionic polymer can also be varied where the trend in hydrophilicity is phosphocholine > sulfobetaine > carboxybetaine.<sup>44</sup> Despite their recent developments and excellent choices for several applications, much remains to be explored for the structure-property relationship of polybetaines.

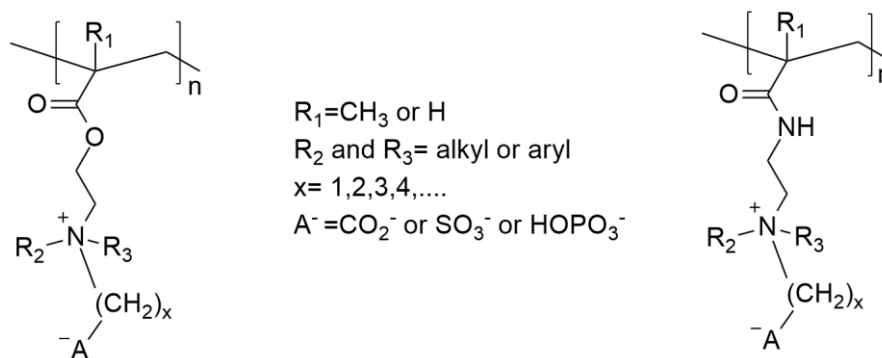


**Figure 1.2: General representation of polybetaines**

### 1.3 Introduction to Amphiphilic Copolymers

The entire class of polyzwitterions is often viewed as a subcategory of amphiphilic polymers.<sup>20,45</sup> Amphiphilic copolymers are defined as a polymeric chain synthesized from two or more types of monomers each exhibiting opposing chemical properties for example cationic/anionic, polar/non-polar, hydrophilic/hydrophobic.<sup>46,47</sup> For block copolymers, each block is comprised of chemically different monomers, each one maintaining its own homopolymer characteristics. Amphiphilic copolymers, over a range of pH, temperature, and ionic strength, show either globular or extended chain conformations.<sup>48</sup> Another interesting property of these polymers is complexation with polyelectrolytes,

biomolecules, or surfactants. This complexation is electrostatic in nature.<sup>49–52</sup> Over the past few decades this class of copolymer has attracted a lot of research interest attributed to its superior self-assembly properties.<sup>46,53</sup> This self-assembly gives rise to different nanostructures which have been extensively used as nanoreactors, nano templates, and nanocarriers for use in drug delivery.<sup>54</sup> Amphiphilic block copolymers with the hydrophilic block being a zwitterionic polybetaine and the corresponding hydrophobic block providing mechanical integrity of the system are referred to as amphiphilic zwitterionic (A-Z) copolymers.

#### **1.4 Synthetic Routes and Their Advantages and Disadvantages for Amphiphilic Zwitterionic Copolymer**

The properties discussed above depend solely on the chemical nature and composition of each segment comprising the block copolymer. Thus, a robust synthetic approach is a decisive factor to control the effectiveness of the behavior of the polymers.<sup>20</sup> A-Z copolymers with complex architecture and interesting functionalization have attracted attention for the development of different synthetic routes. In this section, two pathways for the synthesis of A-Z copolymers will be discussed.

##### **1.4.1 Direct Polymerization**

One of the commonly used synthetic routes is direct polymerization. In this route precursor monomers with desired functionality are directly polymerized using living or controlled polymerization methodologies.<sup>55–57</sup> The major advantage of this route is that a copolymer with tailored architecture, comonomer composition and narrow molecular weight distribution can be directly synthesized.<sup>47</sup> A-Z copolymers consists of two or more

repeat units having opposing polarity. A disadvantage of using direct polymerization to synthesize this type of copolymer is due to poor compatibility of different blocks in the same reaction media.

#### **1.4.2 Post-Polymerization Modification**

To overcome the shortcoming of direct polymerization, chemo-selective and efficient post-polymerization modifications are adopted. A facile organic chemistry reaction is utilized to functionalize one block within the polymer precursor to give a desired A-Z copolymer.<sup>58</sup> This route provides opportunities for tailoring A-Z copolymer with interesting functionality from a single parent polymer precursor ensuring fixed molecular weight and dispersity.<sup>59</sup> Two important criteria to consider for post polymerization modifications are<sup>58</sup> i) mild and selective chemistry *e.g.*, the functionalization of the pendent group in the selected block without compromising the other polymer block or backbone chemical characteristics like degree of polymerization or dispersity ii) effective chemistry that can ideally lead to 100% functionalization.

#### **1.5 Block Copolymer Microphase Separation**

Copolymer systems under certain conditions self-assemble into an array of morphologies. Block copolymers which consist of two or more covalently bonded chemically incompatible blocks, microphase separate based of their composition into diverse morphologies.<sup>60</sup> Self-assembly of block copolymer in bulk and solutions are both complex and an extensive area for active research from both experimental and theoretical perspectives.<sup>60,61</sup> Three classical and practically applicable phases are lamellae (L), hexagonally packed cylinders (H), and body centered spheres (S), whereas a fourth phase



double-gyroid (Q) are limited due to its instability at higher segregation region,<sup>61</sup> (Figure 1.3).

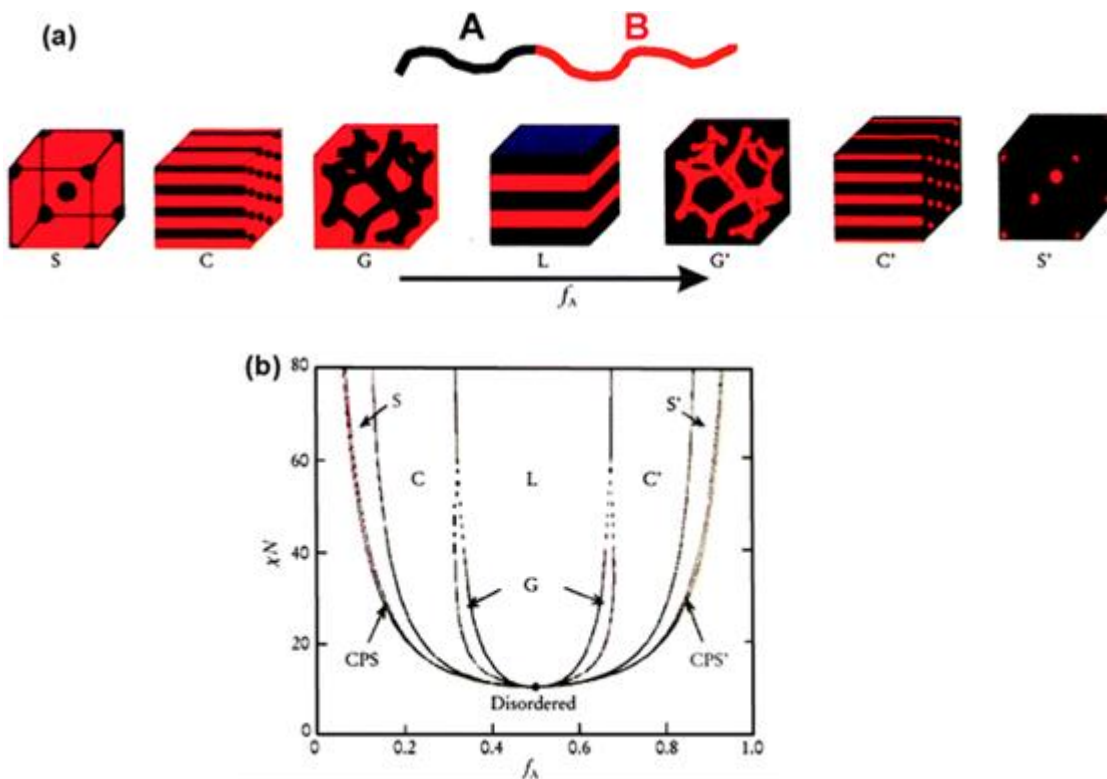


**Figure 1.3: Microphase separation of Diblock Copolymer. (a) topological structure of the microphase (b) the theoretical phase diagram of a symmetric diblock copolymer. Image taken from ref 60.**

Parameters affecting the formation of these morphologies are degree of polymerization ( $N$ ), immiscibility of the block ( $\chi$ ), and the relative volume fraction of the blocks ( $f$ ). Two competing factors contributing to these microphase separations are interfacial energy between the blocks (enthalpy) and chain stretching (entropy). To minimize the interfacial energy, two incompatible blocks organize themselves in an ordered state to reduce their interfacial area (Figure 1.4). The extent of the stretching depends on the relative volume fraction of the blocks.<sup>60,62</sup> Other factors which affect the phase separations are

conformational asymmetry,<sup>63,64</sup> polymer architecture,<sup>65,66</sup> molecular weight distribution,<sup>67</sup> and electrostatic interactions.<sup>68</sup>

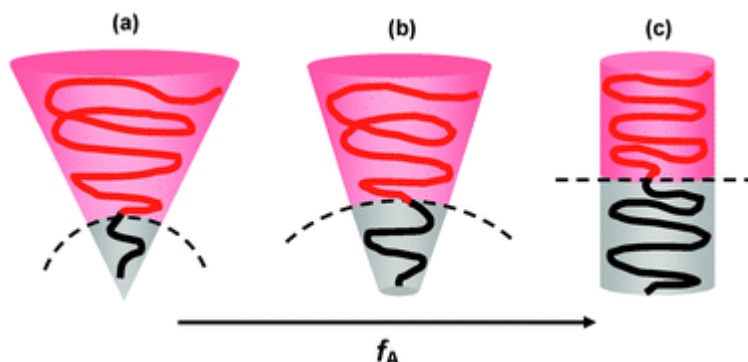


**Figure 1.4: Schematic representation of polymer chain arrangement in different morphology from sphere (a) to cylindrical (b) to lamella (c), as a function of relative volume fraction. Image is taken from ref. 60.**

These self-assemblies are promising in the formation of various nanostructures with potential applications in electrical devices, photonic crystals, biomedicine, and high-performance separation membrane.<sup>60,61,63–68</sup> They also created a broad platform for structure-property relationship studies of copolymeric materials. These morphologies can be tuned by incorporating functionalities in block copolymers by post polymerization modification to enhance the material performance.

Literature on block polyelectrolytes has shown how incorporating charges in one of the blocks leads to formation of different nanostructures that are inaccessible to uncharged block copolymers.<sup>68</sup> Varying charges can tune the material spectrum of self-assembled structures and enhance the efficiency of the ion transport.<sup>69</sup> This complexity in the nanostructures arises because of counterion entropy leading to suppression of phase separation and charge ionization in the surrounding medium leading to enhancement of

phase separation.<sup>70-73</sup> Introducing charges at the monomer level reorganizes the charged species and leads to higher solubility. This shifts the phase diagram vertically which is linearly proportional (with the constant  $C=-160.0$ , equation 1.5.1) to the fraction of charged monomer (Figure 1.5).<sup>70,71</sup>

$$\chi N \rightarrow \chi_{eff} N = \chi N - C f_q \dots \dots \dots \text{Equation 1.1}$$

where  $\chi$  is the Flory parameter defined as chemical mismatch between the two blocks,  $N$  is the number of monomers along the chain,  $f_q$  is the fraction of charged monomer and  $C$  is the shift constant.

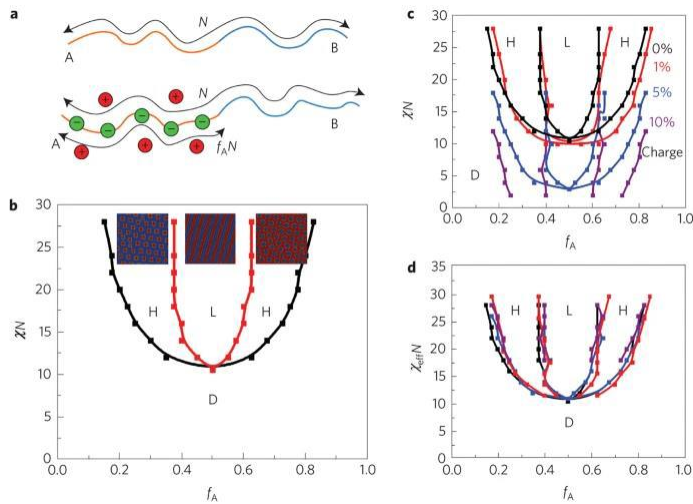


**Figure 1.5: Effect of charge entropy and solubility effect on block copolyelectrolyte nanostructure. a cartoon of neutral block copolymer (top) and block copolyelectrolyte (bottom). b neutral block copolymer phase diagram. original phase boundary with the influence of ion entropy and solubility effect for block copolyelectrolyte with different charge fractions. d adjustment of the phase diagram to overlap with the uncharge phase boundary with the shifted  $\chi_{eff}$ , using  $C=-160.0$ .**

**Image taken from ref 68**

This simple correction of  $\chi$  becomes insufficient to describe the effect of charges on the morphology when the electrostatic cohesive strength becomes larger than unity. Strong Coulombic coupling starts shifting the phase diagram towards the left where minority charged phase becomes the continuous domain giving an inverse hexagonal morphology.<sup>72,73</sup> The electrostatic cohesion energetically prefers high density of charges which overwhelms the entropy effect of the counterion which has the opposite effect of preferring lower density of counterion (Figure 1.6).<sup>68</sup> This gives rise to percolating nanodomain of the minority phase by charge manipulation making uninterrupted pathways for ion transport (Figure 1.7).<sup>68</sup>

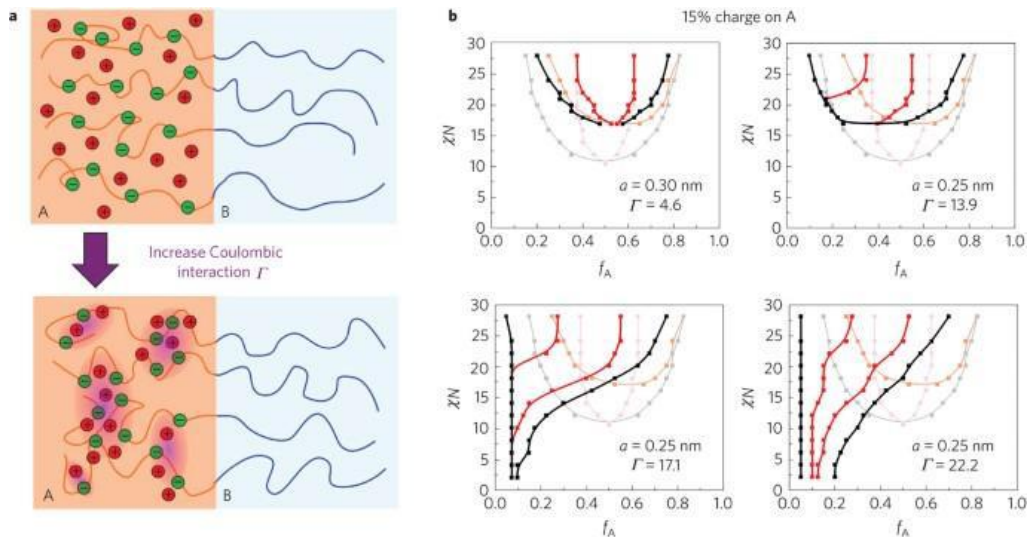


**Figure 1.6:effect of charge cohesion on block copolyelectrolyte morphology.**

**Electrostatic cohesion between charged block and the counterions. It is an asymmetric effect as it only affects the charged block. b shift of phase diagram based of coulombic interaction strength. Higher strength value results in phase separated morphology even at  $\chi=0$ . Image is taken from ref 68.**

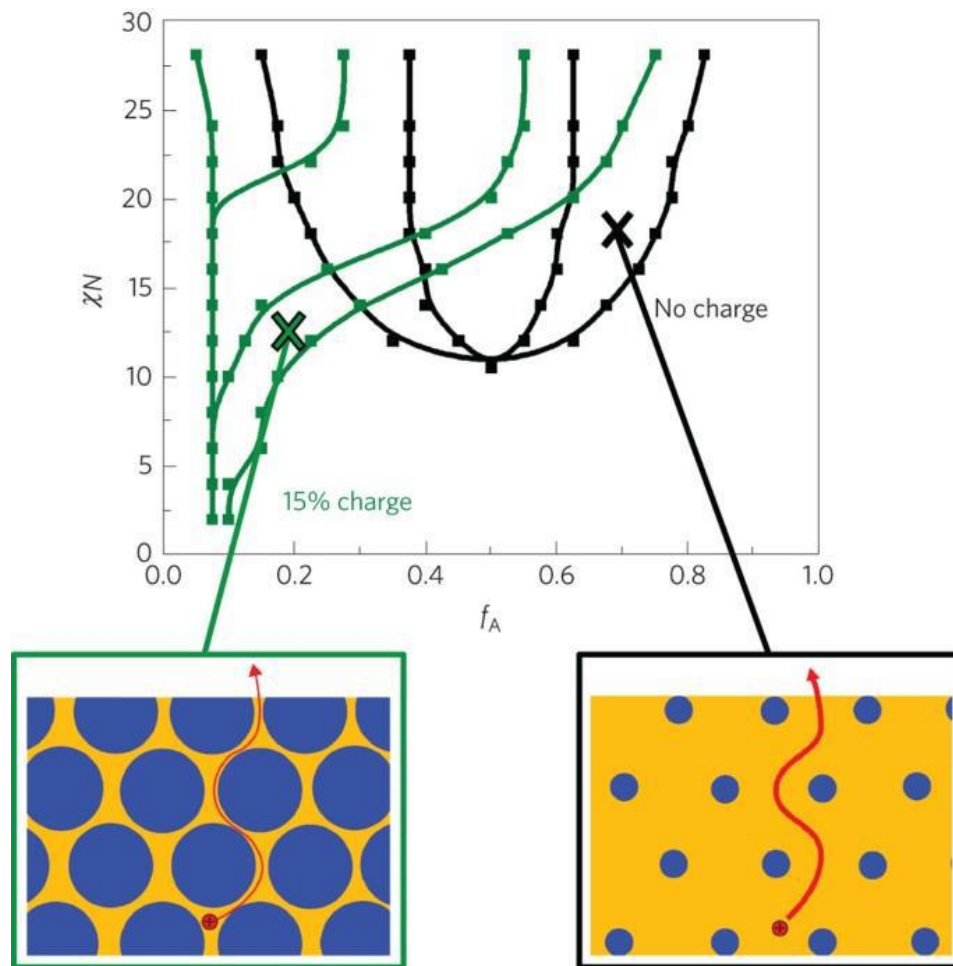


**Figure 1.7: Ion transport in charged system through percolating minority charged phase vs in uncharged system which is primarily bulk domain percolating around minority phase. Image is taken from ref 68.**

Following the phase separation trend in uncharged block copolymer and charged block copolyelectrolyte, it would be interesting to investigate the self-assembly behavior of block copolymer zwitterions. In this category of block copolymer two opposite charges are covalently bonded. Therefore, the entropy effect of the counterion will be nullified whereas the electrostatic cohesive strength will be highly enhanced. The contribution of these effects on morphology and the efficiency of the resultant morphology as the transport channels for water and ions is yet to be explored.

## **1.6 Advanced Material Applications for Polyzwitterions**

### **1.6.1 Antifouling Coating**

Fouling occurs when cells, proteins, and other microbes are attached to a surface. Antifoul coatings are of great importance in marine engineering and biomedical applications.<sup>22</sup> Polyzwitterions, especially polybetaines, have been explored over traditional PEG based material for their superior anti-fouling properties.<sup>74,75</sup> Due to polyzwitterion's high level of surface hydration and fixed charges on polymer backbone, the electrostatic force results in a low degree of protein attachment to the surface.<sup>76</sup>

### **1.6.2 Hydrogel Material**

Hydrogels are three-dimensional hydrophilic polymer networks held together by crosslinking that undergo swelling in aqueous medium. Opposed to the classical hydrogel where polymer chains are chemically held together by the covalently bonded crosslinker, polyzwitterions crosslinking points are the interchain electrostatically interacted opposite charges. The crosslinked zwitterions exhibit reversible swelling behavior with change in salt concentration and pH.<sup>75,77</sup> Due to their softness, responsive behavior, and water compatibility, polyzwitterion hydrogels have found use in many biomedicines'

applications. In addition to the electrostatic force between the opposite charges, entanglement of polymer chain and interaction with the environment provide added toughness.<sup>78</sup> These hydrogels can be reversible broken and healed when stretched or cut making them a self-healable material finding applications in tissue engineering (Figure 1.8).<sup>78,79</sup>

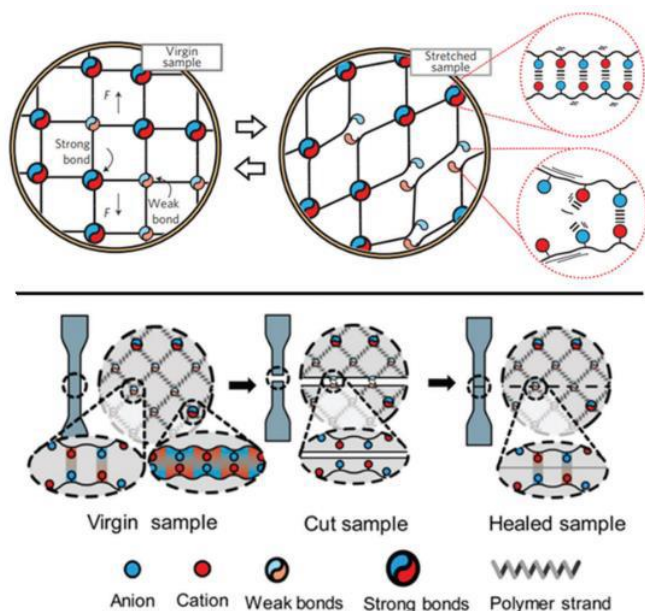


**Figure 1.8: Structure of zwitterionic polymer exhibiting self-healing properties upon stretching and cutting. Image taken from ref 76**

### 1.6.3 Dispersant and Stabilizers

Nanomaterials, which are highly important for advancement of nanotechnology, are often difficult to handle due to a lack of stability and have a tendency for agglomeration. Due to the “salt-in” behavior of polyelectrolytes, they have been utilized as a dispersing agent for nanomaterials.<sup>80</sup> These polyelectrolytes have been shown to act as a reversible stabilizer for gold nanoparticles at a pH range of 2-14 and precipitate the particle at pH 0

(Figure 1.9). Polyzwitterion's pH responsiveness makes it an interesting material for catalytic recovery of expensive or toxic nanoparticles.<sup>81</sup>

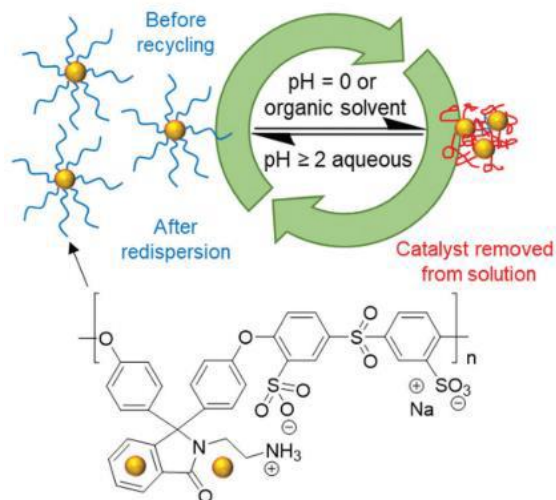


**Figure 1.9: Catalytic stabilization of gold nanoparticle. Image taken from ref 76**

#### 1.6.4 Antifreeze Material

Amphiphilic zwitterionic copolymers due to their antifreeze property have found large potential applications in cryopreservation of blood and tissue, freeze thaw expansion prevention of steel and concrete at construction sites, minimizing crop damage in agriculture, and aerospace.<sup>22</sup> The exact mechanisms of their antifreeze properties have yet to be firmly established. One theory is that these materials have a hydrophobic and a hydrophilic part which are capable of binding with the surface and with water molecules, preventing crystallization.<sup>82</sup>

#### 1.6.5 Drug Delivery and Gene Therapy

Owing to self-assembly, low toxicity due to charge neutrality and water compatibility, zwitterionic polymers have found applications in delivery of many classes of protein, nucleic acid, and small molecule therapeutics.<sup>22</sup> These materials also mimic



many zwitterionic moieties present in nature which enhance cell attachment and uptake efficiency.<sup>83</sup> Their amphoteric nature can also be used for a multitude of therapeutic purposes due to interactions with proteins.<sup>84</sup>

## **1.7 Zwitterionic Amphiphilic Copolymer for Water Transport Membrane**

The most widely used processes for water purification applications are reverse osmosis (RO) forward osmosis (FO), electrodialysis (EDI), pressure retarded osmosis (PRO), reverse electrodialysis (RED), nanofiltration (NF), ultrafiltration (UF) and microfiltration (MF).<sup>85-87</sup> OF these methods MF and UF are used to treat oil and other organic solutes while NF and RO are used for desalination or removal of other dissolved solutes.<sup>88</sup> To date, most water purification membranes are typically made of hydrophobic polymers. Hydrophobic-hydrophobic interactions between the membranes and the mixture of oil, salt and other dissolved particulates often lead to membrane fouling which is a drawback in the field of water treatment. Constant chemical treatment is needed to keep them foulant free which leads to a shortened life span of the membranes.<sup>88</sup> To overcome this problem, synthesized surface modified polymer membranes with improved hydrophilicity and reduced interaction with possible foulants have opened a broad scope of study.<sup>89</sup>

A hydrophilic surface attracts a tightly bound water layer, physically and energetically preventing direct interaction between a foulant and the membrane surface.<sup>44</sup> Polyethylene glycol (PEG)-containing materials due to their improved hydrophilicity and good antifouling property are being used widely in desalination and waste-water

management.<sup>88,90,91</sup> However, PEG being amphiphilic in nature exhibits some hydrophobic interaction and lacks resistance to certain proteins adsorption.<sup>92</sup>

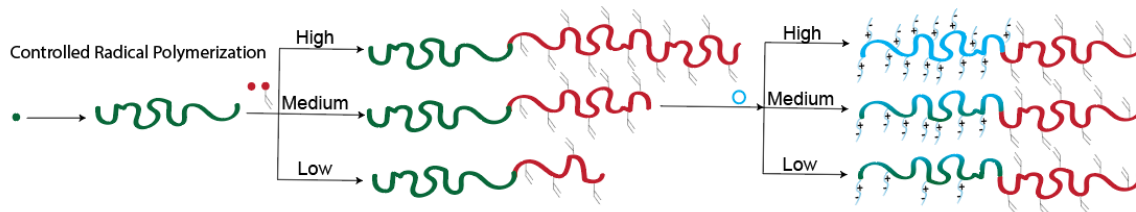
Zwitterionic polymers are a new class of polymeric films widely studied to replace the PEG based membrane and solve some of the problems associated with water treatment membranes. Due to incorporation of the charges on the membrane surface they show improved water and salt transport behavior along with better antifouling property. Polyzwitterions showing improved resistance to protein adsorption can be directly used for tailoring new generations of NF membranes.<sup>93</sup> Despite being a promising material in the field of waste-water treatment and desalination, the fundamentals of water and salt transport properties are not yet clearly understood. The polymer structures influence water uptake and salt transport.<sup>87</sup> Charged and uncharged polymers differ widely in their water and salt absorption, diffusion, and permeation.<sup>94</sup> For uncharged polymers without any ionizable functional group swollen with water utilize the partition mechanism for water transport and osmotic deswelling (dependent on the external salt concentration) for salt transport.<sup>94,95</sup> Charged polymers with fixed charged groups, or ionizable functional groups that are swollen with water, use both simple partition mechanism and electrostatic interaction for improved water and salt transport.<sup>94,96,97</sup> The zwitterions have packed density of both positive and negative charges, but they are covalently bonded (non-ionizable) with the backbone giving an overall charge neutrality. It is not yet clear whether zwitterionic polymers would mimic the charged or uncharged polymer for water and salt transport properties.

## 1.8 Dissertation Overview

The primary focus of this dissertation is to investigate the synthesis of tailored amphiphilic-zwitterionic (A-Z) block copolymers. The synthetic designs are chosen such that these novel A-Z block copolymers can be converted to mechanically robust membranes through photo crosslinking. Preliminary investigations on the effect of molecular weight, morphology and zwitterionic identity on water transport are reported. The organization of this dissertation has two specific objectives.

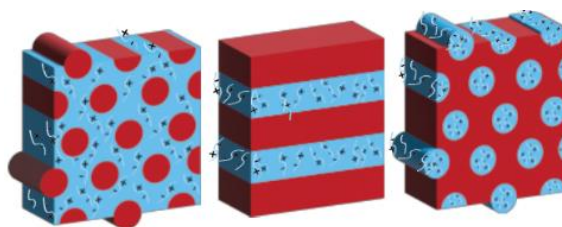
### 1.8.1 Tailoring of a Novel Amphiphilic-Zwitterionic Block Copolymer to Form Photo Crosslinked Free-Standing Films

Neutral block copolymer precursors of poly (n butyl acrylate-*ran*-allyl methacrylate)-*b*-poly (dimethylamino ethyl methacrylate) (P(nBA-*ran*-AMA)-*b*-PDMAEMA) with different copolymer volume fractions were synthesized using controlled radical polymerization. Advantage of using this technique is the ability to synthesize a polymer chain with predetermined molecular weight and well-defined chemical composition while also maintaining a narrow dispersity. Variation of the zwitterionic groups; sulfobetaine, carboxybetaine or cholinephosphate were attempted through post-polymerization modification of the PDMAEMA block using nucleophilic ring-opening reactions of 1,3-propane sultone,  $\beta$ -propiolactone or n-butyl substituted phospholane. The molecular properties of the polymer were investigated via NMR, GPC, FTIR analysis. Thermal stability of these zwitterionic systems was investigated by using thermogravimetric analysis (TGA) and differential scanning calorimetry (DSC).



## 1.8.2 Analyzing the Effect of Composition and Identity of Zwitterionic Block on Morphology

A mechanically robust free-standing amphiphilic zwitterionic copolymer poly (n butyl acrylate-*ran*-allyl methacrylate)-*b*-polybetaine methacrylate



membrane were tailored using thiol-ene click chemistry on the pendent double bond of the allyl methacrylate repeating unit with a dithiol crosslinking agent under UV source. The systematic variations in volume fractions of each block were targeted to generate different morphologies. There is also an expectation that by choosing different zwitterionic groups the dipole moment of the block can be varied, which in turn will affect the self-assembled nanostructure of the system. NMR spectroscopy data are analyzed to calculate degree of polymerization (DP) from the distinct peaks of each repeating unit of pendent groups in parent neutral block copolymers and its modified amphiphilic-zwitterionic counterpart. These DP values of the neutral block copolymer were used to calculate the relative volume fraction of each block and aid the future calculation of post-polymerization modification on PDMAEMA block and crosslinking chemistry on PAMA block. The impact of the copolymer composition and the identity of various zwitterionic blocks on the morphology were analyzed using small angle X-ray scattering (SAXS). Various relative humidity

sweeps and temperature sweep SAXS were performed through collaboration with Argonne National Laboratory to investigate the effect of different environmental conditions of these morphologies. In addition to SAXS, transmission electron microscopy (TEM) was performed to study real space imaging of these structures. With these characterizations it is possible to perform a structure-property relationship study of these novel Amphiphilic-Zwitterionic block copolymer system. This study also has a potential application in the field of water transport filtration membrane. The effect of morphology (contributed by zwitterionic identity and composition) on water uptake property will be studied using gravimetric analysis and dead-end filtration and on salt transport property using kinetic desorption method.

## 1.9 Reference

- (1) Pummerer, R. Die Hochmolekularen Organischen Verbindungen Kautschuk Und Cellulose. Von Dr. Phil. Hermann Staudinger, o. Prof., Direktor Des Chemischen Laboratoriums Der Universität Freiburg i. Br. 540 Seiten in Großoktav, 113 Abbildungen, Ein Ausführliches Sachverzeic. *Angew. Chemie* **1932**.  
<https://doi.org/10.1002/ange.19320455113>.
- (2) Miller, D. J.; Huang, X.; Li, H.; Kasemset, S.; Lee, A.; Agnihotri, D.; Hayes, T.; Paul, D. R.; Freeman, B. D. Fouling-Resistant Membranes for the Treatment of Flowback Water from Hydraulic Shale Fracturing: A Pilot Study. *J. Memb. Sci.* **2013**.  
<https://doi.org/10.1016/j.memsci.2013.03.019>.
- (3) Cheng, X. Q.; Liu, Y.; Guo, Z.; Shao, L. Nanofiltration Membrane Achieving Dual Resistance to Fouling and Chlorine for “Green” Separation of Antibiotics. *J. Memb. Sci.* **2015**. <https://doi.org/10.1016/j.memsci.2015.06.048>.
- (4) Geise, G. M.; Freeman, B. D.; Paul, D. R. Characterization of a Sulfonated Pentablock Copolymer for Desalination Applications. *Polymer (Guildf)*. **2010**, *51* (24), 5815–5822. <https://doi.org/10.1016/j.polymer.2010.09.072>.
- (5) Sujanani, R.; Landsman, M. R.; Jiao, S.; Moon, J. D.; Shell, M. S.; Lawler, D. F.; Katz, L. E.; Freeman, B. D. Designing Solute-Tailored Selectivity in Membranes: Perspectives for Water Reuse and Resource Recovery. *ACS Macro Lett.* **2020**, *9* (11), 1709–1717. <https://doi.org/10.1021/acsmacrolett.0c00710>.
- (6) Hickner, M. A.; Ghassemi, H.; Kim, Y. S.; Einsla, B. R.; McGrath, J. E. Alternative Polymer Systems for Proton Exchange Membranes (PEMs). *Chem. Rev.* **2004**, *104* (10),

4587–4611. <https://doi.org/10.1021/cr020711a>.

(7) Hickner, M. A.; Herring, A. M.; Coughlin, E. B. Anion Exchange Membranes: Current Status and Moving Forward. *Journal of Polymer Science, Part B: Polymer Physics*. 2013. <https://doi.org/10.1002/polb.23395>.

(8) Grady, B. P. Review and Critical Analysis of the Morphology of Random Ionomers across Many Length Scales. *Polymer Engineering and Science*. 2008. <https://doi.org/10.1002/pen.21024>.

(9) Neuse, E. W.; Perlwitz, A. G. As Drug Carriers Polyamides. **1991**, 394–404.

(10) Muthukumar, M. 50th Anniversary Perspective: A Perspective on Polyelectrolyte Solutions. *Macromolecules* **2017**, *50* (24), 9528–9560. <https://doi.org/10.1021/acs.macromol.7b01929>.

(11) Yethiraj, A. Liquid State Theory of Polyelectrolyte Solutions. *J. Phys. Chem. B* **2009**, *113* (6), 1539–1551. <https://doi.org/10.1021/jp8069964>.

(12) Lindquist, G. M.; Stratton, R. A. The Role of Polyelectrolyte Charge Density and Molecular Weight on the Adsorption and Flocculation of Colloidal Silica with Polyethylenimine. *J. Colloid Interface Sci.* **1976**, *55* (1), 45–59. [https://doi.org/10.1016/0021-9797\(76\)90007-2](https://doi.org/10.1016/0021-9797(76)90007-2).

(13) Ward, T. C.; Tobolsky, A. V. Viscoelastic Study of Ionomers. *J. Appl. Polym. Sci.* **1967**, *11* (12), 2403–2415. <https://doi.org/10.1002/app.1967.070111201>.

(14) Schanze, K. S.; Shelton, A. H. Functional Polyelectrolytes. *Langmuir* **2009**, *25* (24), 13698–13702. <https://doi.org/10.1021/la903785g>.

- (15) Lowe, A. B.; McCormick, C. L. Synthesis and Solution Properties of Zwitterionic Polymers. *Chem. Rev.* **2002**, *102* (11), 4177–4189. <https://doi.org/10.1021/cr020371t>.
- (16) Astafieva, I.; Khougaz, K.; Eisenberg, A. Micellization in Block Polyelectrolyte Solutions. 2. Fluorescence Study of the Critical Micelle Concentration as a Function of Soluble Block Length and Salt Concentration. *Macromolecules* **1995**, *28* (21), 7127–7134. <https://doi.org/10.1021/ma00125a015>.
- (17) Astafieva, I.; Zhong, X. F.; Eisenberg, A. Critical Micellization Phenomena in Block Polyelectrolyte Solutions. *Macromolecules* **1993**, *26* (26), 7339–7352. <https://doi.org/10.1021/ma00078a034>.
- (18) Chelushkin, P. S.; Lysenko, E. A.; Bronich, T. K.; Eisenberg, A.; Kabanov, V. A.; Kabanov, A. V. Polyion Complex Nanomaterials from Block Polyelectrolyte Micelles and Linear Polyelectrolytes of Opposite Charge. 2. Dynamic Properties. *J. Phys. Chem. B* **2008**, *112* (26), 7732–7738. <https://doi.org/10.1021/jp8012877>.
- (19) Zhu, J.; Lennox, R. B.; Eisenberg, A. Interfacial Behavior of Block Polyelectrolytes. 4. Polymorphism of (Quasi) Two-Dimensional Micelles. *J. Phys. Chem.* **1992**, *96* (12), 4727–4730. <https://doi.org/10.1021/j100191a002>.
- (20) Laschewsky, A. Structures and Synthesis of Zwitterionic Polymers. *Polymers (Basel)*. **2014**, *6* (5), 1544–1601. <https://doi.org/10.3390/polym6051544>.
- (21) Leng, C.; Sun, S.; Zhang, K.; Jiang, S.; Chen, Z. Molecular Level Studies on Interfacial Hydration of Zwitterionic and Other Antifouling Polymers in Situ. *Acta Biomaterialia*. 2016. <https://doi.org/10.1016/j.actbio.2016.02.030>.



- (22) Blackman, L. D.; Gunatillake, P. A.; Cass, P.; Locock, K. E. S. An Introduction to Zwitterionic Polymer Behavior and Applications in Solution and at Surfaces. *Chem. Soc. Rev.* **2019**, *48* (3), 757–770. <https://doi.org/10.1039/c8cs00508g>.
- (23) Wever, D. A. Z.; Picchioni, F.; Broekhuis, A. A. Polymers for Enhanced Oil Recovery: A Paradigm for Structure-Property Relationship in Aqueous Solution. *Progress in Polymer Science (Oxford)*. 2011. <https://doi.org/10.1016/j.progpolymsci.2011.05.006>.
- (24) Schulz, D. N.; Peiffer, D. G.; Agarwal, P. K.; Larabee, J.; Kaladas, J. J.; Soni, L.; Handwerker, B.; Garner, R. T. Phase Behaviour and Solution Properties of Sulphobetaine Polymers. *Polymer (Guildf)*. **1986**. [https://doi.org/10.1016/0032-3861\(86\)90269-7](https://doi.org/10.1016/0032-3861(86)90269-7).
- (25) Zhu, Y.; Noy, J. M.; Lowe, A. B.; Roth, P. J. The Synthesis and Aqueous Solution Properties of Sulfoethylbetaine (Co)Polymers: Comparison of Synthetic Routes and Tuneable Upper Critical Solution Temperatures. *Polym. Chem.* **2015**, *6* (31), 5705–5718. <https://doi.org/10.1039/c5py00160a>.
- (26) Wischerhoff, E.; Badi, N.; Laschewsky, A.; Lutz, J. F. Smart Polymer Surfaces: Concepts and Applications in Biosciences. *Adv. Polym. Sci.* **2010**. [https://doi.org/10.1007/12\\_2010\\_88](https://doi.org/10.1007/12_2010_88).
- (27) Peng, S.; Bhushan, B. Smart Polymer Brushes and Their Emerging Applications. *RSC Adv.* **2012**. <https://doi.org/10.1039/c2ra20451g>.
- (28) Hildebrand, V.; Laschewsky, A.; Päch, M.; Müller-Buschbaum, P.; Papadakis, C. M. Effect of the Zwitterion Structure on the Thermo-Responsive Behaviour of Poly(Sulfobetaine Methacrylates). *Polym. Chem.* **2017**, *8* (1), 310–322. <https://doi.org/10.1039/c6py01220e>.

- (29) Ni, L.; Meng, J.; Geise, G. M.; Zhang, Y.; Zhou, J. Water and Salt Transport Properties of Zwitterionic Polymers Film. *J. Memb. Sci.* **2015**, *491*, 73–81. <https://doi.org/10.1016/j.memsci.2015.05.030>.
- (30) Johnston, D. S.; Sanghera, S.; Pons, M.; Chapman, D. Phospholipid Polymers—Synthesis and Spectral Characteristics. *Biochim. Biophys. Acta - Biomembr.* **1980**. [https://doi.org/10.1016/0005-2736\(80\)90289-8](https://doi.org/10.1016/0005-2736(80)90289-8).
- (31) Koga, Y.; Morii, H. Biosynthesis of Ether-Type Polar Lipids in Archaea and Evolutionary Considerations. *Microbiol. Mol. Biol. Rev.* **2007**. <https://doi.org/10.1128/membr.00033-06>.
- (32) Jones, M. N. The Surface Properties of Phospholipid Liposome Systems and Their Characterisation. *Advances in Colloid and Interface Science.* 1995. [https://doi.org/10.1016/0001-8686\(94\)00223-Y](https://doi.org/10.1016/0001-8686(94)00223-Y).
- (33) Binder, H.; Zschörnig, O. The Effect of Metal Cations on the Phase Behavior and Hydration Characteristics of Phospholipid Membranes. *Chem. Phys. Lipids* **2002**. [https://doi.org/10.1016/S0009-3084\(02\)00005-1](https://doi.org/10.1016/S0009-3084(02)00005-1).
- (34) Zhao, L.; Li, N.; Wang, K.; Shi, C.; Zhang, L.; Luan, Y. A Review of Polypeptide-Based Polymersomes. *Biomaterials.* 2014. <https://doi.org/10.1016/j.biomaterials.2013.10.063>.
- (35) Ramachandran, G. N.; Ramakrishnan, C.; Sasisekharan, V. Stereochemistry of Polypeptide Chain Configurations. *Journal of Molecular Biology.* 1963. [https://doi.org/10.1016/S0022-2836\(63\)80023-6](https://doi.org/10.1016/S0022-2836(63)80023-6).

- (36) Priftis, D.; Laugel, N.; Tirrell, M. Thermodynamic Characterization of Polypeptide Complex Coacervation. *Langmuir* **2012**. <https://doi.org/10.1021/la302729r>.
- (37) Tarannum, N.; Singh, M. Advances in Synthesis and Applications of Sulfo and Carbo Analogues of Polybetaines: A Review. *Rev. Adv. Sci. Eng.* **2013**. <https://doi.org/10.1166/rase.2013.1036>.
- (38) Zhang, Z.; Chen, S.; Jiang, S. Dual-Functional Biomimetic Materials: Nonfouling Poly(Carboxybetaine) with Active Functional Groups for Protein Immobilization. *Biomacromolecules* **2006**. <https://doi.org/10.1021/bm060750m>.
- (39) Zhang, Z.; Vaisocherová, H.; Cheng, G.; Yang, W.; Xue, H.; Jiang, S. Nonfouling Behavior of Polycarboxybetaine-Grafted Surfaces: Structural and Environmental Effects. *Biomacromolecules* **2008**. <https://doi.org/10.1021/bm800407r>.
- (40) Cao, B.; Li, L.; Tang, Q.; Cheng, G. The Impact of Structure on Elasticity, Switchability, Stability and Functionality of an All-in-One Carboxybetaine Elastomer. *Biomaterials* **2013**. <https://doi.org/10.1016/j.biomaterials.2013.06.063>.
- (41) Cao, B.; Tang, Q.; Li, L.; Humble, J.; Wu, H.; Liu, L.; Cheng, G. Switchable Antimicrobial and Antifouling Hydrogels with Enhanced Mechanical Properties. *Adv. Healthc. Mater.* **2013**. <https://doi.org/10.1002/adhm.201200359>.
- (42) Vaisocherová, H.; Zhang, Z.; Yang, W.; Cao, Z.; Cheng, G.; Taylor, A. D.; Piliarik, M.; Homola, J.; Jiang, S. Functionalizable Surface Platform with Reduced Nonspecific Protein Adsorption from Full Blood Plasma-Material Selection and Protein Immobilization Optimization. *Biosens. Bioelectron.* **2009**. <https://doi.org/10.1016/j.bios.2008.09.035>.

- (43) Vaisocherová, H.; Yang, W.; Zhang, Z.; Cao, Z.; Cheng, G.; Piliarik, M.; Homola, J.; Jiang, S. Ultralow Fouling and Functionalizable Surface Chemistry Based on a Zwitterionic Polymer Enabling Sensitive and Specific Protein Detection in Undiluted Blood Plasma. *Anal. Chem.* **2008**. <https://doi.org/10.1021/ac8015888>.
- (44) Shah, S.; Liu, J.; Ng, S.; Luo, S.; Guo, R.; Cheng, C.; Lin, H. Transport Properties of Small Molecules in Zwitterionic Polymers. *J. Polym. Sci. Part B Polym. Phys.* **2016**, *54* (19), 1924–1934. <https://doi.org/10.1002/polb.24096>.
- (45) Blackman, L. D.; Gunatillake, P. A.; Cass, P.; Locock, K. E. S. An Introduction to Zwitterionic Polymer Behavior and Applications in Solution and at Surfaces. *Chem. Soc. Rev.* **2019**, *48* (3), 757–770. <https://doi.org/10.1039/c8cs00508g>.
- (46) Narayanan Nair, A. K.; Martinez Jimenez, A.; Sun, S. Complexation Behavior of Polyelectrolytes and Polyampholytes. *J. Phys. Chem. B* **2017**, *121* (33), 7987–7998. <https://doi.org/10.1021/acs.jpcc.7b04582>.
- (47) Kaditi, E.; Mountrichas, G.; Pispas, S. Amphiphilic Block Copolymers by a Combination of Anionic Polymerization and Selective Post-Polymerization Functionalization. *Eur. Polym. J.* **2011**, *47* (4), 415–434. <https://doi.org/10.1016/j.eurpolymj.2010.09.012>.
- (48) Narayanan Nair, A. K.; Uyaver, S.; Sun, S. Conformational Transitions of a Weak Polyampholyte. *J. Chem. Phys.* **2014**. <https://doi.org/10.1063/1.4897161>.
- (49) Koutalas, G.; Pispas, S.; Hadjichristidis, N. Micelles of Poly(Isoprene-*b*-2-Vinylpyridine-*b*-Ethylene Oxide) Terpolymers in Aqueous Media and Their Interaction with Surfactants. *Eur. Phys. J. E* **2004**. <https://doi.org/10.1140/epje/i2004-10075-3>.

- (50) Hammond, M. R.; Li, C.; Tsitsilianis, C.; Mezzenga, R. Hierarchical Self-Organization in Polyelectrolyte-Surfactant Complexes Based on Heteroarm Star Block Copolyampholytes. *Soft Matter* **2009**. <https://doi.org/10.1039/b817219f>.
- (51) Annaka, M.; Morishita, K.; Okabe, S. Electrostatic Self-Assembly of Neutral and Polyelectrolyte Block Copolymers and Oppositely Charged Surfactant. *J. Phys. Chem. B* **2007**. <https://doi.org/10.1021/jp074404q>.
- (52) Harada, A.; Kataoka, K. Chain Length Recognition: Core-Shell Supramolecular Assembly from Oppositely Charged Block Copolymers. *Science* (80-. ). **1999**. <https://doi.org/10.1126/science.283.5398.65>.
- (53) Förster, S. Amphiphilic Block Copolymers for Templating Applications BT - Colloid Chemistry I; Antonietti, M., Ed.; Springer Berlin Heidelberg: Berlin, Heidelberg, 2003; pp 1–28. [https://doi.org/10.1007/3-540-36408-0\\_1](https://doi.org/10.1007/3-540-36408-0_1).
- (54) Lazzari, M.; Liu, G.; Lecommandoux, S. *Block Copolymers in Nanoscience*; 2008. <https://doi.org/10.1002/9783527610570>.
- (55) Hadjichristidis, N.; Pispas, S.; Iatrou, H.; Pitsikalis, M. Linking Chemistry and Anionic Polymerization. *Curr. Org. Chem.* **2005**. <https://doi.org/10.2174/1385272023374463>.
- (56) Bielawski, C. W.; Grubbs, R. H. Living Ring-Opening Metathesis Polymerization. *Progress in Polymer Science (Oxford)*. 2007. <https://doi.org/10.1016/j.progpolymsci.2006.08.006>.
- (57) Matyjaszewski, K. Atom Transfer Radical Polymerization (ATRP): Current Status

and Future Perspectives. *Macromolecules* **2012**, *45* (10), 4015–4039. <https://doi.org/10.1021/ma3001719>.

(58) Eisenberg, A. *Block Copolymers: Synthetic Strategies, Physical Properties, and Applications* By Nikos Hadjichristidis and Stergios Pispas (University of Athens) and George Floudas (University of Ioannina). John Wiley and Sons, Inc.: Hoboken, NJ. 2003. Xx + 420 Pp. \$12. *J. Am. Chem. Soc.* **2003**. <https://doi.org/10.1021/ja025357c>.

(59) Blasco, E.; Sims, M. B.; Goldmann, A. S.; Sumerlin, B. S.; Barner-Kowollik, C. 50th Anniversary Perspective: Polymer Functionalization. *Macromolecules* **2017**, *50* (14), 5215–5252. <https://doi.org/10.1021/acs.macromol.7b00465>.

(60) Mai, Y.; Eisenberg, A. Self-Assembly of Block Copolymers. *Chem. Soc. Rev.* **2012**, *41* (18), 5969–5985. <https://doi.org/10.1039/c2cs35115c>.

(61) Cochran, E. W.; Garcia-Cervera, C. J.; Fredrickson, G. H. Stability of the Gyroid Phase in Diblock Copolymers at Strong Segregation. *Macromolecules* **2006**, *39* (7), 2449–2451. <https://doi.org/10.1021/ma0527707>.

(62) Discher, D. E.; Ahmed, F. POLYMERSOMES. *Annu. Rev. Biomed. Eng.* **2006**, *8* (1), 323–341. <https://doi.org/10.1146/annurev.bioeng.8.061505.095838>.

(63) Vavasour, J. D.; Whitmore, M. D. Self-Consistent Field Theory of Block Copolymers with Conformational Asymmetry. *Macromolecules* **1993**, *26* (25), 7070–7075. <https://doi.org/10.1021/ma00077a054>.

(64) Tang, J.; Jiang, Y.; Zhang, X.; Yan, D.; Chen, J. Z. Y. Phase Diagram of Rod-Coil Diblock Copolymer Melts. *Macromolecules* **2015**, *48* (24), 9060–9070.

<https://doi.org/10.1021/acs.macromol.5b02235>.

(65) Matsen, M. W. Effect of Architecture on the Phase Behavior of AB-Type Block Copolymer Melts. *Macromolecules* **2012**, *45* (4), 2161–2165.

<https://doi.org/10.1021/ma202782s>.

(66) Shi, W.; Lynd, N. A.; Montarnal, D.; Luo, Y.; Fredrickson, G. H.; Kramer, E. J.; Ntaras, C.; Avgeropoulos, A.; Hexemer, A. Toward Strong Thermoplastic Elastomers with Asymmetric Miktoarm Block Copolymer Architectures. *Macromolecules* **2014**, *47* (6), 2037–2043. <https://doi.org/10.1021/ma402566g>.

(67) Asai, Y.; Yamada, K.; Yamada, M.; Takano, A.; Matsushita, Y. Formation of Tetragonally-Packed Rectangular Cylinders from ABC Block Terpolymer Blends. *ACS Macro Lett.* **2014**, *3* (2), 166–169. <https://doi.org/10.1021/mz400647v>.

(68) Sing, C. E.; Zwanikken, J. W.; Olvera De La Cruz, M. Electrostatic Control of Block Copolymer Morphology. *Nat. Mater.* **2014**, *13* (7), 694–698. <https://doi.org/10.1038/nmat4001>.

(69) Wanakule, N. S.; Virgili, J. M.; Teran, A. A.; Wang, Z. G.; Balsara, N. P. Thermodynamic Properties of Block Copolymer Electrolytes Containing Imidazolium and Lithium Salts. *Macromolecules* **2010**, *43* (19), 8282–8289. <https://doi.org/10.1021/ma1013786>.

(70) Wang, Z.-G. Effects of Ion Solvation on the Miscibility of Binary Polymer Blends. *J. Phys. Chem. B* **2008**, *112* (50), 16205–16213. <https://doi.org/10.1021/jp806897t>.

(71) Nakamura, I.; Balsara, N. P.; Wang, Z.-G. Thermodynamics of Ion-Containing

Polymer Blends and Block Copolymers. *Phys. Rev. Lett.* **2011**, *107* (19), 198301.  
<https://doi.org/10.1103/PhysRevLett.107.198301>.

(72) Zwanikken, J. W.; Jha, P. K.; De La Cruz, M. O. A Practical Integral Equation for the Structure and Thermodynamics of Hard Sphere Coulomb Fluids. *J. Chem. Phys.* **2011**, *135* (6). <https://doi.org/10.1063/1.3624809>.

(73) Sing, C. E.; Zwanikken, J. W.; de la Cruz, M. O. Interfacial Behavior in Polyelectrolyte Blends: Hybrid Liquid-State Integral Equation and Self-Consistent Field Theory Study. *Phys. Rev. Lett.* **2013**, *111* (16), 168303.  
<https://doi.org/10.1103/PhysRevLett.111.168303>.

(74) Chang, Y.; Liao, S. C.; Higuchi, A.; Ruaan, R. C.; Chu, C. W.; Chen, W. Y. A Highly Stable Nonbiofouling Surface with Well-Packed Grafted Zwitterionic Polysulfobetaine for Plasma Protein Repulsion. *Langmuir* **2008**.  
<https://doi.org/10.1021/la800228c>.

(75) Sagle, A. C.; Sharma, M. M.; Freeman, B. D. Structure-Property Relationships in PEG-Based Hydrogels for Potential Hydrophilic Membrane Coating Materials. *PMSE Prepr.* **2007**.

(76) Jiang, S.; Cao, Z. Ultralow-Fouling, Functionalizable, and Hydrolyzable Zwitterionic Materials and Their Derivatives for Biological Applications. *Adv. Mater.* **2010**, *22* (9), 920–932. <https://doi.org/10.1002/adma.200901407>.

(77) Hoffman, A. S. Hydrogels for Biomedical Applications. *Advanced Drug Delivery Reviews.* 2012. <https://doi.org/10.1016/j.addr.2012.09.010>.



- (78) Sun, T. L.; Kurokawa, T.; Kuroda, S.; Ihsan, A. Bin; Akasaki, T.; Sato, K.; Haque, M. A.; Nakajima, T.; Gong, J. P. Physical Hydrogels Composed of Polyampholytes Demonstrate High Toughness and Viscoelasticity. *Nat. Mater.* **2013**. <https://doi.org/10.1038/nmat3713>.
- (79) Ihsan, A. Bin; Sun, T. L.; Kurokawa, T.; Karobi, S. N.; Nakajima, T.; Nonoyama, T.; Roy, C. K.; Luo, F.; Gong, J. P. Self-Healing Behaviors of Tough Polyampholyte Hydrogels. *Macromolecules* **2016**. <https://doi.org/10.1021/acs.macromol.6b00437>.
- (80) Ciferri, a.; Kudaibergenov, S. Natural and Synthetic Polyampholytes, 2, Functions and Applications. *Macromol. Rapid Commun.* **2007**. <https://doi.org/10.1002/marc.200700162>.
- (81) Rodriguez, A. K.; Ayyavu, C.; Iyengar, S. R.; Bazzi, H. S.; Masad, E.; Little, D.; Hanley, H. J. M. Polyampholyte Polymer as a Stabiliser for Subgrade Soil. *Int. J. Pavement Eng.* **2018**. <https://doi.org/10.1080/10298436.2016.1175561>.
- (82) Mitchell, D. E.; Cameron, N. R.; Gibson, M. I. Rational, yet Simple, Design and Synthesis of an Antifreeze-Protein Inspired Polymer for Cellular Cryopreservation. *Chem. Commun.* **2015**. <https://doi.org/10.1039/c5cc04647e>.
- (83) Kim, Y.; Binauld, S.; Stenzel, M. H. Zwitterionic Guanidine-Based Oligomers Mimicking Cell-Penetrating Peptides as a Nontoxic Alternative to Cationic Polymers to Enhance the Cellular Uptake of Micelles. *Biomacromolecules* **2012**. <https://doi.org/10.1021/bm301351e>.
- (84) Shen, H.; Akagi, T.; Akashi, M. Polyampholyte Nanoparticles Prepared by Self-Complexation of Cationized Poly( $\gamma$ -Glutamic Acid) for Protein Carriers. *Macromol.*

*Biosci.* **2012**. <https://doi.org/10.1002/mabi.201200062>.

(85) Greenlee, L. F.; Lawler, D. F.; Freeman, B. D.; Marrot, B.; Moulin, P. Reverse Osmosis Desalination: Water Sources, Technology, and Today's Challenges. *Water Research*. 2009. <https://doi.org/10.1016/j.watres.2009.03.010>.

(86) Cheryan, M.; Rajagopalan, N. Membrane Processing of Oily Streams. Wastewater Treatment and Waste Reduction. *J. Memb. Sci.* **1998**, *151* (1), 13–28. [https://doi.org/10.1016/S0376-7388\(98\)00190-2](https://doi.org/10.1016/S0376-7388(98)00190-2).

(87) Geise, G. M.; Lee, H. S.; Miller, D. J.; Freeman, B. D.; McGrath, J. E.; Paul, D. R. Water Purification by Membranes: The Role of Polymer Science. *J. Polym. Sci. Part B Polym. Phys.* **2010**. <https://doi.org/10.1002/polb.22037>.

(88) Miller, D. J.; Huang, X.; Li, H.; Kasemset, S.; Lee, A.; Agnihotri, D.; Hayes, T.; Paul, D. R.; Freeman, B. D. Fouling-Resistant Membranes for the Treatment of Flowback Water from Hydraulic Shale Fracturing: A Pilot Study. *J. Memb. Sci.* **2013**, *437*, 265–275. <https://doi.org/10.1016/j.memsci.2013.03.019>.

(89) Schönemann, E.; Laschewsky, A.; Wischerhoff, E.; Koc, J.; Rosenhahn, A. Surface Modification by Polyzwitterions of the Sulfobetaine-Type, and Their Resistance to Biofouling. *Polymers (Basel)*. **2019**, *11* (6), 1–34. <https://doi.org/10.3390/polym11061014>.

(90) Ju, H.; McCloskey, B. D.; Sagle, A. C.; Kusuma, V. A.; Freeman, B. D. Preparation and Characterization of Crosslinked Poly(Ethylene Glycol) Diacrylate Hydrogels as Fouling-Resistant Membrane Coating Materials. *J. Memb. Sci.* **2009**. <https://doi.org/10.1016/j.memsci.2008.12.054>.

- (91) Wu, Y. H.; Park, H. B.; Kai, T.; Freeman, B. D.; Kalika, D. S. Water Uptake, Transport and Structure Characterization in Poly(Ethylene Glycol) Diacrylate Hydrogels. *J. Memb. Sci.* **2010**. <https://doi.org/10.1016/j.memsci.2009.10.025>.
- (92) Roosjen, A.; Van Der Mei, H. C.; Busscher, H. J.; Norde, W. Microbial Adhesion to Poly(Ethylene Oxide) Brushes: Influence of Polymer Chain Length and Temperature. *Langmuir* **2004**. <https://doi.org/10.1021/la048469l>.
- (93) Ji, Y. L.; An, Q. F.; Zhao, Q.; Sun, W. D.; Lee, K. R.; Chen, H. L.; Gao, C. J. Novel Composite Nanofiltration Membranes Containing Zwitterions with High Permeate Flux and Improved Anti-Fouling Performance. *J. Memb. Sci.* **2012**. <https://doi.org/10.1016/j.memsci.2011.11.047>.
- (94) Geise, G. M.; Paul, D. R.; Freeman, B. D. Fundamental Water and Salt Transport Properties of Polymeric Materials. *Progress in Polymer Science.* 2014. <https://doi.org/10.1016/j.progpolymsci.2013.07.001>.
- (95) Lonsdale, H. K.; Merten, U.; Riley, R. L. Transport Properties of Cellulose Acetate Osmotic Membranes. *J. Appl. Polym. Sci.* **1965**. <https://doi.org/10.1002/app.1965.070090413>.
- (96) Geise, G. M.; Freeman, B. D.; Paul, D. R. Sodium Chloride Diffusion in Sulfonated Polymers for Membrane Applications. *J. Memb. Sci.* **2013**. <https://doi.org/10.1016/j.memsci.2012.09.029>.
- (97) Geise, G. M.; Falcon, L. P.; Freeman, B. D.; Paul, D. R. Sodium Chloride Sorption in Sulfonated Polymers for Membrane Applications. *J. Memb. Sci.* **2012**. <https://doi.org/10.1016/j.memsci.2012.08.014>.

- (98) Banerjee, S. L.; Bhattacharya, K.; Samanta, S.; Singha, N. K. Self-Healable Antifouling Zwitterionic Hydrogel Based on Synergistic Phototriggered Dynamic Disulfide Metathesis Reaction and Ionic Interaction. *ACS Appl. Mater. Interfaces* **2018**, *10* (32), 27391–27406. <https://doi.org/10.1021/acsami.8b10446>.
- (99) Hu, G.; Parelkar, S. S.; Emrick, T. A Facile Approach to Hydrophilic, Reverse Zwitterionic, Choline Phosphate Polymers. *Polym. Chem.* **2015**, *6* (4), 525–530. <https://doi.org/10.1039/c4py01292e>.
- (100) Bates, F. S.; Fredrickson, G. H. Block Copolymer Thermodynamics: Theory and Experiment. *Annu. Rev. Phys. Chem.* **1990**, *41* (1), 525–557. <https://doi.org/10.1146/annurev.pc.41.100190.002521>.
- (101) Matsen, M. W. The Standard Gaussian Model for Block Copolymer Melts. *J. Phys. Condens. Matter* **2002**, *14* (2). <https://doi.org/10.1088/0953-8984/14/2/201>.
- (102) Chan, E. P.; Frieberg, B. R.; Ito, K.; Tarver, J.; Tyagi, M.; Zhang, W.; Coughlin, E. B.; Stafford, C. M.; Roy, A.; Rosenberg, S.; Soles, C. L. Insights into the Water Transport Mechanism in Polymeric Membranes from Neutron Scattering. *Macromolecules* **2020**, *53* (4), 1443–1450. <https://doi.org/10.1021/acs.macromol.9b02195>.
- (103) Ertem, S. P.; Tsai, T. H.; Donahue, M. M.; Zhang, W.; Sarode, H.; Liu, Y.; Seifert, S.; Herring, A. M.; Coughlin, E. B. Photo-Cross-Linked Anion Exchange Membranes with Improved Water Management and Conductivity. *Macromolecules* **2016**, *49* (1), 153–161. <https://doi.org/10.1021/acs.macromol.5b01784>.
- (104) Tsai, T. H.; Ertem, S. P.; Maes, A. M.; Seifert, S.; Herring, A. M.; Coughlin, E. B. Thermally Cross-Linked Anion Exchange Membranes from Solvent Processable Isoprene

Containing Ionomers. *Macromolecules* **2015**, 48 (3), 655–662.  
<https://doi.org/10.1021/ma502362a>.

(105) Ilčíková, M.; Tkáč, J.; Kasák, P. Switchable Materials Containing Polyzwitterion Moieties. *Polymers (Basel)*. **2015**, 7 (11), 2344–2370.  
<https://doi.org/10.3390/polym7111518>.

## CHAPTER 2

# MODULAR CHEMISTRY FOR DEVELOPING A LIBRARY OF NOVEL AMPHIPHILIC ZWITTERIONIC (A-Z) BLOCK COPOLYMERS

### 2.1 Background and Motivation

The hydrophobic and hydrophilic (zwitterionic) blocks of the A-Z block copolymer are usually not compatible to undergo a sequential copolymerization technique due to the expected lack of a common solvent to allow for solution polymerizations. To mitigate this challenge a neutral block copolymer precursor of poly [dimethylamino ethyl methacrylate-*b*-(*n* butyl acrylate-*ran*-allyl methacrylate)] (D-HyphB) was chosen to allow for synthesis using RAFT polymerization, which is a living/controlled radical polymerization. Advantages of using this technique are the ability to synthesize a polymer chain with a predetermined molecular weight and well-defined chemical composition also maintaining a narrow dispersity. Poly(*n* butyl acrylate-*ran*-allyl methacrylate) (HyphB) was chosen as the hydrophobic part of the copolymer for its low glass transition temperature ( $T_g$ ) that would provide flexibility. The pendent allyl group from the allyl methacrylate comonomer affords sites for future crosslinking to enhance mechanical integrity. The poly(dimethylamino ethyl methacrylate) (D) has two sites for modification chemistry - an acrylate ester group making it susceptible for nucleophilic substitution chemistry and a basic tertiary amine group suitable for nucleophilic ring-opening reactions that simultaneously results in quaternization. After sequential RAFT polymerization is used to synthesize the parent block copolymer a post-polymerization modification can be performed using the latent functionality of the tertiary amine pendent group. Nucleophilic

ring-opening reactions of different heterocycles were performed to achieve the hydrophilic zwitterionic segments of the block copolymers. This synthetic methodology provides flexibility to tailor a broad array of A-Z copolymers by obviating the synthetic challenges of the incompatibility of HyphB and zwitterionic blocks while also giving well-controlled overall molecular weights, volume fractions of the copolymer block, dispersity, and zwitterion content.

This chapter will focus on developing a platform series of A-Z block copolymers with different volume fractions of the hydrophilic block and identity of zwitterionic block from the same parent polymer. Post-polymerization modification of the PDMAEMA block will be performed using ring-opening of 1,3-propane sultone,  $\beta$ -propiolactone, and n-Butyl substituted choline phospholane heterocyclic rings. Characterizations methods employed include NMR, GPC, FT-IR, TGA and DSC were performed to investigate the molecular composition and thermal properties of the copolymers.

## **2.2 Instrumentation and Characterization**

NMR spectroscopy was performed using a Bruker Avance III HD 500 MHz spectrometer. Gel permeation chromatography (GPC) was performed in DMF with a RI detector. Infrared spectroscopy was performed on a Perkin-Elmer Spectrum One FT-IR spectrometer with ATR sampling accessory recorded between  $650\text{ cm}^{-1}$  and  $4000\text{ cm}^{-1}$  with 8 scans. Thermogravimetric analysis (TGA) Q500 was used with a heating rate of  $10\text{ K min}^{-1}$  from  $21\text{ }^{\circ}\text{C}$  to  $150\text{ }^{\circ}\text{C}$  then an isothermal hold for 30 minutes under a nitrogen environment. Differential scanning calorimetry (DSC) was performed using a TA

Instruments DSC Q200 equipped with a refrigerated cooling system (RCS90). Samples of approximately 3-8 mg were loaded into hermetically sealed aluminum pans and subjected to a heat/cool/heat cycle at a heating/cooling rate of 10 K/min over a temperature range of -70 to 150 °C. The  $T_g$ 's were determined from the second heating cycle.

## **2.3 Homopolymerization of PDMAEMA**

### **2.3.1 Kinetic Study for Synthesis of PDMAEMA**

A kinetic study of the synthesis of macro chain transfer agents containing DMAEMA (Scheme 2.1) has been performed to study the reaction time required to achieve the D block with targeted molecular weight and low dispersity. A commercially available chain transfer agent (CTA) was chosen containing trithiocarbonate group which is less susceptible than the dithioester group to nucleophilic attack from the tertiary amine group present in the monomer. The CTA contains a methylene group that provides a distinct traceable signal in  $^1\text{H-NMR}$ , not overlapping with any of the polymer characteristic signals, for end-group analysis and DP measurements. The CTA, 4-Cyano-4-[(dodecylsulfanylthiocarbonyl)sulfanyl]pentanoic acid (CDTCPA), and the initiator 4,4'-Azobis (4-cyanovaleric acid) (ABCVA) are purchased from Sigma Aldrich. Monomer (DMAEMA) and solvent (DMF, anhydrous 99.8%) were purchased from Alfa Aesar. The monomer was purified by passing through an alumina column to remove inhibitors. All the other reagents were used without further purification.

Synthesis of poly DMAEMA was performed under a nitrogen atmosphere at 60°C. Selected quantities of CTA and initiator are dissolved in DMF (10ml) in a 50 ml round bottom flask. The solution was purged under nitrogen for 20 min. Into the purged solution,



a known amount purified DMAEMA (10ml) was then added. The resulting stock solution was kept under nitrogen flow for a further 10 min more to ensure complete removal of dissolved oxygen. The flask was then transferred to a stir plate pre-heated to 60°C. An aliquot of 0.5 ml of the reaction mixture was removed with a nitrogen flushed syringe every 2 hours. <sup>1</sup>H-NMR and DMF-GPC measurements were performed on the crude aliquot to observe changes in monomer concentration to determine % conversion, molecular weight, and dispersity (Table 2.1).

**Table 2.1: Kinetic study data for homopolymer block**

<b>Time</b>	<b>conversion [%]</b>	<b>Đ</b>	<b>M<sub>n</sub> [KDa]</b>
<b>2 h</b>	11	1.9	28
<b>4 h</b>	19	1.6	41
<b>6 h</b>	26	1.5	56
<b>8 h</b>	28	1.5	61
<b>10 h</b>	34	1.4	71
<b>11 h</b>	32	1.5	65
<b>14 h</b>	48	1.5	90
<b>16 h</b>	44	1.3	98
<b>18 h</b>	44	1.4	90
<b>20 h</b>	37	1.4	85
<b>22 h</b>	46	1.4	91

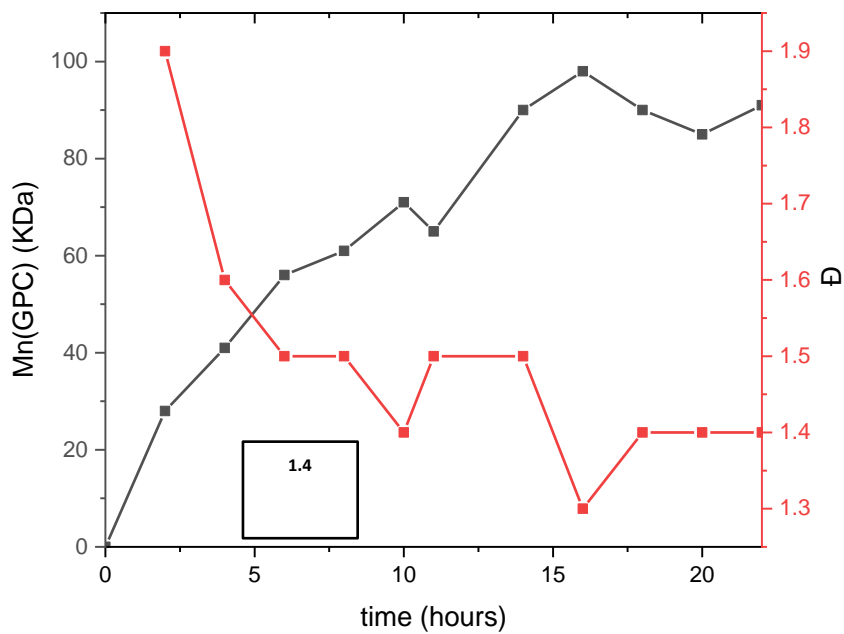
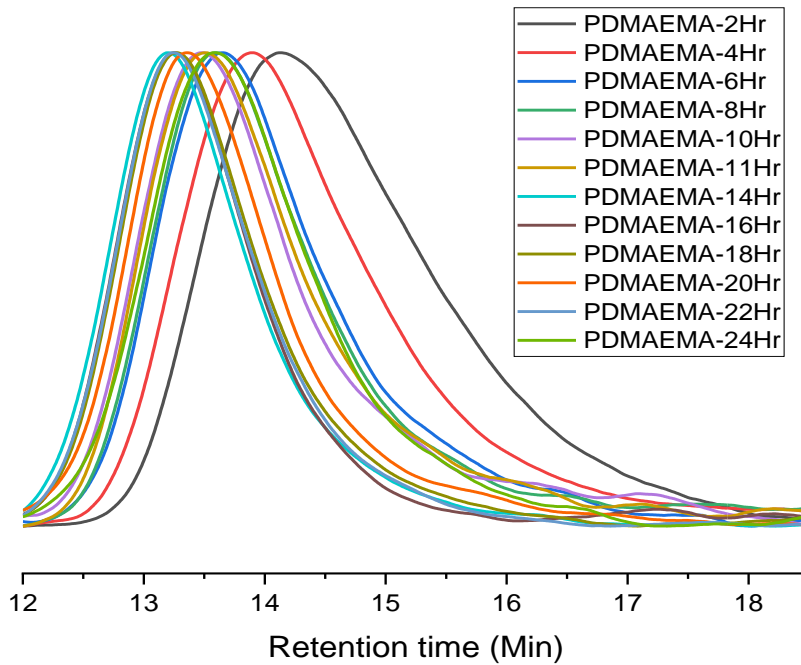


**Figure 2.1: a) GPC trace of the crude aliquot at 2hr interval b)  $M_n$  and  $\bar{D}$  plot as indicated by GPC value**

**a**

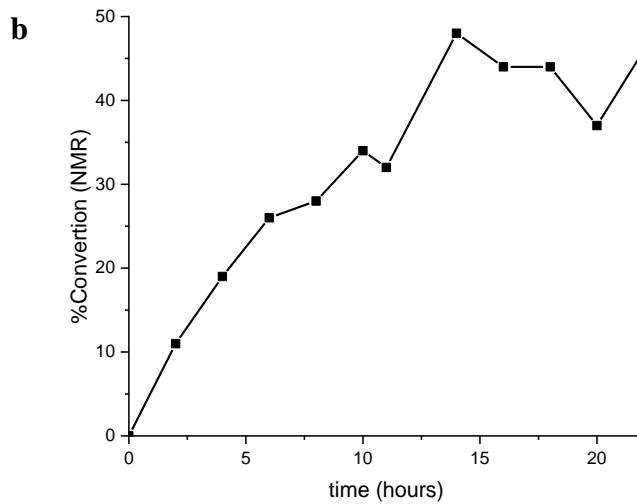
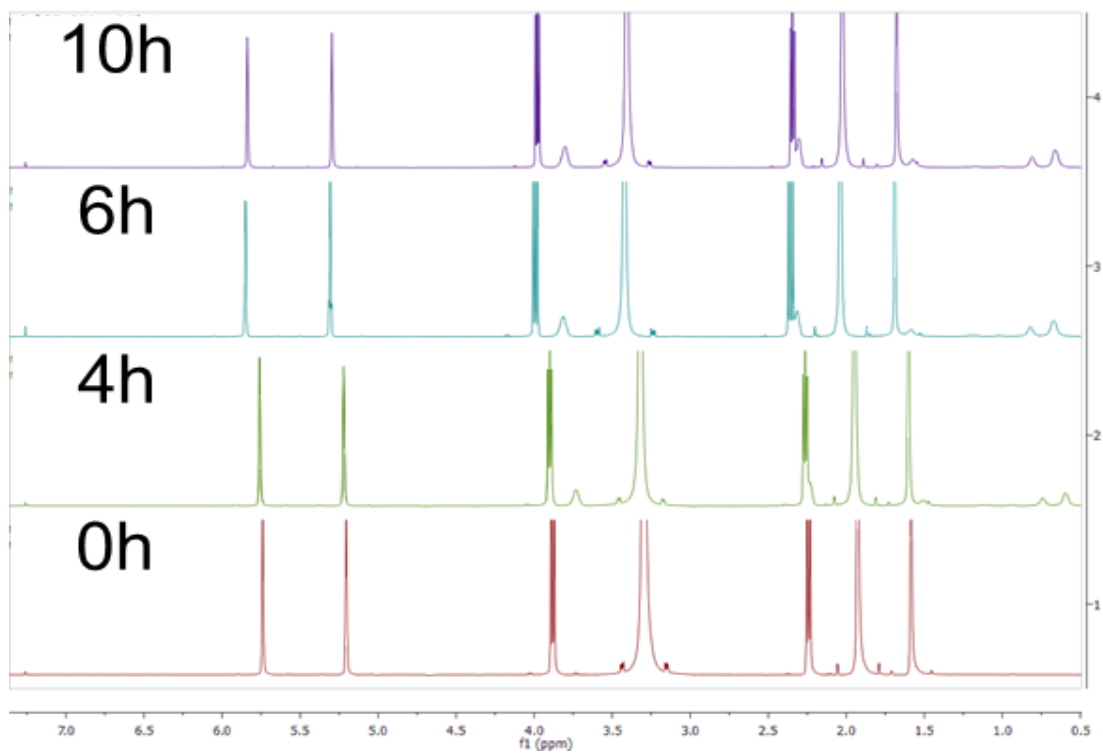
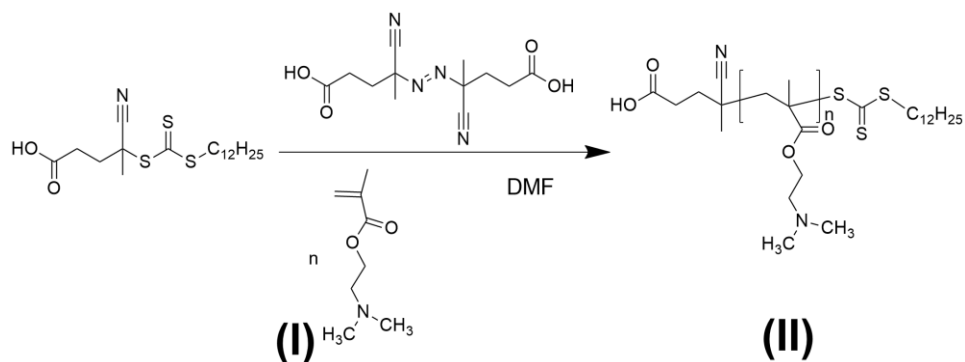


**Figure 2.2: a) <sup>1</sup>H-NMR spectra of the crude aliquot at different time interval b) % conversion plot as calculated from the unreacted monomer to polymer peak ration**

The percent conversion (Table 2.1) of the poly DMAEMA were studied through  $^1\text{H-NMR}$  by calculating the relative ratio of the methylene proton alpha to the carbonyl group of the pendant group of the unreacted monomer and polymer. This study shows a linear increase in polymer formation up to 10 h with a gradual decrease in the rate of increase of molecular weight over time (Figure 2.2). A similar trend is followed by molecular weight and as studied by DMF-GPC with PMMA standard (Figure 2.1). The overall dispersity values were low, but it gradually reduced for the first 10 h and after that it became constant. This study demonstrates that the polymerization remained controlled for the initial 10 h time period, after that the rate drops. This observation is attributed to two factors: 1) reduction is the concentration of the unreacted monomer, 2) possible nucleophilic attack of the tertiary amine on the trithiocarbonyl end-group on the CTA, terminating the chain-end. Based on this observation, the selection duration of polymerization reactions was fixed at 10 h.

### 2.3.2 Synthesis of PDMAEMA with Different Molecular Weight



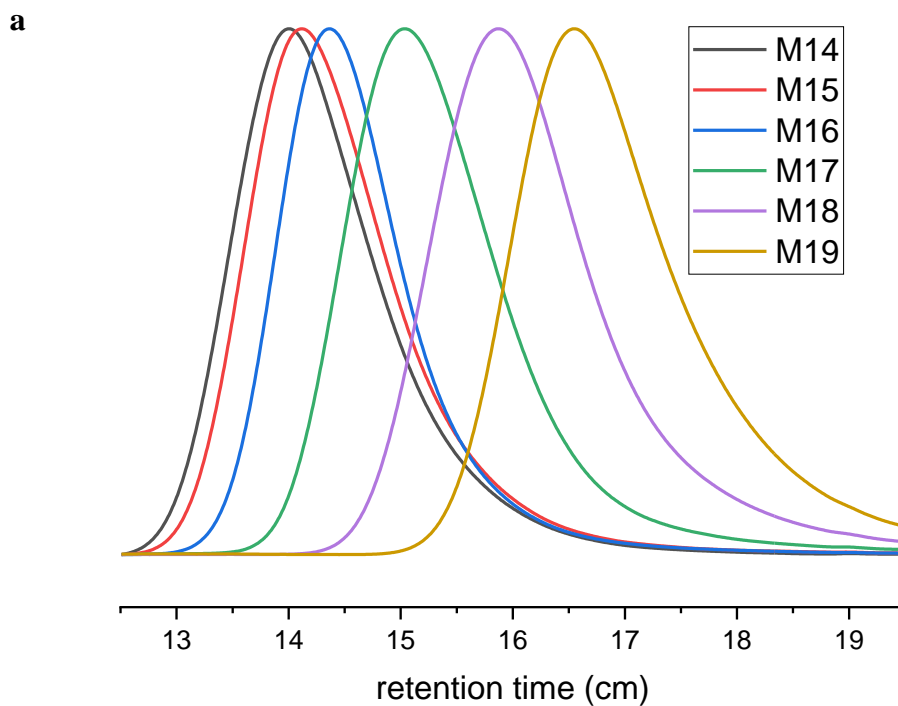
**Scheme 2.1: Homopolymerization of PDMAEMA**

The synthesis of six batches of PDMAEMA macro-CTAs with different molecular weights were performed based on the observation obtained from the kinetic study (Scheme 2.1). The CTA and initiator were first dissolved in DMF (10ml) in a 50 ml round bottom flask. The solution was purged under nitrogen for 20 min. Into the purged solution, purified DMAEMA (10ml) was added. The stock solution was kept under nitrogen flow for 10 min more to ensure complete removal of dissolved oxygen. The flask was then transferred to a stir plate pre-heated to 60 °C for 10 h. CTA and monomer concentrations ratio were varied in order to obtain different molecular weights. After 10 h the vials were quenched by exposure to air with the reaction vial chilled in an ice bath. The DMF solvent was removed by freeze drying. The resultant polymer was dissolved in THF and purified by precipitating into hexane. The samples were dried for 24 h under vacuum at 70°C. The resultant polymer was pale yellowish in color, ranging from soft and sticky to hard and brittle depending on the molecular weight.

The synthesized homopolymer series are listed (Table 2.2). The molar ratio of CTA to initiator ABCVA was 10:1, and the molecular weight of PDMAEMA block in the di-block copolymer will be controlled by adjusting the feed ratio DMAEMA monomer to CTA. The molecular weight of the homopolymers will vary between 5,000-55,000 g/mol of relative volume fraction of PDMAEMA. The DP and copolymer composition will be calculated by end-group analysis from <sup>1</sup>H-NMR and DMF-GPC. DP is chosen over  $M_n$  to report the chain length of the homopolymer.

**Table 2.2: Overview of the Synthesis and Corresponding Properties of the PDMAEMA Homopolymer Series**

Name	Target			GPC		NMR			Nomenclature
	$M_n$	DP	%conv	$M_n$	$\bar{D}$	%Conv	DP	$M_n$	
M14	55,000	359	30	46,000	1.37	26.5	317	50,000	PDMAEMA <sub>290</sub>
M15	45,000	286	30	41,000	1.35	28.7	277	43,500	PDMAEMA <sub>260</sub>
M16	30,000	191	30	35,000	1.31	49.6	315	50,000	PDMAEMA <sub>223</sub>
M17	20,000	127	30	17,000	1.41	42.6	178	28,000	PDMAEMA <sub>110</sub>
M18	10,000	64	30	10,000	1.34	48.2	102	16,000	PDMAEMA <sub>64</sub>
M19	5,000	32	30	4,000	1.41	70	74	10,000	PDMAEMA <sub>25</sub>



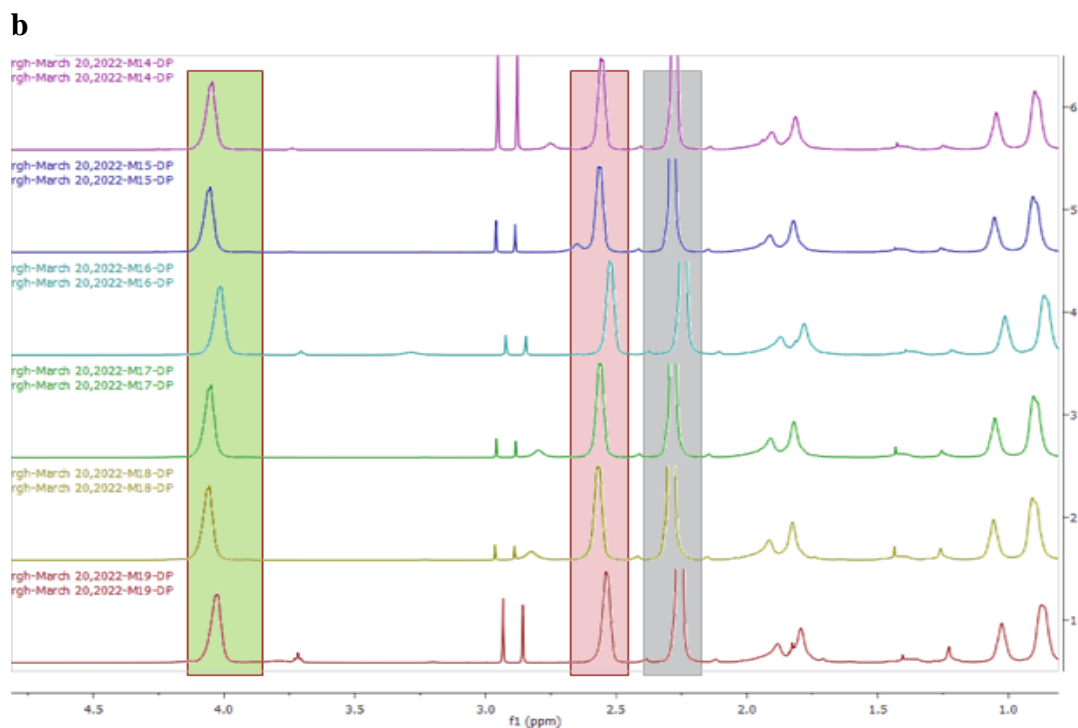


**Figure 2.3: a) DMF-GPC Trace b) $^1\text{H-NMR}$  spectra of DMAEMA homopolymer**

The percent conversion of the poly DMAEMA was studied through  $^1\text{H-NMR}$  by calculating the relative ratio of the methylene proton alpha to the carbonyl group of the pendant group of the unreacted monomer and polymer. The analysis shows that with an increase in the targeted molecular weight, the percent conversion of monomer decreases. For higher targeted molecular weights, the monomer to CTA ratio is high (figure 2.3). The CTA added could not polymerize a large amount of monomer within the selected 10 h reaction time leading to lower overall monomer conversion. According to DMF GPC the dispersity was low, and a monotonic increase in molecular weight was observed with higher targeted molecular weight (figure 2.2). A tailing was observed near the lower molecular weight regime, more prominently for lower molecular weight due to column

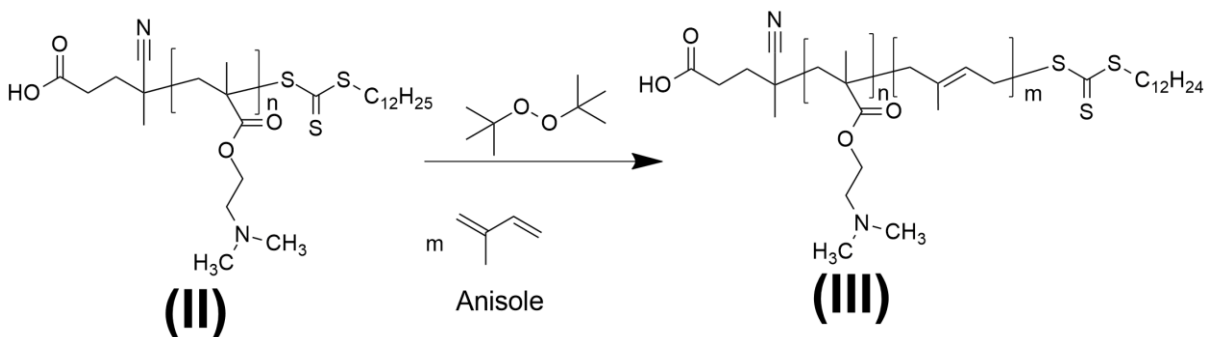
interaction between DMF-GPC column and tertiary amine group of the polymer pendant group.

PDMAEMA with six different molecular weights were synthesized successfully. After characterizing these six batches, they were ready for chain extension to make the parent amphiphilic diblock copolymer system.

## 2.4 Chain Extension of PDMAEMA with Different Hydrophobic block

### 2.4.1 Chain Extension with Polyisoprene

The macroCTA (II) (CTA-PDMAEMA) was used for chain extension reaction with isoprene (III) (Scheme 2.2). To mediate the slow polymerization rate of isoprene, the reaction was performed at higher temperature, 125°C and di-tert butyl peroxide (DTBPO) was chosen as initiator for its elongated half-life at 120°C. Polymerization reactions were performed under N<sub>2</sub> using thick walled Schlenk tubes after 3-4 cycles of freeze-pump-thaw. The reaction was performed at 125°C for 17 h. The polymer was dried under vacuum for 48 hours to remove any unreacted monomer.



**Scheme 2.2: Chain Extension with Isoprene**



From the  $^1\text{H}$  NMR spectra (Figure 2.4) a successful synthesis of polyisoprene was observed, but it was not sufficient to confirm whether block copolymer or a mixture of homopolymers were synthesized. The copolymer was not soluble in DMF, and thus we were not able to perform DMF-GPC. For THF-GPC due to column interaction with the tertiary amine of the pendent group, performing GPC to detect the dispersity of the polymer chain was beyond the scope of the instrumentation.

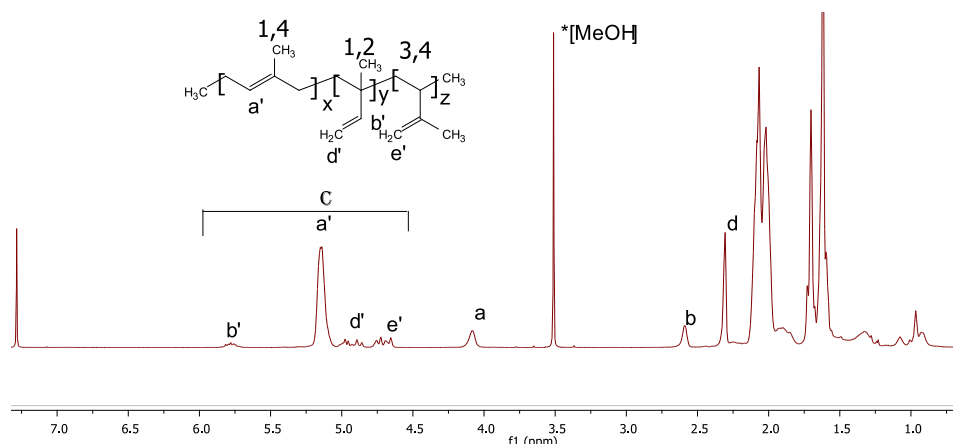
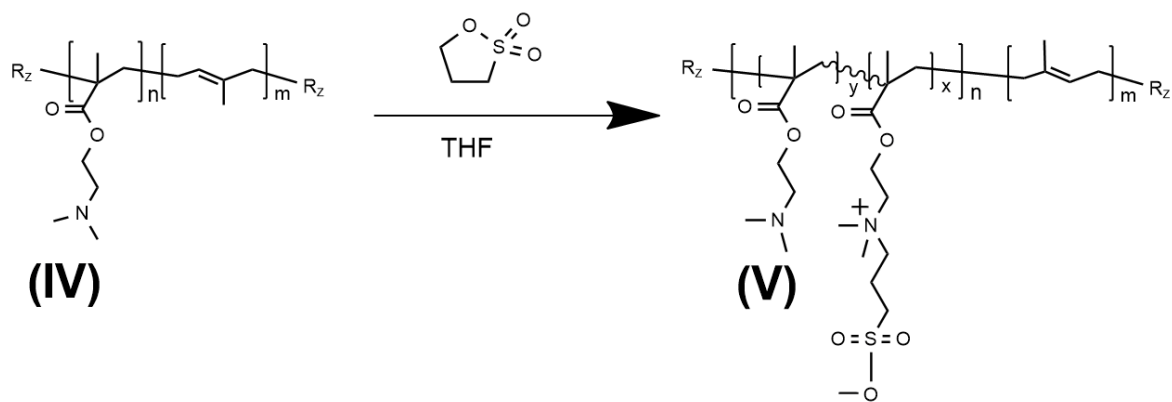
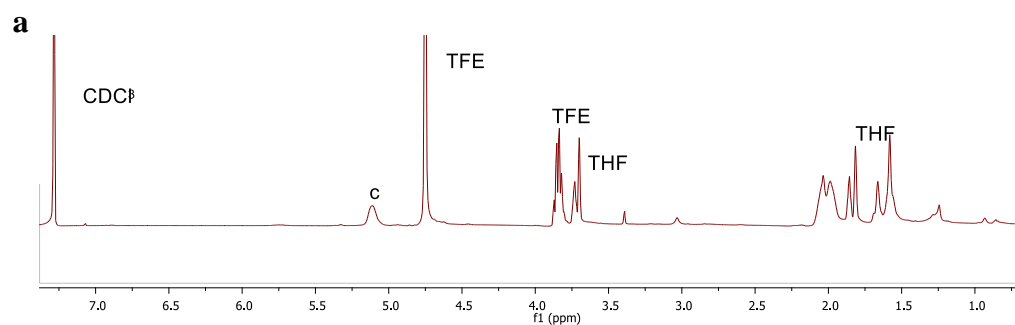


**Figure 2.4:**  $^1\text{H}$ -NMR of PDMAEMA-b-PI

Post polymerization modification of the synthesized polymer was performed by nucleophilic ring-opening of 1,3-propane sultone (Scheme 2.3). After 24 hours, the modified polymer became insoluble in any organic solvent at room temperature.  $^1\text{H}$ -NMR (figure 2.5) shows no peak visible for sulfobetaine proving that the zwitterionic portion is not going in the solution. This led to difficulty in measurement of percent zwitterion formation. This incompatibility with any organic solvent led to difficulty in characterization as well as future processing of this block copolymer.



**Scheme 2.3: Post-polymerization Modification of PDMAEMA-*b*-PI by 1,3-Propane Sultone**



**b**



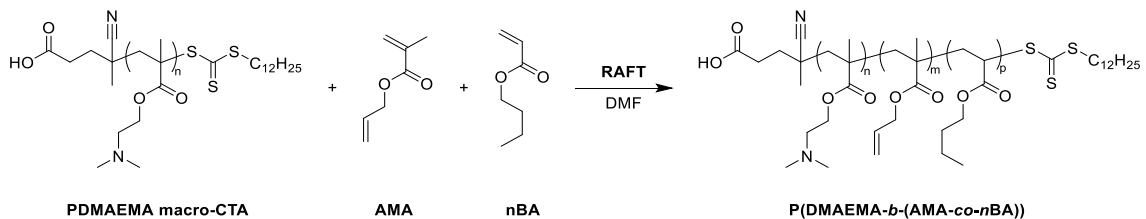
**Figure 2.5:a) <sup>1</sup>H-NMR Spectra of PSBMA-PI b) Solubility of PDMAEMA-*b*-PI vs PSBMA-*b*-PI in TFE**

#### 2.4.2 Chain Extension with Poly Allyl Acrylate

Chain extension of PDMAEMA was performed with allyl acrylate under nitrogen atmosphere at 60°C. Macro CTA and initiator ABCVA were dissolved in DMF (10 ml) in 50 ml round bottom flasks. The solutions were purged under nitrogen for 20 min. In the purged solutions, allyl acrylate was added. The stock solution is kept under nitrogen flow for 10 min more to ensure complete removal of dissolved oxygen. The flasks were then transferred to a stir plate pre heated to 60°C. After 1 h the reaction gelled into a solid mass which was insoluble in any solvent. Allyl acrylate has two radical generating sites. The vinylic group is more active than the allyl group. So in the initial phase radicals were being generated in the vinylic site leading to incorporation of allyl acrylate at the chain-end. With the reduction in allyl acrylate monomer concentration, there is a reduction in vinylic group and increase in pendant allyl group which started contributing to generating free radical reactive sites. These radical generating sites lead to crosslinking of the di-block copolymer resulting in gelation.

The use of allyl acrylate comonomer was then substituted by a mixture of *n*-butyl acrylate and allyl methacrylate with the feed ratio of *n*-butyl acrylate : allyl methacrylate as 19 : 1 to reduce pendant allylic group concentration in the polymer backbone (scheme 2.4). In this way the hydrophobic block still retains its low  $T_g$ , rubbery phase along with having allyl pendant group providing the possibility for future controlled crosslinking. Chain extension of the DMAEMA macro CTA using the mixture of *n*-butyl acrylate and allyl methacrylate in an equal volume of DMF resulting in the formation of a copolymer that was soluble in DMF after 1 h or reaction time. In <sup>1</sup>H-NMR peaks for both hydrophobic and hydrophilic block can be visible (Figure 2.6). Analysis of the resulting copolymer in

DMF GPC with the crude aliquot shows multimodal peak at higher molecular weight region showing crosslinking is still occurring but at slow rate (figure 2.6a).



**scheme 2.4: Chain extension via random mixture of n-butyl acrylate and allyl methacrylate**

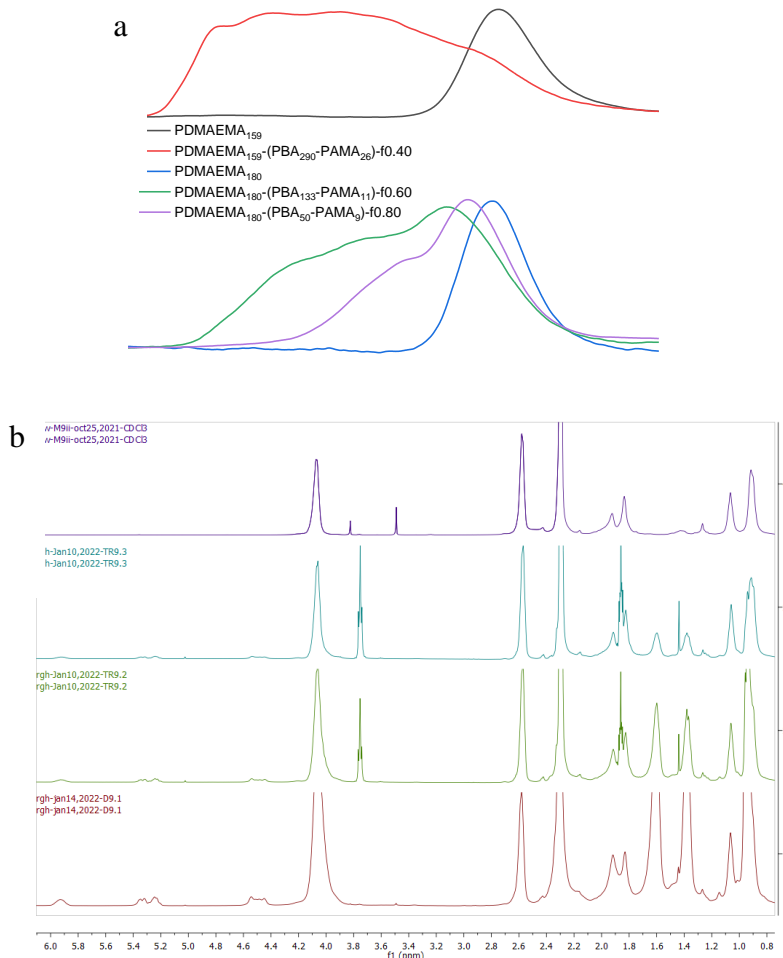


**Figure 2.6: a) DMF-GPC Trace b) 1H-NMR spectra of block copolymer**

The procedure was repeated in 4 times excess DMF as compared to comonomer volume. The polymers synthesized remain soluble in DMF even after 24 hours. We then proceeded for kinetic study to set the time required to achieve a polymer with no significant crosslinking.

### **2.4.3 Kinetic Study for Synthesis of Poly[(dimethyl aminoethyl methacrylate)-*b*-(*n*-butyl acrylate-*ran*-allyl methacrylate)]**

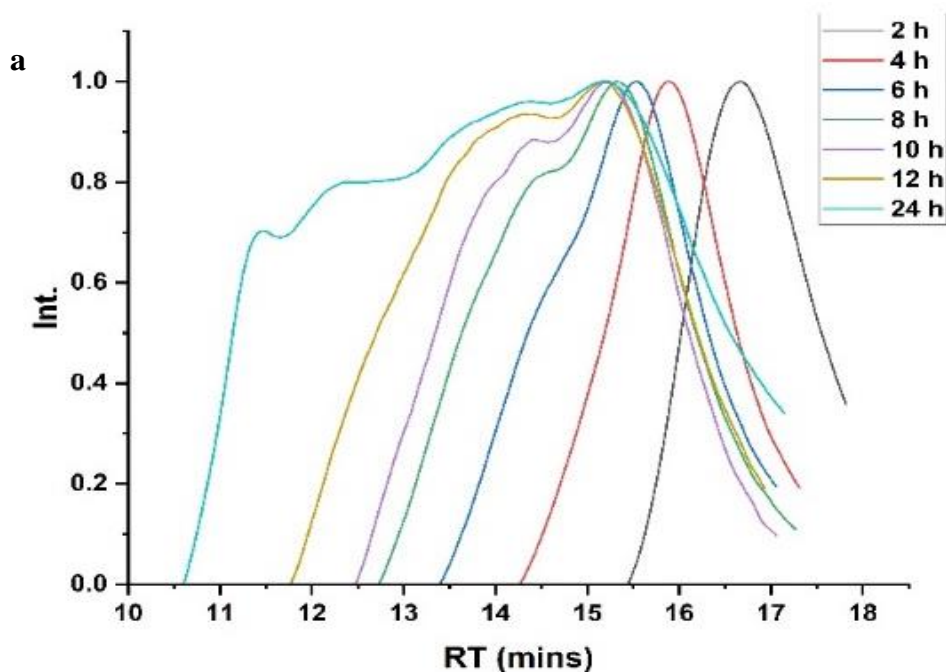
A kinetic study of the chain extension of poly DMAEMA hydrophobic block (HyphB) has been performed to study the reaction time required to achieve a diblock copolymer with targeted volume fraction and low dispersity. Purified PDMAEMA from previously described steps were used as macro CTAs. The initiator 4,4'-Azobis (4-cyanovaleric acid) (ABCVA) are purchased from Sigma Aldrich. Monomers (*n*-butyl acrylate and allyl methacrylate) and solvent (DMF, anhydrous 99.8%) were purchased from Alfa Aesar. The monomers are purified by passing through alumina column to remove inhibitors. The rest of the reagents were used without further purification

Chain extension of poly DMAEMA was performed under nitrogen atmosphere at 60°C. The prescribed amounts of macro CTA and initiator are dissolved in DMF (10 ml) in a 50 ml round bottom flask. The solution was purged under nitrogen for 20 min. In the purged solution, purified *n*-butyl acrylate (10 ml) and allyl methacrylate were added. The stock solution was kept under nitrogen flow for a further 10 min to ensure complete removal of dissolved oxygen. The flask was then transferred to a stir plate pre-heated to 60 °C. An aliquot of 0.5 ml of the reaction mixture was removed with a nitrogen flushed syringe every 2 hours. <sup>1</sup>H-NMR and DMF-GPC were performed on the crude aliquot to

observe change in percent conversion of monomer, molecular weight and dispersity (Table 2.3).

**Table 2.3: Kinetic study of synthesis of PDMAEMA-b-P(BA-ran-AMA)**

time	DMF-GPC				<sup>1</sup> H-NMR						
	PDMAEMA	Di-Block Copolymer			PBA		PAMA		Di-Block Copolymer		
	D.P.	M <sub>n</sub> [g/mol]	M <sub>w</sub> [g/mol]	Đ	D.P.	conversion [%]	D.P.	conversion [%]	conversion (monomer signal) [%]	M <sub>n</sub> [g/mol]	
0 h	40	800	1,000	1.3	0	0	0	0	0	0	
2 h	40	4,100	5,400	1.3	42	29	2	75	27	11,800	
4 h	40	8,600	12,900	1.5	76	53	5	93	49	16,500	
6 h	40	13,400	24,700	1.8	105	66	8	93	64	20,600	
8 h	40	15,600	39,300	2.5	103	76	8	93	73	20,400	
10 h	40	18,000	52,300	2.9	128	80	8	93	80	23,600	
12 h	40	22,000	81,600	3.7	151	85	8	93	83	26,500	
22 h	40	23,300	192,700	8.3	142	93	8	93	92	25,400	



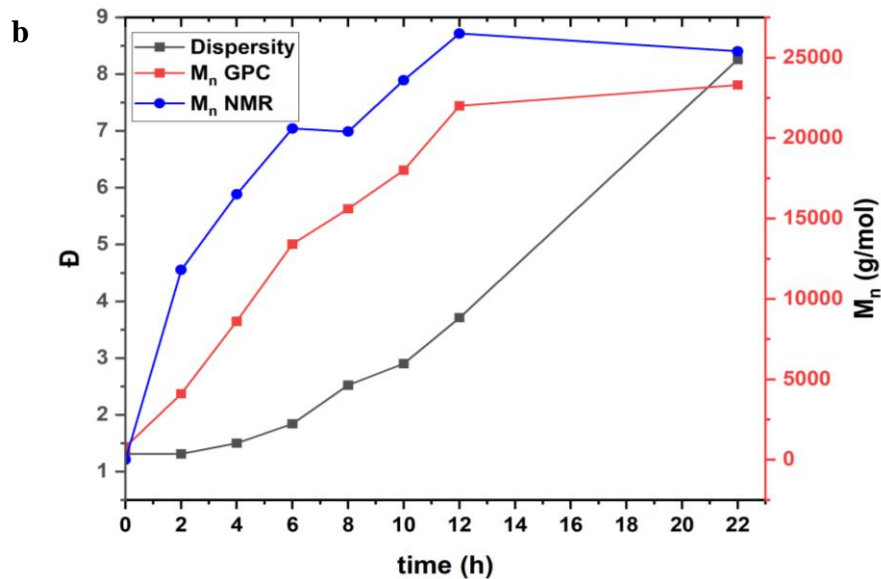
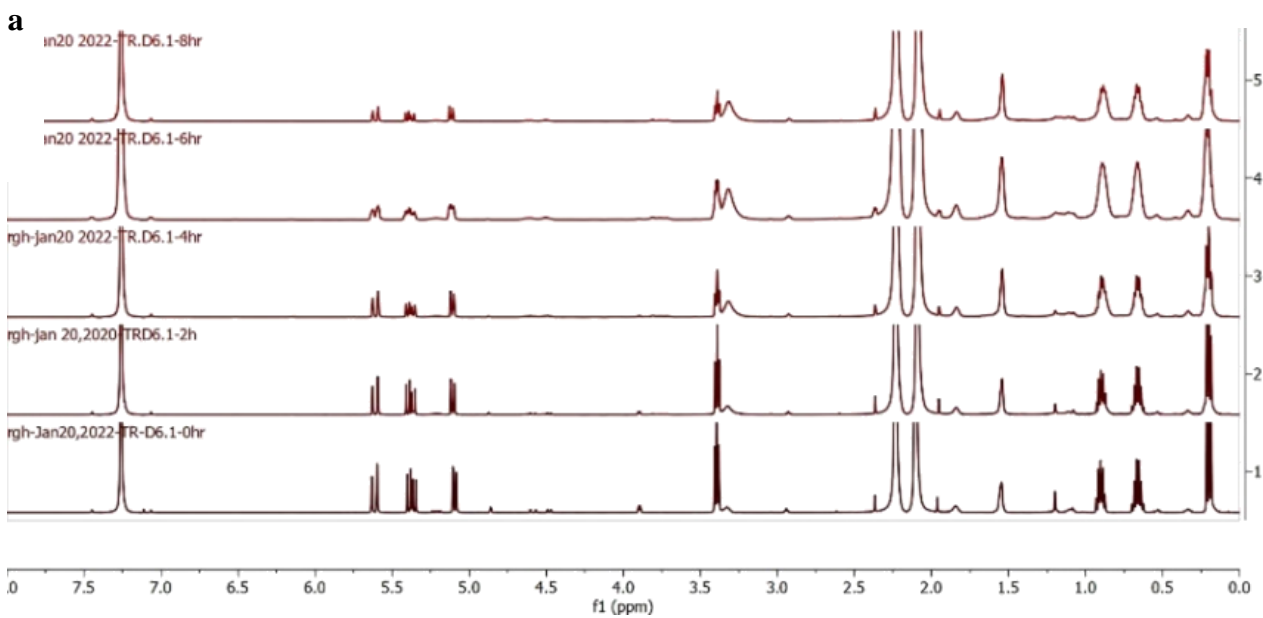
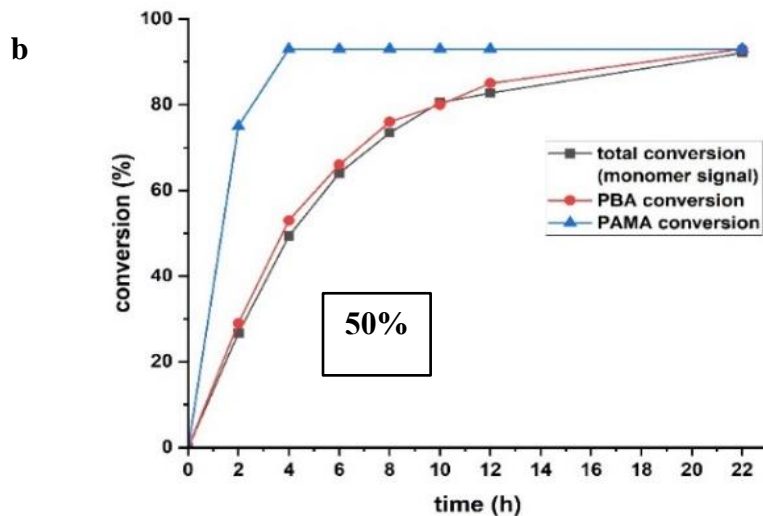


Figure 2.7: a) GPC trace of the crude aliquot at 2 h interval b)  $M_n$  and  $\bar{D}$  plot as indicated by GPC value





**Figure 2.8: a)  $^1\text{H-NMR}$  spectra of the crude aliquot at different time interval b) percent conversion plot as calculated from the unreacted monomer to polymer**

The percent conversion of the *n*-butyl acrylate and allyl methacrylate were studied through  $^1\text{H-NMR}$  by calculating relative ratios of the methylene proton alpha to the carbonyl group of the pendant group of the unreacted monomers and polymer (Figure 2.8 a). Butyl acrylate exhibits a linear increase in percent conversion for an initial 4 h with gradual reduction in rate of increase in percent conversion. For allyl acrylate, the rate of increase in percent conversion is high and reaches almost 95% in the initial 4 h, after which it becomes constant due to a very low monomer concentration (Figure 2.8 b). The analysis by DMF-GPC with PMMA standard shows a gradual increase in molecular weight up to 4 h with gradual decrease in the rate of increase over time whereas the opposite trend is followed by dispersity as studied (Figure 2.7 b). The overall dispersity was initially low then it increases exponentially after 4 hrs. The GPC chromatogram also shows an appearance of a shoulder at higher molecular weight (Figure 2.7 a). This observation can be attributed to the fact that initially the vinyl unit of the allyl methacrylate were reacting with the chain-end of the macro CTA, but with the reduction of the monomer



concentration, radical generation begins to happen from the allyl group resulting in branching and crosslinking of the pendent sidechains. Based on this observation, the duration of the polymerization reaction was fixed at 4 h.

#### **2.4.4 Synthesis of Poly[(dimethyl aminoethyl methacrylate)-*b*-(*n*-butyl acrylate-*ran*-allyl methacrylate)] with Different Volume Fraction**

Chain extension of PDMAEMA to target different molecular weight copolymers were performed under nitrogen atmosphere at 60 °C for 4 h. The macro CTAs with six different molecular weights and the initiator were dissolved in DMF (10 ml) in separate 50 ml round bottom flasks. Different volume fractions were targeted by changing the ratio of macro CTA and comonomers feed ratios. The solutions were purged under nitrogen for 20 min. In the purged solutions, purified *n*-butyl acrylate (10 ml) and allyl methacrylate were added. The stock solutions were kept under nitrogen flow for a further 10 min to ensure complete removal of dissolved oxygen. The flasks were then transferred to a stir plate pre-heated to 60°C. After 4 h the reactions were quenched by exposing to air in the vials that were chilled to an ice-cold temperature. The DMF was removed by freeze drying and the copolymers were dissolved in THF and purified by precipitating in hexane. The isolated copolymers were dried under vacuum for 24 h under room temperature.

The synthesized copolymer series are listed (Table 2.4). The molar ratio of macro-CTA to initiator (DTBPO) was 10:1, and the chemical composition of the (*n*-butyl acrylate-*ran*-allyl methacrylate) and PDMAEMA block in the diblock copolymer was controlled by adjusting the feed ratio of comonomer and PDMAEMA. The composition of the copolymers varied between 0.10-0.65 of relative volume fraction of PDMAEMA.

The chain-ends of the macro CTA were active and successfully chain extended without any noticeable dead chains observed at the lower molecular weight region in GPC (Figure 2.9a). From the DMF-GPC trace molecular weight of each block copolymer and their respective volume fractions can be calculated (Table 2.4). <sup>1</sup>H-NMR spectra (Figure 2.9b) were recorded using CDCl<sub>3</sub> as solvent to calculate the molar ratio of each block in the copolymer (Table 2.5). Batch 16 shows that the ratio between *n*-butyl acrylate and allyl acrylate is high. The dispersity of the batch is also higher than the rest. This observation can be attributed to the fact that premature crosslinking started in the allyl pendant group resulting in higher composition of *n*-butyl acrylate as compared to allyl methacrylate.

**Table 2.4: Overview of the Synthesis and Corresponding Properties of the PDMAEMA-*b*-P(BA-AMA) Series as Indicated by GPC**

Name	f <sub>PDMAEMA</sub>	GPC(M)		GPC(D)		Nomenclature
		M <sub>n</sub>	Đ	M <sub>n</sub>	Đ	
14	.66	46,000	1.37	70,200	1.34	PDMAEMA <sub>290</sub> - <i>b</i> -P(BA- <i>ran</i> - <sup>5%</sup> AMA) <sub>185</sub> - <sup>f</sup> 0.66
15	.69	41,000	1.35	60,100	1.36	PDMAEMA <sub>260</sub> - <i>b</i> -P(BA- <i>ran</i> - <sup>5%</sup> AMA) <sub>150</sub> - <sup>f</sup> 0.69
16	.47	35,000	1.31	75,300	1.70	PDMAEMA <sub>223</sub> - <i>b</i> -P(BA- <i>ran</i> - <sup>5%</sup> AMA) <sub>312</sub> - <sup>f</sup> 0.47
17	.22	17,000	1.41	78,400	1.37	PDMAEMA <sub>110</sub> - <i>b</i> -P(BA- <i>ran</i> - <sup>5%</sup> AMA) <sub>480</sub> - <sup>f</sup> 0.22
18	.18	10,000	1.34	56,300	1.34	PDMAEMA <sub>94</sub> - <i>b</i> -P(BA- <i>ran</i> - <sup>5%</sup> AMA) <sub>360</sub> - <sup>f</sup> 0.18
19	.10	4,000	1.41	37,900	1.35	PDMAEMA <sub>25</sub> - <i>b</i> -P(BA- <i>ran</i> - <sup>5%</sup> AMA) <sub>265</sub> - <sup>f</sup> 0.10

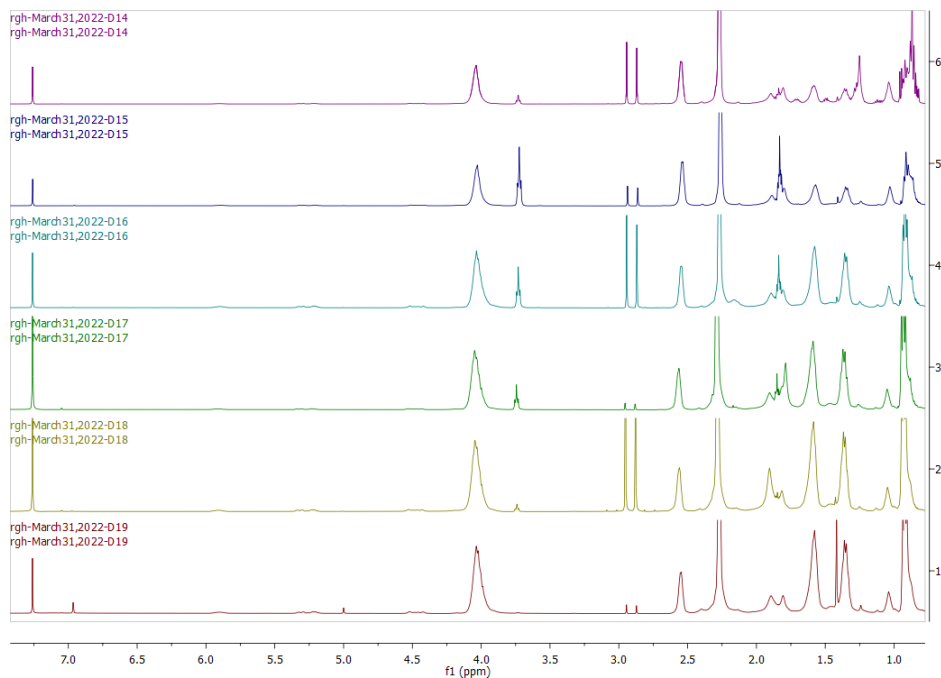
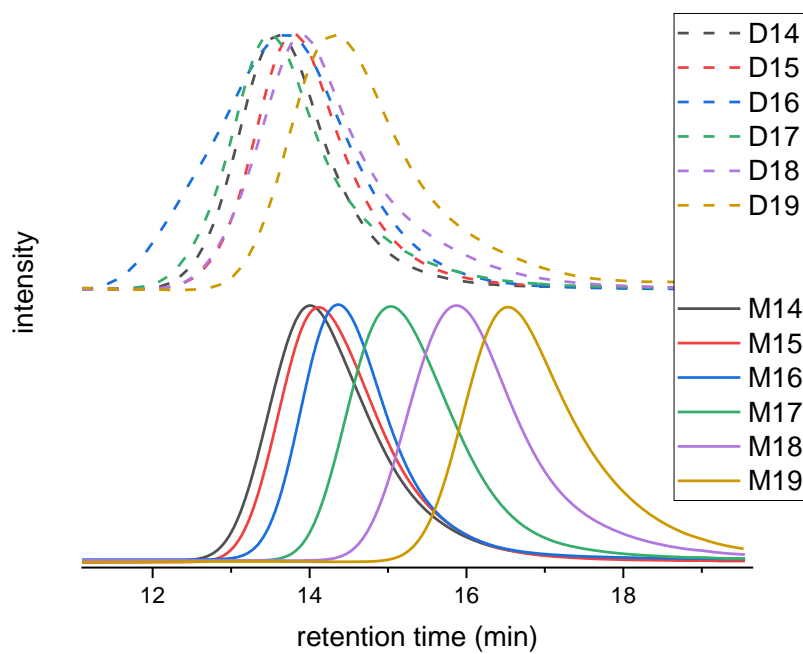


**Figure 2.9: : a) DMF-GPC Trace b) <sup>1</sup>H-NMR spectra of parent block copolymer**

**Table 2.5: Overview of the Synthesis and Corresponding Properties of the PDMAEMA-*b*-P(BA-AMA) Series as Indicated by NMR**

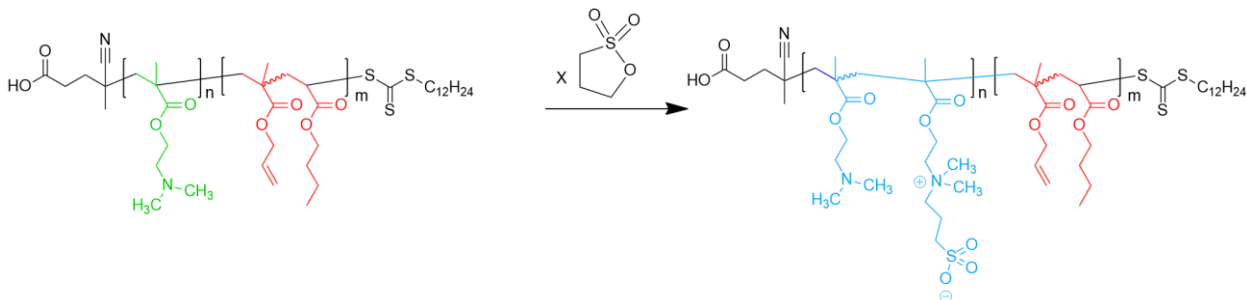
Name	$f_{\text{PDMAEMA}}$	PDMAEMA (M)		PBA		PAMA		Name	PDMAEMA	PBA	PAMA
		DP	$M_n$	DP	$M_n$	DP	$M_n$				
14	0.78	317	50,000	114	14,600	15	2,000	14	21	7.6	1
15	0.76	277	43,500	110	14,100	15	2,000	15	18	7.3	1
16	0.45	315	50,000	497	63,700	22	3,000	16	14	23	1
17	0.43	178	28,000	297	38,100	22	3,000	17	8.1	14	1
18	0.39	102	16,000	204	26,100	22	3,000	18	4.6	9.3	1
19	0.34	74	10,000	157	20,100	22	3,000	19	3.4	7.1	1

## 2.5 Post Polymerization Modification with Different Heterocyclic Rings

### 2.5.1 Ring-Opening of 1,3-Propane Sultone

A series of A-Z copolymers have been synthesized by ring-opening of 1,3-propane sultone using the previously synthesized parent copolymer PDMAEMA-*b*-P(*n*-BA-*ran*-AMA) copolymers. A typical synthetic procedure was as follows, the copolymers (1 gm) and .5 and 1 equivalent 1,3-propane sultone as compared with the PDMAEMA monomer calculated by NMR were dissolved in tetrahydrofuran (THF) (12 ml), and stirred vigorously for 24 h at room temperature (Scheme 2.5).<sup>1</sup> At the end of the reaction time the polymer appeared as transparent solid gel. The gel was then dissolved in TFE and precipitated into toluene to remove any excess 1,3-propane sultone. From each parent copolymer synthesized, three different A-Z copolymers were synthesized with targeted

30%, 50%, and 100% molar fraction of the heterocyclic ring relative to the DP of DMAEMA.



**scheme 2.5: Post polymerization modification of parent diblock polymer via nucleophilic ring opening of 1,3-propane sultone**

**Table 2.6: Percent quaternization as indicated by NMR**

$D_{290}$ -(HyPhb) <sub>187</sub> <sup>f</sup> -0.66 (14)			$D_{223}$ -(HyPhb) <sub>312</sub> <sup>f</sup> -0.47 (16)			$D_{110}$ -(HyPhB) <sub>480</sub> <sup>f</sup> -0.22 (17)			$D_{25}$ -(HyPhB) <sub>265</sub> <sup>f</sup> -0.10 (19)		
Targeted % Quaternization			Targeted % Quaternization			Targeted % Quaternization			Targeted % Quaternization		
30	50	100	30	50	100	30	50	100	30	50	100
Experimental % Quaternization (x)			Experimental % Quaternization (x)			Experimental % Quaternization (x)			Experimental % Quaternization (x)		
27	40	100	30	54	100	25	35	100	17	35	100

The <sup>1</sup>H-NMR spectrum using TFE-*d*<sub>2</sub> solvent (Figure 2.10.) reveals the distinct peak of the poly sulfobetaine methacrylate. Due to presence of neighboring positive and negative charge a chemical shift of the proton peaks alpha to ester bond and tertiary amine group has been shifted. From the ratio of the proton peaks appearing at δ 3 ppm (methyl proton attached to quaternary ammonium ion), δ 3.75 ppm (methylene proton alpha to the

sulfonate group) and  $\delta$  2.5 ppm (methylene proton alpha to the tertiary amine of the unreacted pendant group) % quaternization was calculated (Table 2.6)

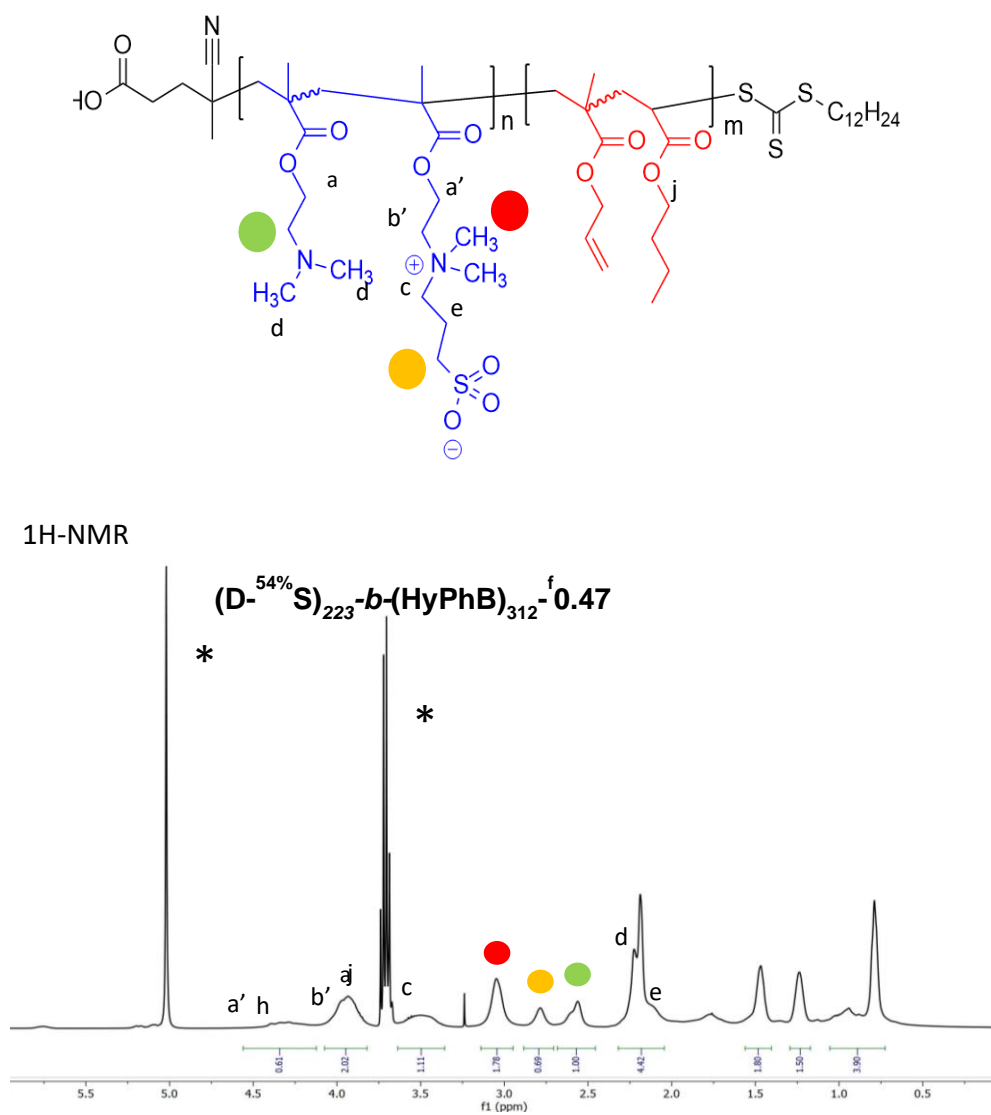


**Figure 2.10: Representative NMR of A-Z block copolymer with 54% of quaternization**

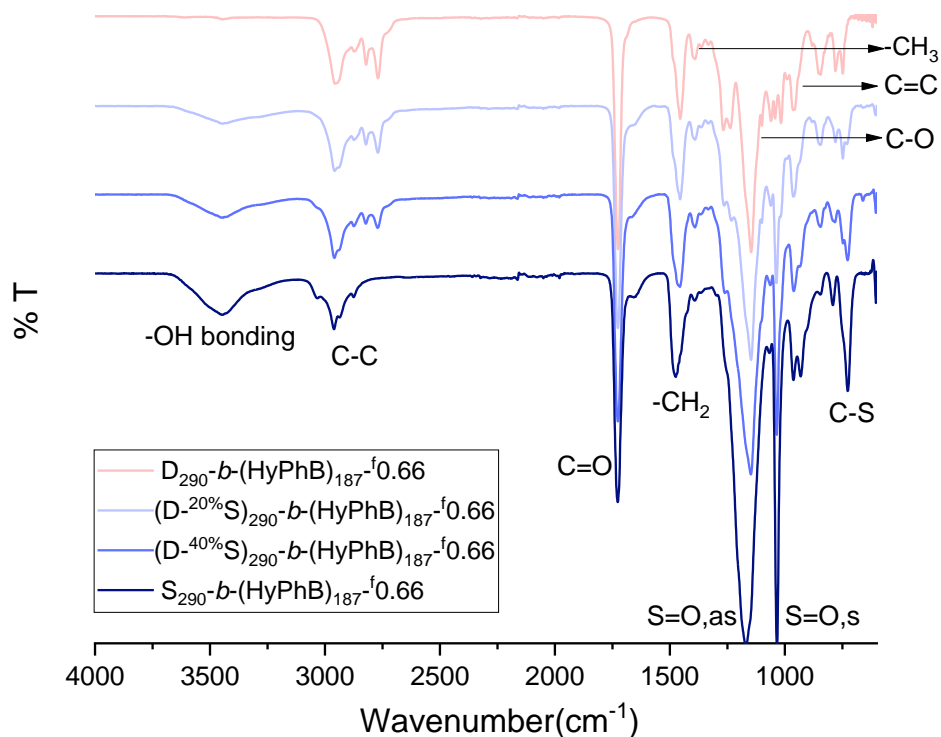


**Figure 2.11: FTIR analysis of the A-Z block copolymer with different percentage quaternization as compared with the parent block copolymer**

FTIR analysis of the A-Z block copolymer with different percentage quaternization as compared with the parent block copolymer were done (Figure 2.11). With the increase in the percent quaternization as indicated by  $^1\text{H-NMR}$  there is also an increase in S=O asymmetric and symmetric stretching bands indicating successful quaternization was. Corresponding to an increase in the percent quaternization, there was also an increase in

bound water peak indicating that the polymer becomes inherently more hygroscopic with the increase in zwitterionic content.

TGA analysis (Figure 2.12) of the polymers were also performed to study the thermal stability of the zwitterions as compared with that of the parent block copolymer. For the parent block copolymers the first degradation temperature was observed at 150°C which is due to the mass loss of bound water. A second degradation step is due to the tertiary amine group and the last degradation is due to the fragmentation of the polymer backbone. With the increase in PDMAEMA volume fraction bound water weight loss and weight loss due to tertiary amine group increases. With the increase in percent quaternization the first mass loss temperature increases as the bound water becomes more tightly bound due to the presence of zwitterionic charges. For 100% quaternized A-Z block copolymer the first degradation temperature is much higher and the mass loss at the higher temperature is greater than the parent block. This analysis showed that the A-Z block copolymers synthesized are thermally stable within the operating temperature range explored.

DSC (Figure 2.13) analysis of the polymers were performed to probe the glass transition temperature of the A-Z block copolymer as compared to its parent block copolymer. In the parent block copolymer, characteristic  $T_g$  of *n*-butyl acrylate appears around -55°C and that of PDMAEMA comes around 117°C. According to literature,  $T_g$  of SBMA is around 200°C in rapid DSC analysis with a 2000 K/min heating rate. The high  $T_g$  of PSBMA is due to the strong cohesive attraction between the positive and negative charges present in the polymer pendant group. In the block copolymer due to the presence of a low  $T_g$  rubbery domain on *n*-butyl acrylate, the  $T_g$  of the PSBMA appears at lower



temperature. At the same time, the  $T_g$  of n-butyl acrylate disappears with the increase in zwitterionic content.

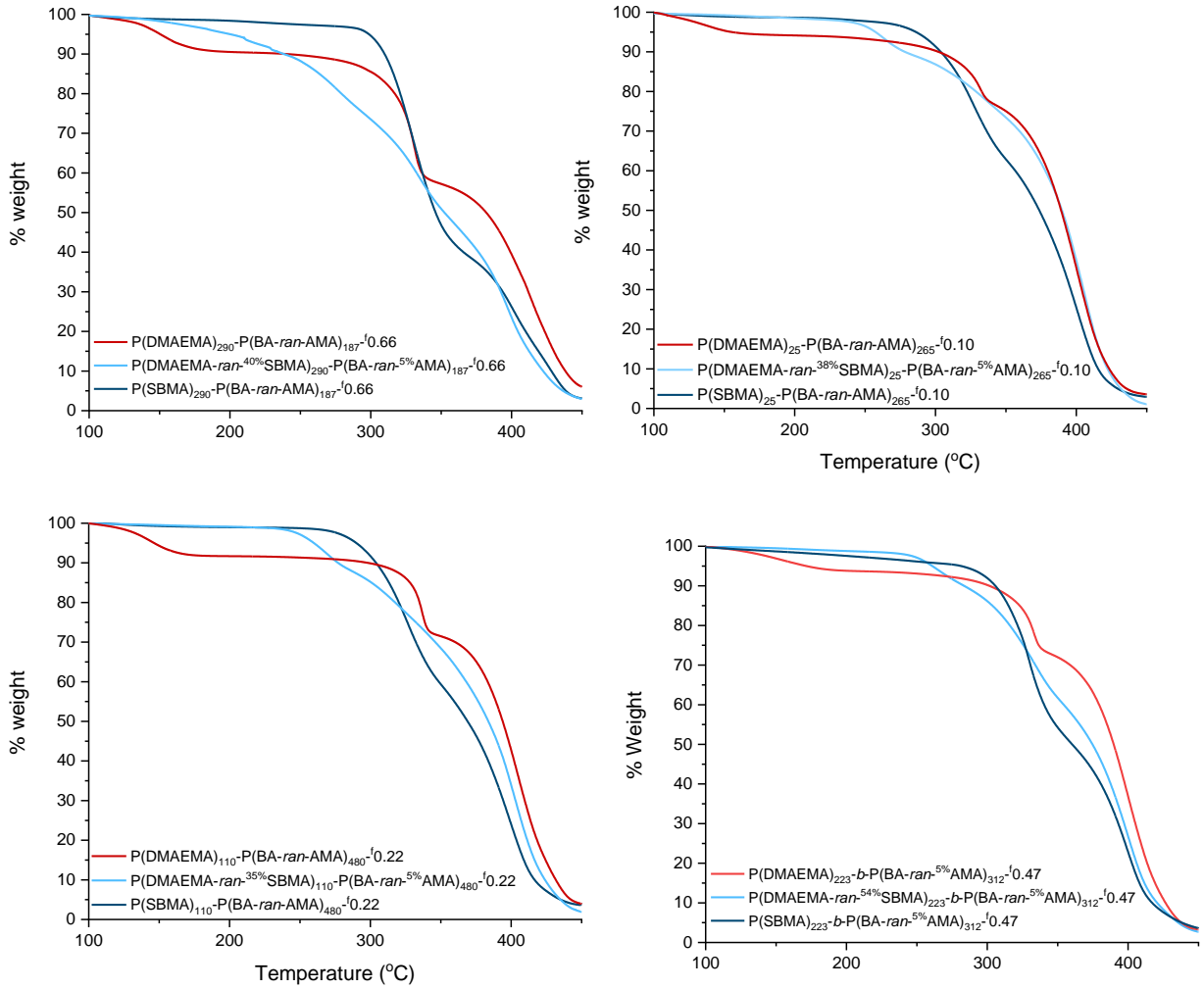


**Figure 2.12: TGA analysis of the A-Z block copolymer as compared with that of the parent block copolymer**

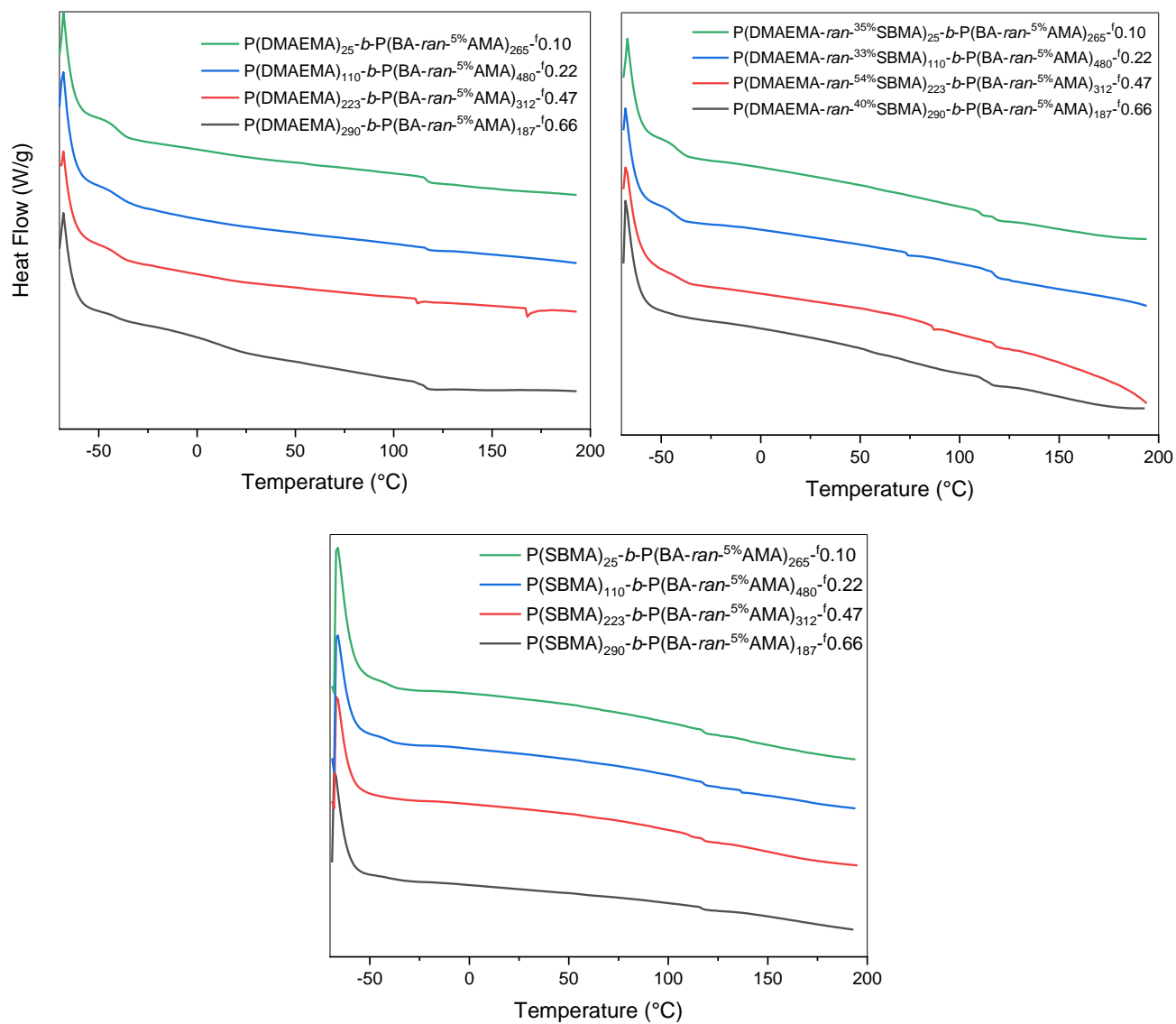


**Figure 2.13: DSC analysis of the A-Z block copolymer as compared with that of the parent block copolymer**

## 2.5.2 Ring-Opening of n-Butyl Substituted Phospholane Ring

### 2.5.2.1 Synthesis of n-Butyl Substituted Phospholane ring

The ring-opening reaction with the phospholane was anticipated to be more challenging than the either sultones or lactones. Reaction of tertiary amines with the phospholane ring shows a competitive pathway to the formation of quaternary ammonium and phosphate salts over the production of zwitterionic moieties (Figure 2.14). This pathway to the formation of phosphate salt becomes prominent and is difficult to separate from the desired zwitterion ionic product in the case of methyl/ethyl/propyl substituted phospholanes. With the increase in the number carbons in the phospholane ring, the ring-opening step becomes more facile to provide a zwitterionic moiety, but the hydrophilicity of the zwitterion decreases accordingly. N-Butyl substituted phospholane shows an optimization between the ring-opening step and hydrophilicity of the produced zwitterionic moiety.<sup>2</sup>

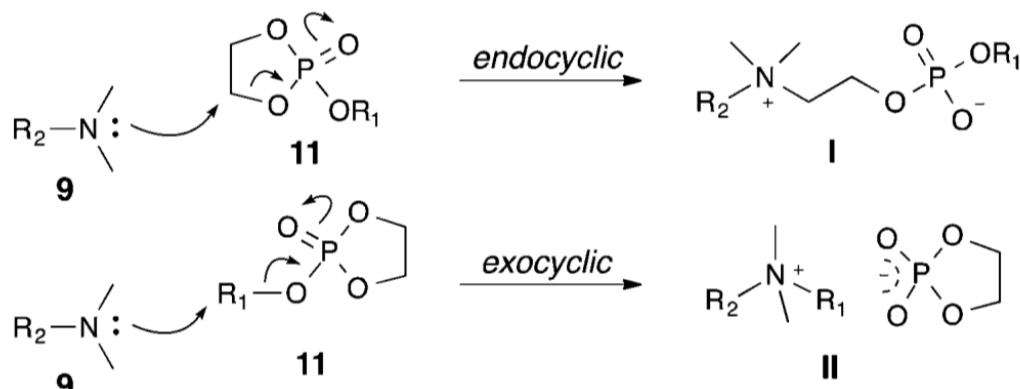
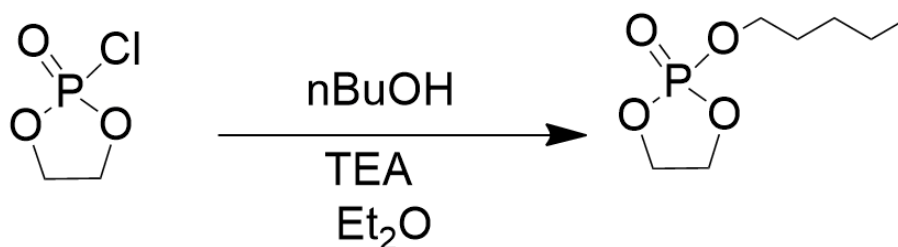


**Figure 2.14: Competitive reaction pathway in the reaction of tertiary amine and alkyl substituted phospholane. Image taken from reference 2**

2-Chloro-1,3,2-dioxaphospholane 2-oxide was purchased from Sigma Aldrich. N-butanol, triethyl amine and diethyl ether (anhydrous) were obtained from Fischer Scientific. 2-Chloro-1,3,2-dioxaphospholane 2-oxide and triethyl amine were distilled prior to use. 2-Chloro-1,3,2-dioxaphospholane 2-oxide was stirred with an equimolar amount of n-Butanol at  $-20^{\circ}\text{C}$  under an inert atmosphere in the presence of dry triethylamine to obtain n-butyl substituted phospholane (Scheme 2.6).<sup>2</sup> The product was separated immediately after synthesis through filtration through a celite pad under  $\text{N}_2$ . Diethyl ether was removed from the filtrate through rotavapor and further dried in vacuum over for 8-9 hour. The product is hydrolytically unstable and readily undergoes ring-opening when in contact with moisture at room temperature, the phospholane proved to be stable at  $-20^{\circ}\text{C}$ .<sup>2</sup>

$^1\text{H-NMR}$ ,  $^{13}\text{C-NMR}$  and  $^{31}\text{P-NMR}$  were performed to show the purity of the product obtained (Figure 2.15).



**scheme 2.6: Synthesis of 2-butyl-1,3,2-dioxaphospholane 2-oxide**

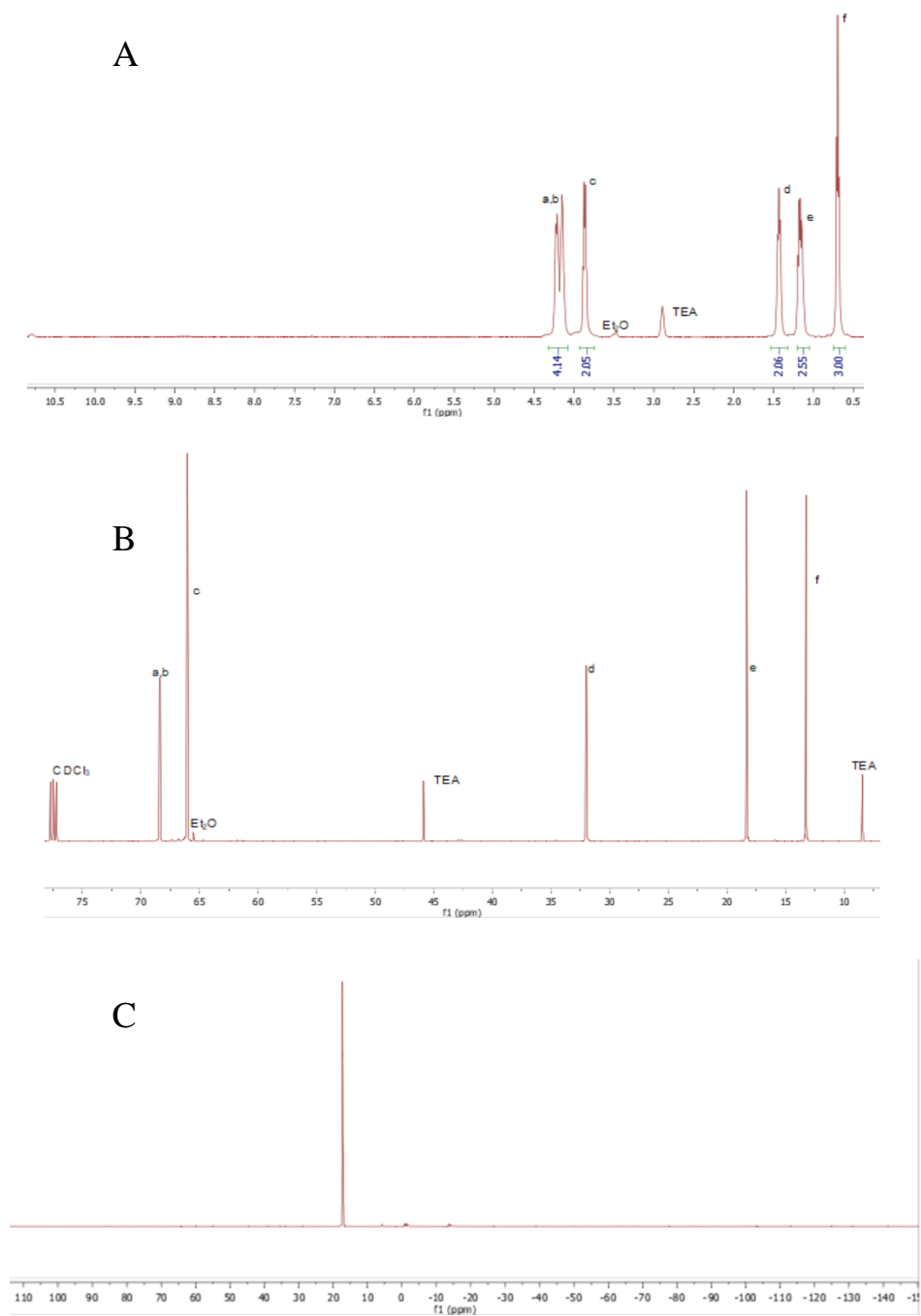
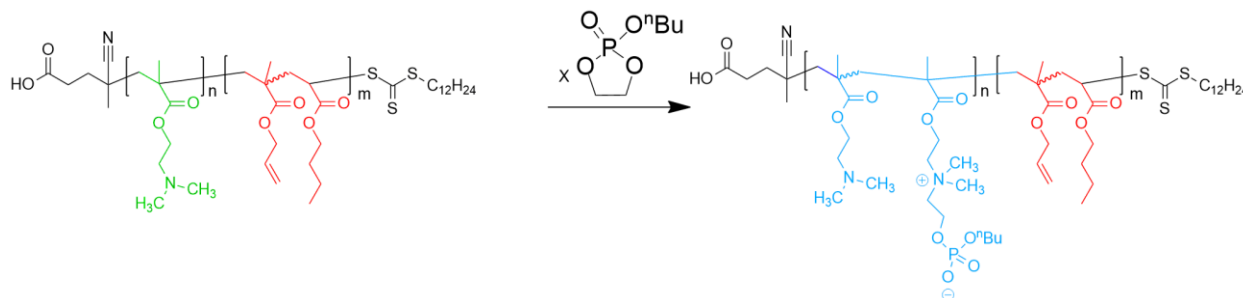


**Figure 2.15: A)  $^1\text{H-NMR}$ , B)  $^{13}\text{C-NMR}$  & C)  $^{31}\text{P-NMR}$  of 2-butyl-1,3,2-dioxaphospholane 2-oxide**

### 2.5.2.2 With n-Butyl Substituted Phospholane

A series of A-Z copolymers have been synthesized by ring-opening of n-Butyl substituted phospholane using the previously synthesized neutral PDMAEMA-*b*-P(nBA-*ran*-AMA) copolymers. A typical synthetic procedure was as follows, the copolymers (1 gm), monomethyl ether hydroquinone (MEHQ) and a threefold excess n-Butyl substituted phospholane ring were dissolved in tetrahydrofuran (THF) (12 ml) and stirred vigorously for 5 day at 60°C (Scheme 2.7) . At the end of the reaction the polymer solution appeared as a transparent viscous liquid. This was then dissolved in TFE and precipitated in toluene to remove any excess n-Butyl substituted phospholane ring. From each neutral copolymer synthesized, A-Z copolymers were synthesized with targeted level 100% molar fraction of the heterocyclic ring relative to the DP of DMAEMA.



**scheme 2.7: Post polymerization modification of parent diblock polymer via nucleophilic ring opening of 2-butyl-1,3,2-dioxaphospholane 2-oxide**

**Table 2.7: Percent quaternization as indicated by NMR**

PBCPMA <sub>290</sub> -P(BA- <i>ran</i> -5%AMA) <sub>187</sub> <sup>-</sup> f0.66 (14)		PBCPMA <sub>223</sub> -P(BA- <i>ran</i> -5%AMA) <sub>312</sub> <sup>-</sup> f0.47 (16)		PBCPMA <sub>25</sub> -P(BA- <i>ran</i> -5%AMA) <sub>265</sub> <sup>-</sup> f0.10 (19)	
Targeted % quaternization	Experimental % quaternization	Targeted % quaternization	Experimental % quaternization	Targeted % quaternization	Experimental % quaternization
100	20	100	20	100	15

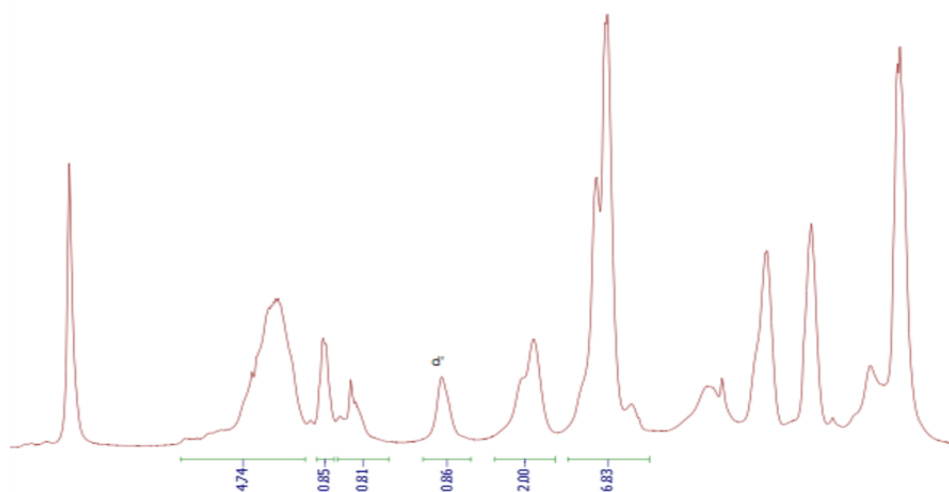


**Figure 2.16: Representative NMR of A-Z block copolymer with 20% of quaternization**

The <sup>1</sup>H-NMR spectrum using TFE-*d*<sub>2</sub> solvent (Figure 2.16) reveals the distinct peak of the poly(choline phosphate methacrylate). Due to presence of neighboring positive and negative charge a chemical shift of the proton peaks alpha to the ester bond and tertiary amine group was observed to have been shifted. From the ratio of the proton peaks appearing at  $\delta$  3.2 ppm (methyl proton attached to quaternary ammonium ion), and  $\delta$  2.5 ppm (methylene proton alpha to the tertiary amine of the unreacted pendant group) the percent quaternization was calculated. Due to slow rate of nucleophilic ring-opening

reaction the percent quaternization achieved was observed to be lower than in the ring-opening reactions with 1,3-propane sultone (Table 2.7)

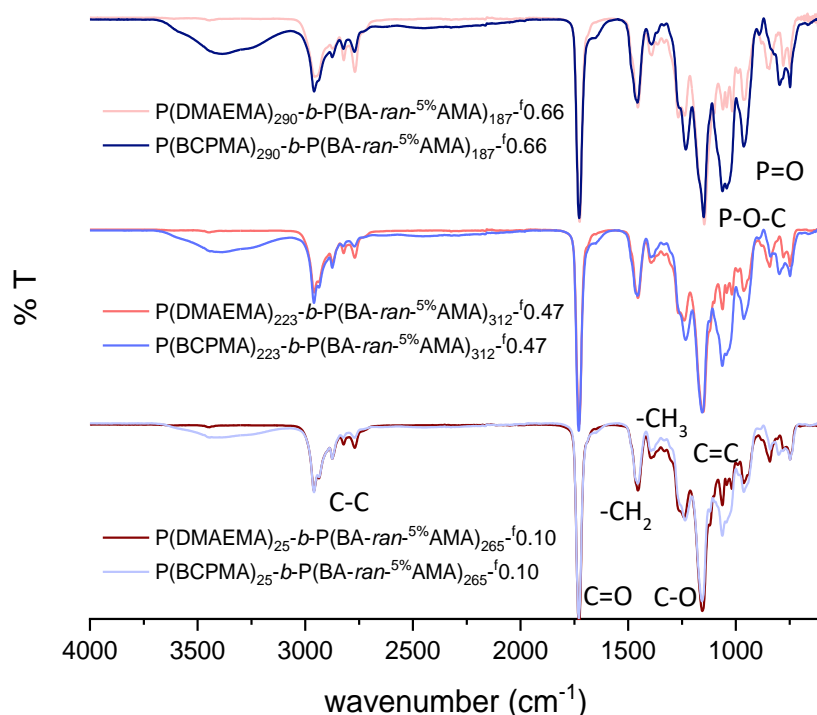


**Figure 2.17: FTIR analysis of the A-Z block copolymer with different percentage quaternization as compared with the parent block copolymer**

FTIR analysis of the A-Z block copolymer with different percent quaternization as compared with the parent block copolymer (Figure 2.17). With the increase in the percent quaternization as indicated by <sup>1</sup>H-NMR there is also an increase in P-O-C and P=O stretching bands, also indicating successful quaternization was possible. Corresponding to the increase in percent quaternization, there was also an increase in bound water peak indicating that the polymer becomes inherently more hygroscopic with the increase in zwitterionic content.



TGA analysis of the polymers were also performed to study the thermal stability of the zwitterions as compared with that of their parent block copolymer (Figure 2.18). For the parent block copolymer the first degradation temperature was observed at 150°C which is due to the mass loss of the bound water. A second degradation was due to the loss of the tertiary amine group and the last degradation step was due to the fragmentation of the polymer backbone. With the increase in PDMAEMA volume fraction the bound water mass loss and mass loss due to tertiary amine group increases. With the increase in the percent quaternization the first mass loss temperature increases as the bound water becomes more rigid due to the presence of the zwitterionic charges. The second mass loss is due to the degradation of the quaternary ammonium groups and the last degradation is due to the fragmentation of the polymer backbone. For 100% quaternized A-Z block copolymer the first degradation temperature is much higher and the mass at the higher temperature is greater than the parent block. This study shows that the A-Z block copolymers synthesized are thermally stable within the range of operating temperatures.

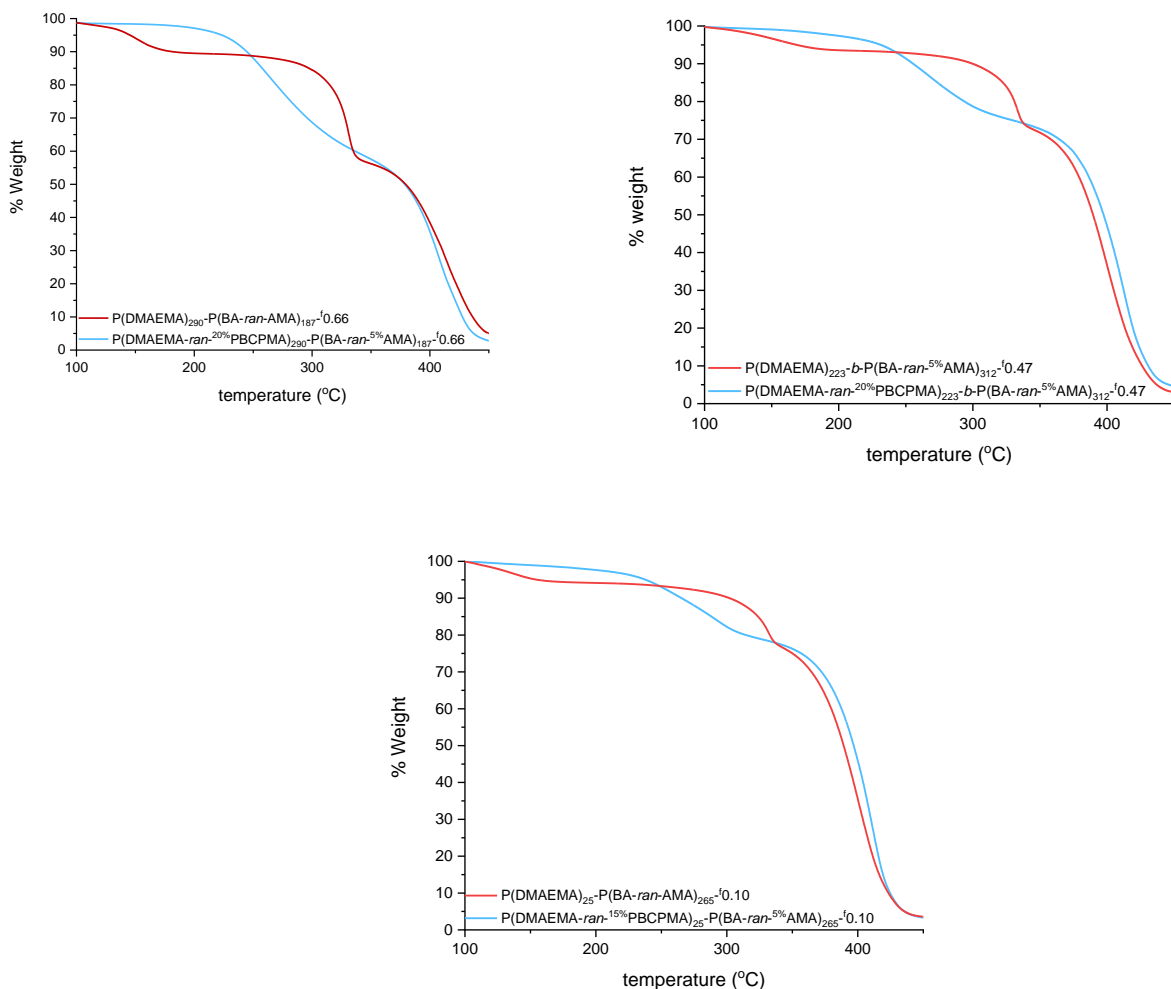


**Figure 2.18: TGA analysis of the A-Z block copolymer as compared with that of the parent block copolymer**

DSC analysis of the polymers were performed to study the glass transition temperature of the A-Z block copolymer as compared to its parent block copolymer (Figure 2.19). In the parent block copolymer, characteristic  $T_g$  of n-butyl acrylate appears around  $-55^\circ\text{C}$  and that of PDMAEMA is observed around  $117^\circ\text{C}$ . The  $T_g$  of the A-Z block copolymer was not very different for the low zwitterionic content. According to literature,  $T_g$  of SBMA is around  $200^\circ\text{C}$  in rapid DSC with a  $2000\text{ K/min}$  heating rate. The high  $T_g$  of PSBMA is due to strong cohesive attractions between the positive and negative charge

present in the polymer pendant group. In the block copolymer due to the presence of a low  $T_g$  rubbery domain on n-butyl acrylate, the  $T_g$  of the PSBMA appears at lower temperature. At the same time  $T_g$  of n-butyl acrylate disappears with the increase in zwitterionic content.

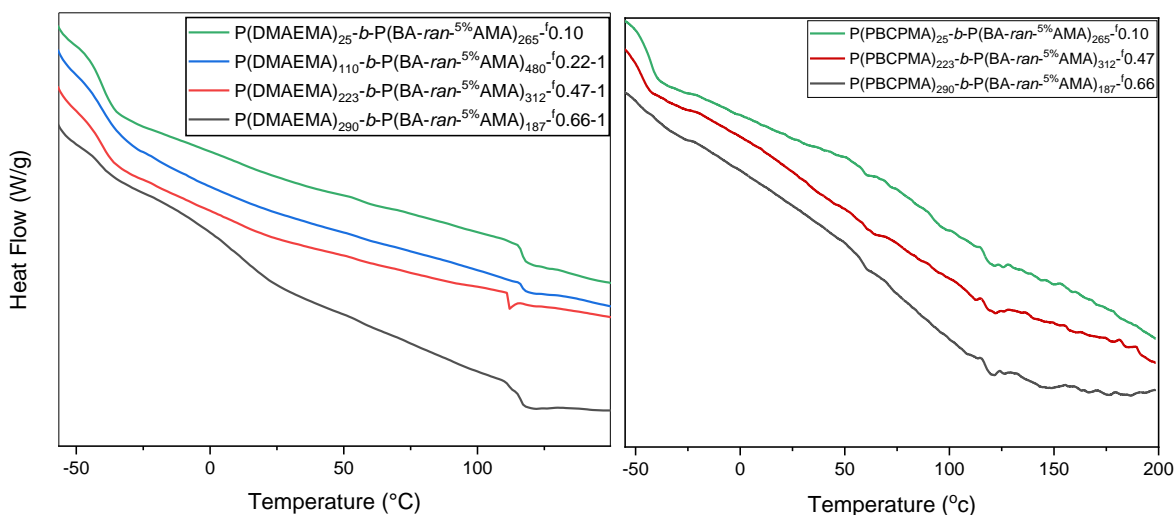
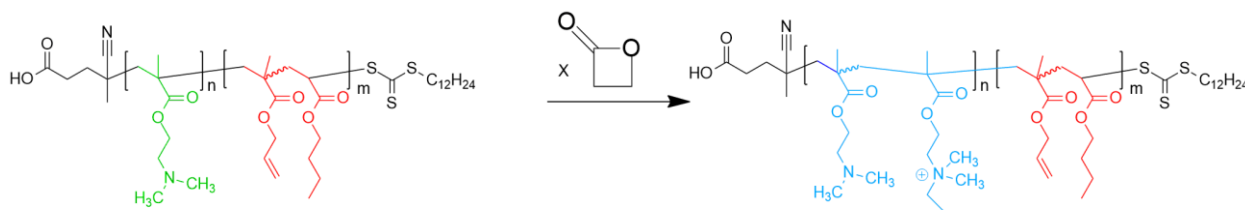


**Figure 2.19: DSC analysis of the A-Z block copolymer as compared with that of the parent block copolymer**

### 2.5.3 Ring-Opening with $\beta$ -propiolactone

A series of A-Z copolymers have been synthesized by ring-opening of by 1,3-propane sultone using the previously synthesized neutral PDMAEMA-*b*-P(nBA-*ran*-AMA) copolymers. A typical synthetic procedure was as follows, the copolymers (1 g) and three times excess  $\beta$ -propiolactone were dissolved in tetrahydrofuran (THF) (12 ml) and stirred vigorously for 24 h at room temperature (Scheme 2.8). This mixture was then dissolved in TFE and precipitated in hexane to isolate the polymer. But <sup>1</sup>H-NMR and FTIR analysis shows no heterocyclic ring opening reaction has been observed (Table 2.8). In the

$^1\text{H-NMR}$  a peak for methyl proton attached to quaternary amine should have appeared at  $\delta$  3.0-3.5 ppm region and a shifted peak 2methylene proton alpha to the tertiary amine group of the unreacted PDMAEMA should have shifted (Figure 2.20). In the FTIR no change in parent copolymer peak and increase of bound water peak should have been observed (figure 2.21). The conclusion drawn from these analyses is that of the reaction the polymer showed no change in appearance, indicating a lack of reaction. The reaction was repeated at higher temperatures, high concentration and longer time all to no avail.



**scheme 2.8: Post polymerization modification of parent diblock polymer via nucleophilic ring opening of  $\beta$ -propiolactone**

**Table 2.8: Percent quaternization as indicated by NMR**

PCBMA <sub>290</sub> -P(BA- <i>ran</i> -5%AMA) <sub>187</sub> -f0.66 (14)		PCBMA <sub>223</sub> -P(BA- <i>ran</i> -5%AMA) <sub>312</sub> -f0.47 (16)		PCBMA <sub>110</sub> -P(BA- <i>ran</i> -5%AMA) <sub>480</sub> -f0.22 (17)		PCBMA <sub>25</sub> -P(BA- <i>ran</i> -5%AMA) <sub>265</sub> -f0.10 (19)	
Targeted % quaternization	Experimental % quaternization	Targeted % quaternization	Experimental % quaternization	Targeted % quaternization	Experimental % quaternization	Targeted % quaternization	Experimental % quaternization
100	0	100	0	100	0	100	0

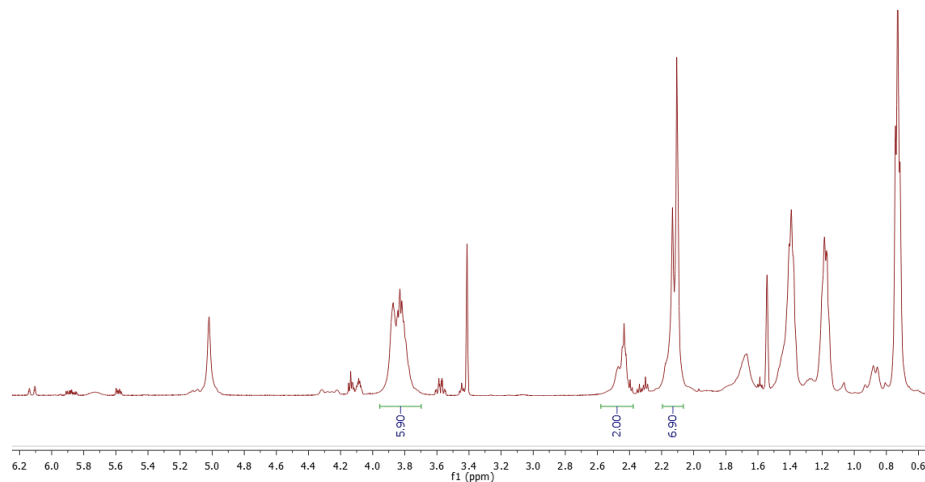


**Figure 2.20: Representative NMR of A-Z block copolymer with 0% of quaternization**

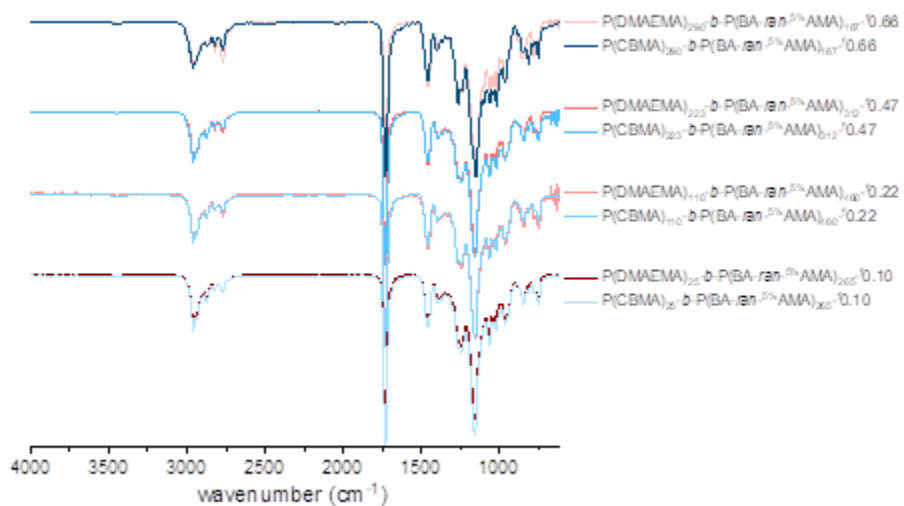


**Figure 2.21: FTIR analysis of the A-Z block copolymer with different percentage quaternization as compared with the parent block copolymer**

## 2.6 Conclusions:

In this chapter, a successful design of a platform parent block copolymer to synthesize amphiphilic zwitterionic block copolymer was discussed. Due to poor compatibility of hydrophobic low  $T_g$  and hydrophilic zwitterionic block post polymerization modification has been utilized. At first a conventional block copolymer consisting of a moderately polar block and a hydrophobic block was synthesized using controlled radical polymerization. This ensured control over molecular weight, dispersity, and volume fraction of each block in the copolymer. The nucleophilic ring-opening of different heterocyclic rings were then performed.

Ring-opening of 1,3-propane sultone showed the most success and high control over the percent quaternization. Ring-opening of n-butyl substituted choline phosphate showed slow reaction rate and low percent quaternization was achieved even when targeted for 100% quaternization. Ring-opening with  $\beta$ -propiolactone did not occur under the reaction conditions explored. More investigation needs to be performed to increase the reaction rate of n-butyl choline phosphate and to find conditions to successfully ring -open  $\beta$ -propiolactone. The synthetic pathway discussed in this chapter also opens broader possibilities of exploring additional copolymers of betaine type zwitterions and chemically incompatible hydrophobic blocks for a range of different applications.

## 2.7 References

- (1) Banerjee, S. L.; Bhattacharya, K.; Samanta, S.; Singha, N. K. Self-Healable Antifouling Zwitterionic Hydrogel Based on Synergistic Phototriggered Dynamic Disulfide Metathesis Reaction and Ionic Interaction. *ACS Appl. Mater. Interfaces* **2018**, *10* (32), 27391–27406. <https://doi.org/10.1021/acsami.8b10446>.
- (2) Hu, G.; Parelkar, S. S.; Emrick, T. A Facile Approach to Hydrophilic, Reverse Zwitterionic, Choline Phosphate Polymers. *Polym. Chem.* **2015**, *6* (4), 525–530. <https://doi.org/10.1039/c4py01292e>.

# CHAPTER 3

## EVALUATION OF AMPHIPHILIC ZWITTERIONIC BLOCK COPOLYMER MEMBRANES FOR WATER TRANSPORT

### 3.1 Introduction

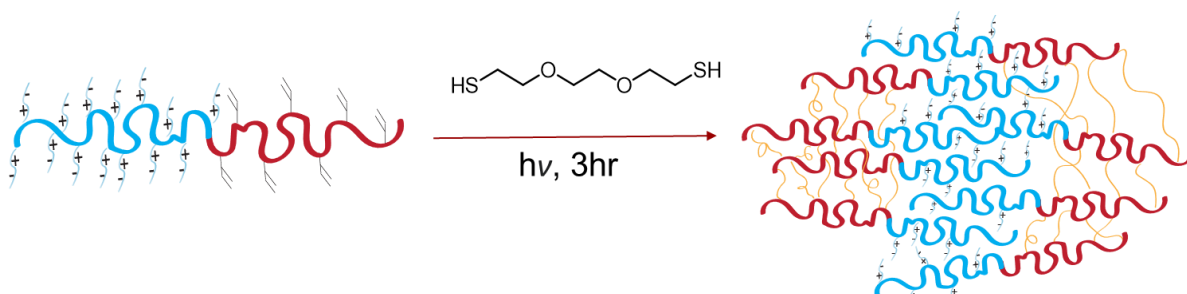
Block copolymers represent a class of materials composed of two or more covalently attached incompatible blocks which can spontaneously segregate into self-assembled structures with controllable dimensions and functionalities. The versatility of block copolymers in terms of their compositional sequence, architecture, and the choice of monomers can lead to dramatic changes in self-assembly and can allow for tailoring mechanical, electrical, optical and other physical properties for the targeted application.<sup>100,101</sup> The simplest and most studied architecture for block copolymers is the linear A-B diblock, whose morphological behavior is dependent on three experimentally controllable factors: the overall degree of polymerization ( $N$ ), the volume fraction of the A component ( $\phi_A$ ) and the Flory-Huggins interaction parameter  $\chi_{AB}$  whose magnitude is determined by the selection of the A-B monomer pair. Depending on the values of  $\phi_A$  and  $\chi_{AB}$ , a diblock copolymer can self-assemble into different equilibrium morphologies with a domain spacing ranging from 10-100 nm.<sup>1-2</sup> By means of incorporating more chemically distinct blocks into a chain, or adapting unique properties such as chiral, crystalline or rod-like structures for one of the blocks; more complex morphologies can be observed which can offer opportunities in designing novel nanostructured materials with improved functionality and properties.<sup>3</sup>



Literature on block copolyelectrolytes has shown how incorporating charges in one of the blocks leads to formation of different nanostructures that are inaccessible to uncharged block copolymers.<sup>4-6</sup> Varying charges can tune the material spectrum of self-assembled structures and enhance the efficiency of the ion transport. This complexity in the nanostructures arises because of counterion entropy leading to suppression of phase separation and charge ionization in the surrounding medium leading to enhancement of phase separation.<sup>4-6</sup> Following the phase separation trend in uncharged block copolymer and charged block copolyelectrolyte, it would be interesting to investigate the self-assembly behavior of block copolymer zwitterions. In this category of block copolymers two opposite charges are covalently bonded. Therefore, the entropy effect of the counterion will be nullified whereas the electrostatic cohesive strength will be highly enhanced. The contribution of these effects on morphology and the efficiency of the resultant morphology as the transport channels for water and ions is yet to be explored.

## 3.2 Experimental Section

### 3.2.1 Fabricating Mechanically Robust A-Z Block Copolymer Membrane via Photo Crosslinking



**scheme 3.1: Fabrication of robust copolymer membrane via photo crosslinking**

Parent block copolymer and their corresponding A-Z block copolymer membranes were prepared by drop-casting from tetrahydrofuran and trifluoroethanol solution respectively following a previously reported procedure (scheme 3.1).<sup>7,8</sup> Polymer (150 mg) was weighed into an aluminum covered scintillation vial equipped with a magnetic stirrer. 10% equivalent of photoinitiator solution (1.8 mL, 5 mg/mL in respective solvent) was then added. The contents of the vial were stirred until the polymer dissolved. Three equivalents of dithiol cross-linker (88  $\mu$ L 2,2'-(ethylenedioxy)-ethanedithiol) was added relative to the total amount of allyl methacrylate units as estimated by <sup>1</sup>H NMR. The solution was thoroughly mixed in the dark for two more minutes. Membranes were then drop cast on a Teflon sheet and were covered with a Petri dish to allow slow evaporation of the solvent and were allowed to dry at ambient conditions overnight in the dark. After 24 h the dried membranes are exposed to solvent vapor annealing of their respective solvent. After that the crosslinking of the membranes was achieved by exposure to UV light for 3 hours (365 nm, 100 mW/cm<sup>2</sup> at working distance). The following photo crosslinking the membranes were soaked into water. Success of the reaction was

determined whether the membrane was retaining its dimensional stability in water (Figure 3.1).

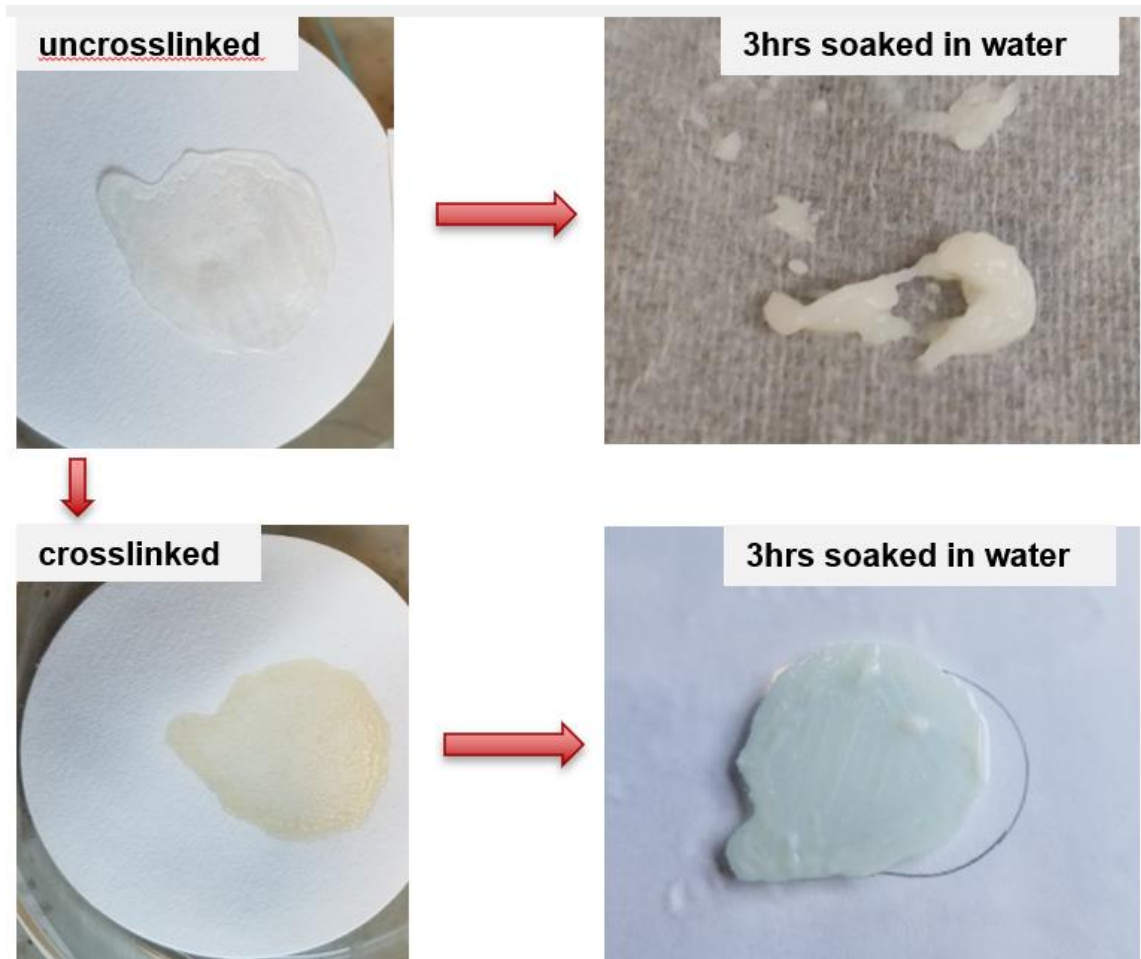


**Figure 3.1: mechanical and dimensional stability of a A-Z block copolymer membrane before and after crosslinking**

It was observed that the flexibility of the membrane changed with the change in the zwitterion content. The lower the zwitterion content, higher is the flexibility and the better the mechanical stability of the membrane (Figure 3.2). On the other hand, the membrane

becomes more brittle with the increase in the zwitterionic content. This result is due to the strong coulombic attraction between the positive and the negative charge between the added zwitterion in the polymer chain.

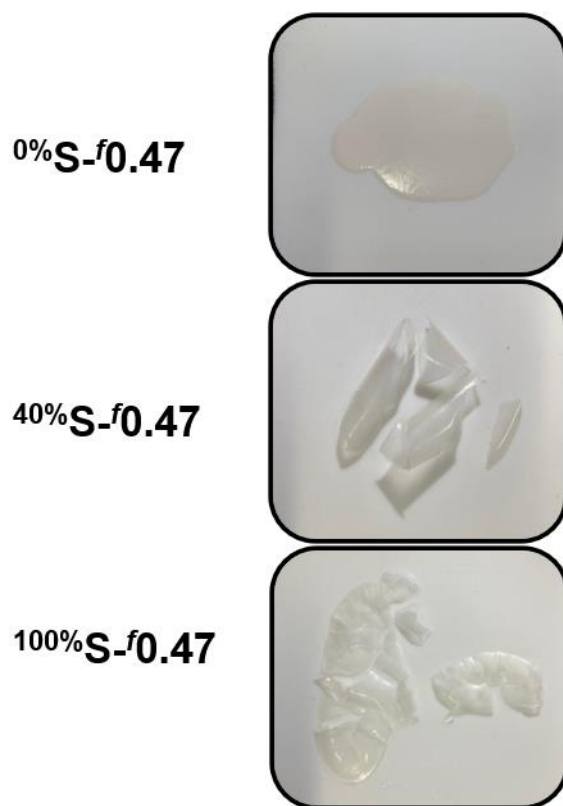


**Figure 3.2: With the increase in percent zwitterion in an A-Z block copolymer system with same hydrophilic volume fraction, the membranes becoming more brittle**

This attractive force should play an important role in determining the self-assembled structure of the material. To compare the effect of these coulombic interactions on the morphology the membranes are soaked in DI water, 0.5M NaCl solution and 1.0 M NaCl solution. The idea behind this is that after soaking in a salt solution ions will get into the

polymer chain screening the opposite charges (anti-polyelectrolytic effect), and thereby reducing the coulombic interaction (Figure 3.3).<sup>9</sup> Membranes were then taken out of the solutions, dried and morphology studies were performed.

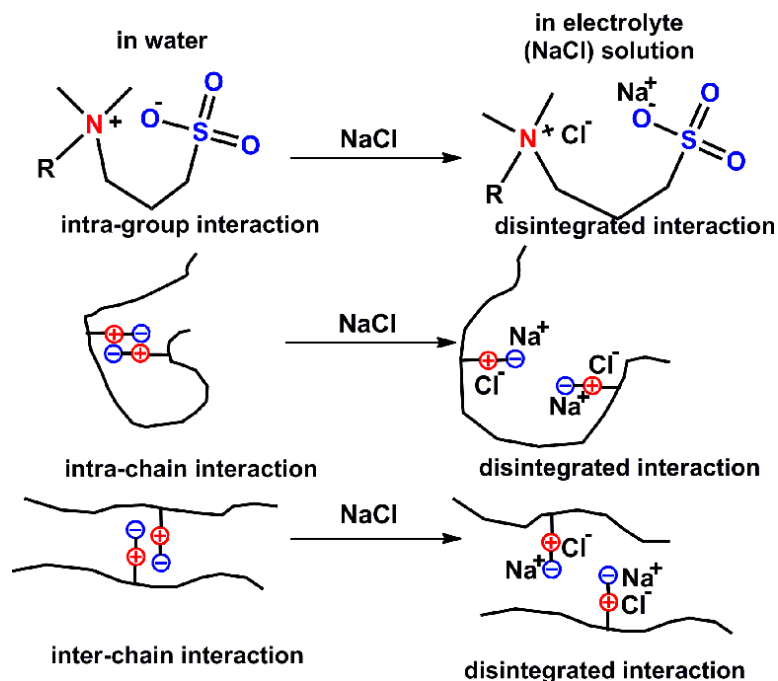


**Figure 3.3: Antipolyelectrolytic effect of zwitterion. Image taken from Ref. 9**

### 3.2.2 Instrument and Characterization

Small angle X-ray scattering (SAXS) experiments were performed at the Advanced Photon Source at Argonne National Laboratory on beamline 12 ID-B. The X-ray beam has a wavelength of 1 Å and power of 12 keV. Scattering data was collected on a Pilatus 2 M SAXS detector with an acquisition time of 1 s. Integration of the 2D scattering pattern with respect to the scattering vector ( $q$ ) provided the intensity ( $I$ ) data. Temperature and humidity of the sample environment during SAXS measurements was controlled using a custom designed oven with four sample slots with Kapton windows, as described

previously.<sup>7,8</sup> In a typical experiment, the oven was loaded with three membranes and one empty sample holder to collect a background spectrum of the environment for each experimental condition. Samples were soaked in water prior to loading. After removing the membranes from water, the superficial water on the surface of the membrane was lightly dried with a Kimwipe. Samples were loaded into the oven at room temperature at dry conditions. Loaded samples were allowed to equilibrate under dry gas flow for 20 min, and for 60 min at 95% RH, prior to X-ray measurements. The chamber temperature was kept constant as the RH increased to 95% RH. Spectra were analyzed by subtracting the background wave of the corresponding experimental condition from the sample wave. Gaussian curve fitting was utilized to detect peak maxima of the scattering curves.

The TEM specimens were prepared by a Leica CryoUltramicrotome. The microtome chamber was cooled down to  $-70\text{ }^{\circ}\text{C}$  by liquid nitrogen, where the bulk sample was microtomed with a diamond knife to a thickness of around 50 nm. The cutting sections were then collected on 400-mesh copper support grids. TEM characterization was performed on a Technai T12 operated at an accelerating voltage of 200 kV.

### **3.2.3 Morphology Study via SAXS**

Morphologies of the photo crosslinked membranes were investigated with SAXS under environmentally controlled conditions. Morphology trace of parent copolymer, 50% zwitterionic form and 100% zwitterionic form are offset for clarity purpose. Each set shows morphology of dry and wet samples. The red traces represent dry samples, and the blue traces represent wet samples. The top traces represent the parent block copolymer, and the bottom trace represents the 100% zwitterion content whereas the middle trace represents intermediated zwitterion content.

The morphology of block copolymer with 0.10 volume fraction of PDMAEMA are done (Figure 3.4). The parent copolymer in a dry state shows no short-range phase separation. But as the zwitterion content starts to increase, a prominent increase in periodic order of the phase separated behavior starts to show. At 50% zwitterion content, the morphology appears as hexagonal while at 100% zwitterion content, the morphology shifts to lamellar. Now when the membranes are fully hydrated, we see a complete disordered morphology for the parent copolymer. But at 50% zwitterion, the d-spacing increases and the periodic arrangement becomes more prominent. Similar changes are also seen for 100% zwitterion. This is due to the fact that water molecules entering in between the chains are swelling the hydrophilic phase, increasing the d-spacing. It is also reducing the coulombic interaction, in the zwitterionic moiety, thus giving a better periodic arrangement.

With the increase in the salt concentration, we see a distinct increase in the periodic arrangement for the parent copolymer. No discernable changes are observed for 50% zwitterion content. For 100% zwitterion content, better periodic arrangements are observed at the lower d-spacing region.

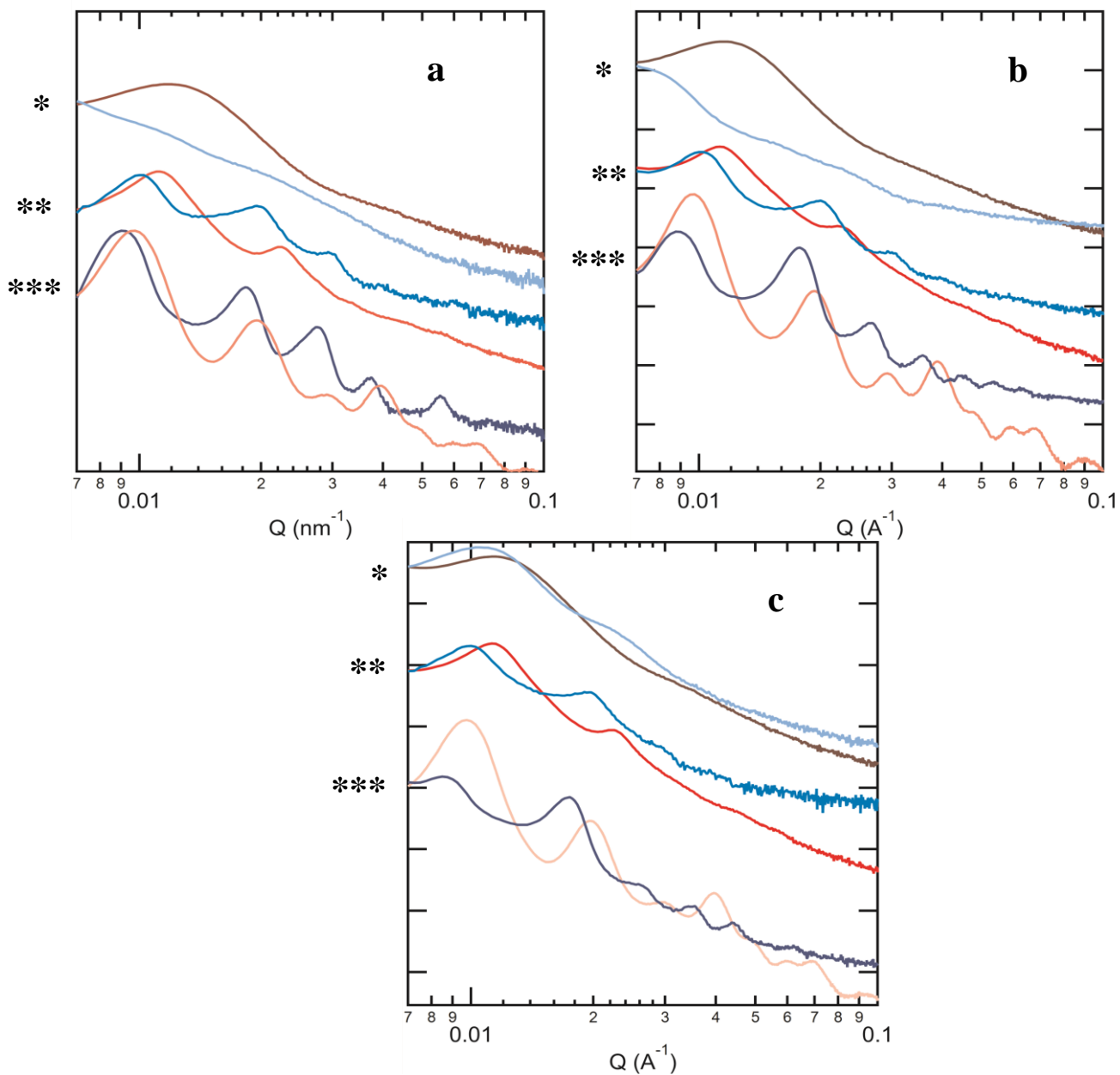


**Figure 3.4: Morphology study of block copolymer membrane with  $f=0.10$  by SAXS under controlled environment pretreated with a) pure DI water b) 0.5 M NaCl aqueous solution c) 1.0 M NaCl aqueous solution.**

\*0% zwitterion, \*\*50% zwitterion, \*\*\*100% zwitterion content

Red Trace : Oven dried sample under dry environment

Blue trace: Fully hydrated membrane under 95% relative humid condition



The morphology of block copolymer with 0.22 volume fraction of PDMAEMA are done (Figure 3.5). In this case a similar trend was observed. The parent copolymer at dry state shows phase separation at a periodic arrangement of hexagonal morphology at a d-spacing of 50 nm. But as the zwitterion content starts to increase, there is a prominent shift in periodic order in the phase separated behavior towards higher d spacing. At 50% zwitterion content, the morphology shifts to lamellar while at 100% zwitterion content, the morphology appears lamellar with d-spacing at 86 nm range. Now when the membranes are fully hydrated, we see more random phase separated arrangement in parent block than its dry state. But at 50% zwitterion and at 100% zwitterion, periodic arrangement becomes more disordered. This is due to the fact that water molecules entering in between the chains swelling the hydrophilic phase, reducing the coulombic interaction, interfering with the periodic arrangement giving a disordered morphology.

With the increase in the salt concentration, we see a distinct increase in the periodic arrangement for the copolymer in the fully hydrated state. But no discernable changes are observed for dry membranes.

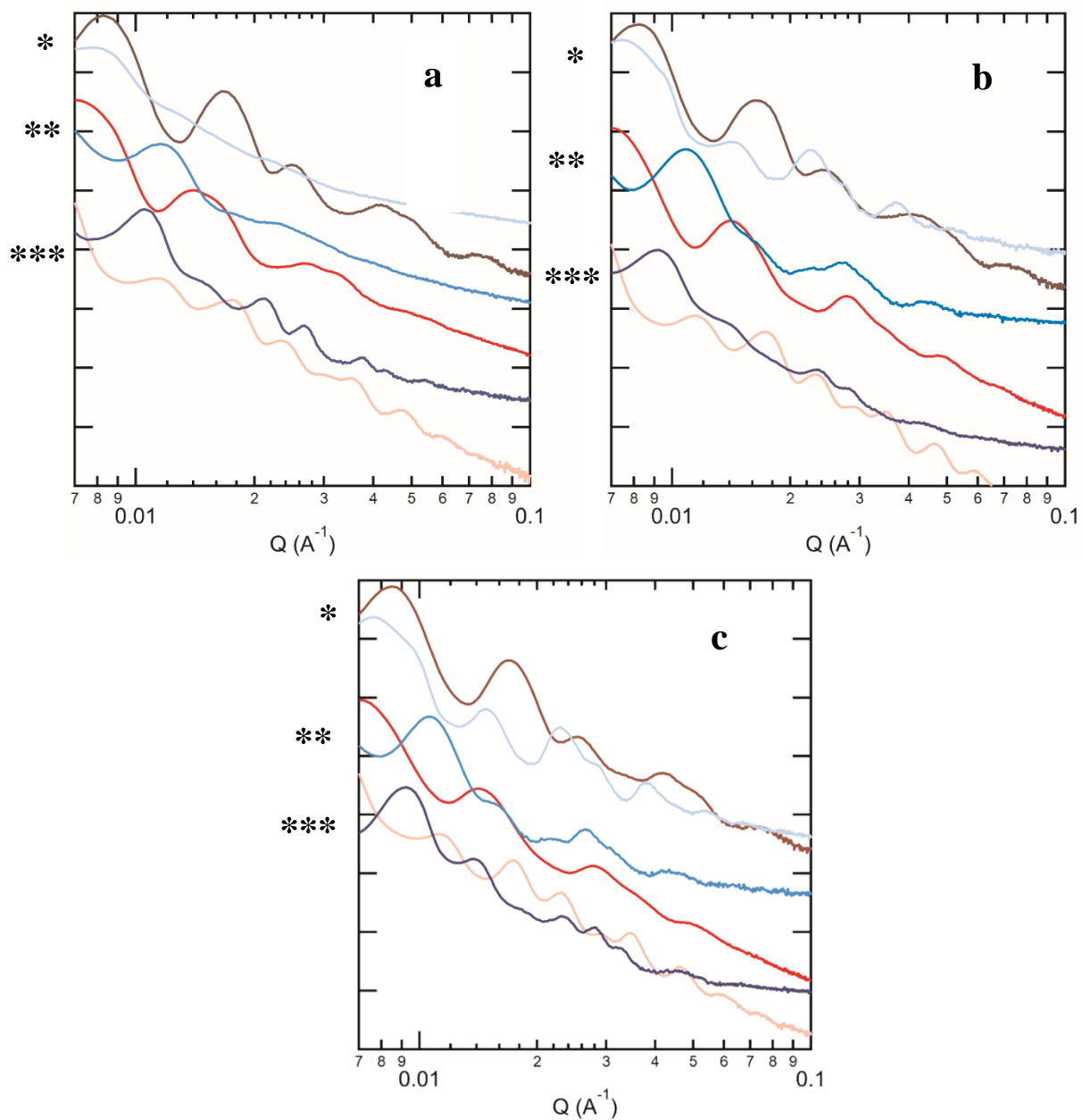


**Figure 3.5.:Morphology study of block copolymer membrane with  $f=0.22$  by SAXS under controlled environment pretreated with a) pure DI water b) 0.5M NaCl aqueous solution c) 1.0M NaCl aqueous solution**

0% zwitterion, \*\*50% zwitterion, \*\*\*100% zwitterion content

Red Trace : Oven dried sample under dry environment

Blue trace: Fully hydrated membrane under 95% relative humid condition

The morphology of block copolymer with 0.47 volume fraction of PDMAEMA are done (Figure 3.6). In this case the opposite trend was observed. The parent copolymer at dry state shows phase separation at a periodic arrangement of lamellar morphology at a d-spacing of 86 nm. But as the zwitterion content starts to increase, there is a prominent shift in periodic order in the phase separated behavior towards lower d-spacing. At 50% zwitterion content, the morphology appears as still lamellar while at 100% zwitterion content, the morphology shifts to hexagonal with d-spacing at 46 nm range. Now when the membranes are fully hydrated, we see a more random phase separated arrangement in parent block than its dry state. But at 50% zwitterion and at 100% zwitterion, periodic arrangement becomes more disordered. This is due to the fact that water molecules entering in between the chains swelling the hydrophilic phase, reducing the coulombic interaction, interfering with the periodic arrangement giving a disordered morphology.

With the increase in the salt concentration, we see a distinct increase in the periodic arrangement for the copolymer on the fully hydrated state. But no discernable changes are observed for dry membranes.

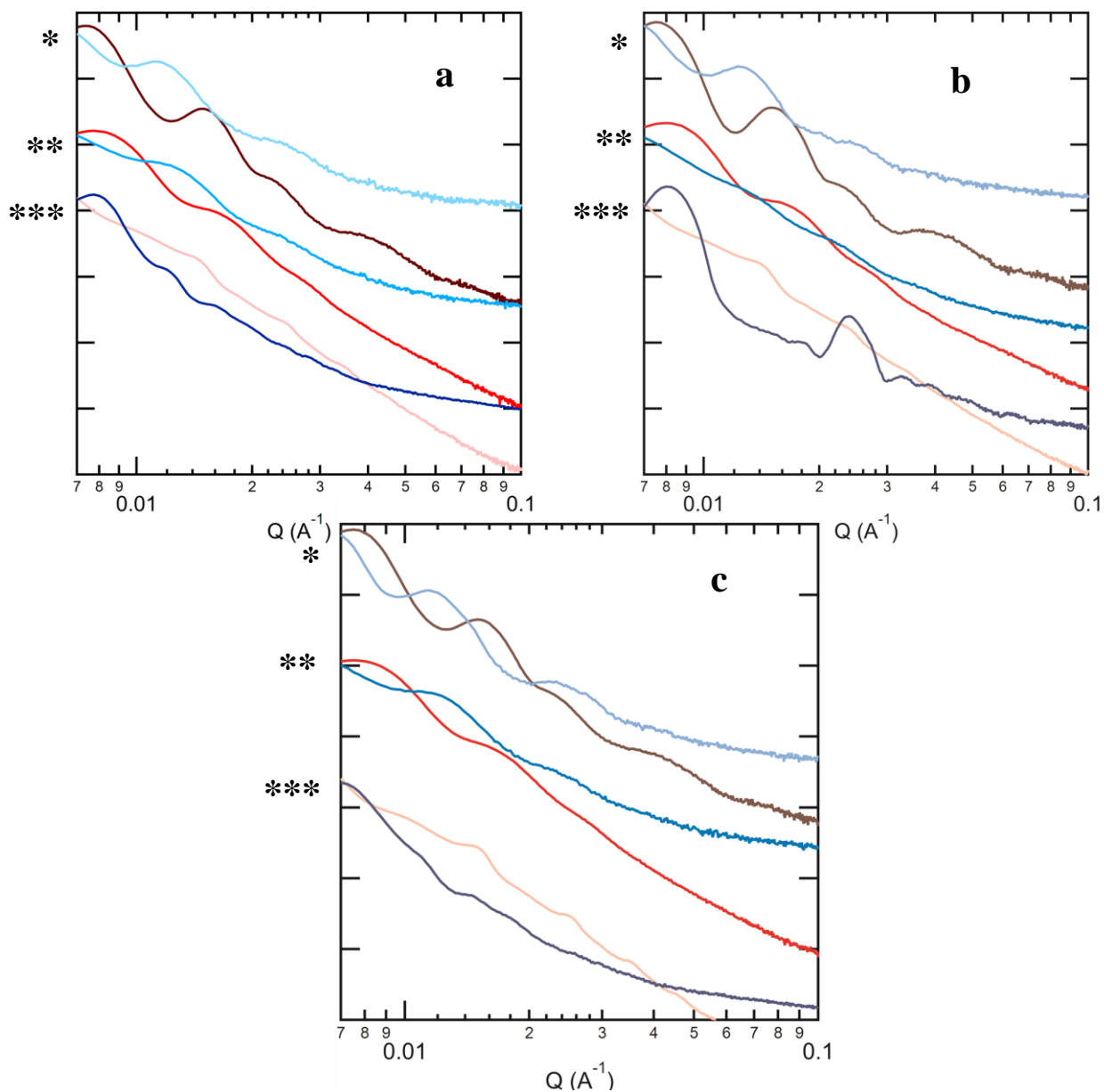


**Figure 3.6: Morphology study of block copolymer membrane with  $f=0.47$  by SAXS under controlled environment pretreated with a) pure DI water b) 0.5M NaCl aqueous solution c) 1.0M NaCl aqueous solution.**

\*0% zwitterion, \*\*50% zwitterion, \*\*\*100% zwitterion content

Red Trace : Oven dried sample under dry environment

Blue trace: Fully hydrated membrane under 95% relative humid condition

The morphology of block copolymer with 0.67 volume fraction of PDMAEMA are done (Figure 3.7). In this case a similar trend was observed as previous. The parent copolymer at dry state shows phase separation at a periodic arrangement of hexagonal morphology at a d-spacing of 50 nm. But as the zwitterion content starts to increase, there is a prominent shift in periodic order in the phase separated behavior towards higher d spacing. At 50% zwitterion content, the morphology appears hexagonal while at 100% zwitterion content, the morphology shifts to lamellar with d-spacing at 86 nm range. Now when the membranes are fully hydrated, we see a morphology more random in parent block than its dry state. But at 50% zwitterion and at 100% zwitterion, periodic arrangement becomes more disordered. This is due to fact, that water molecules entering in between the chains swelling the hydrophilic phase, reducing the coulombic interaction, interfering with the periodic arrangement giving a disordered morphology.

With the increase in the salt concentration, we see a distinct increase in the periodic arrangement for the copolymer on the fully hydrated state. But no discernable changes are observed for dry membranes.

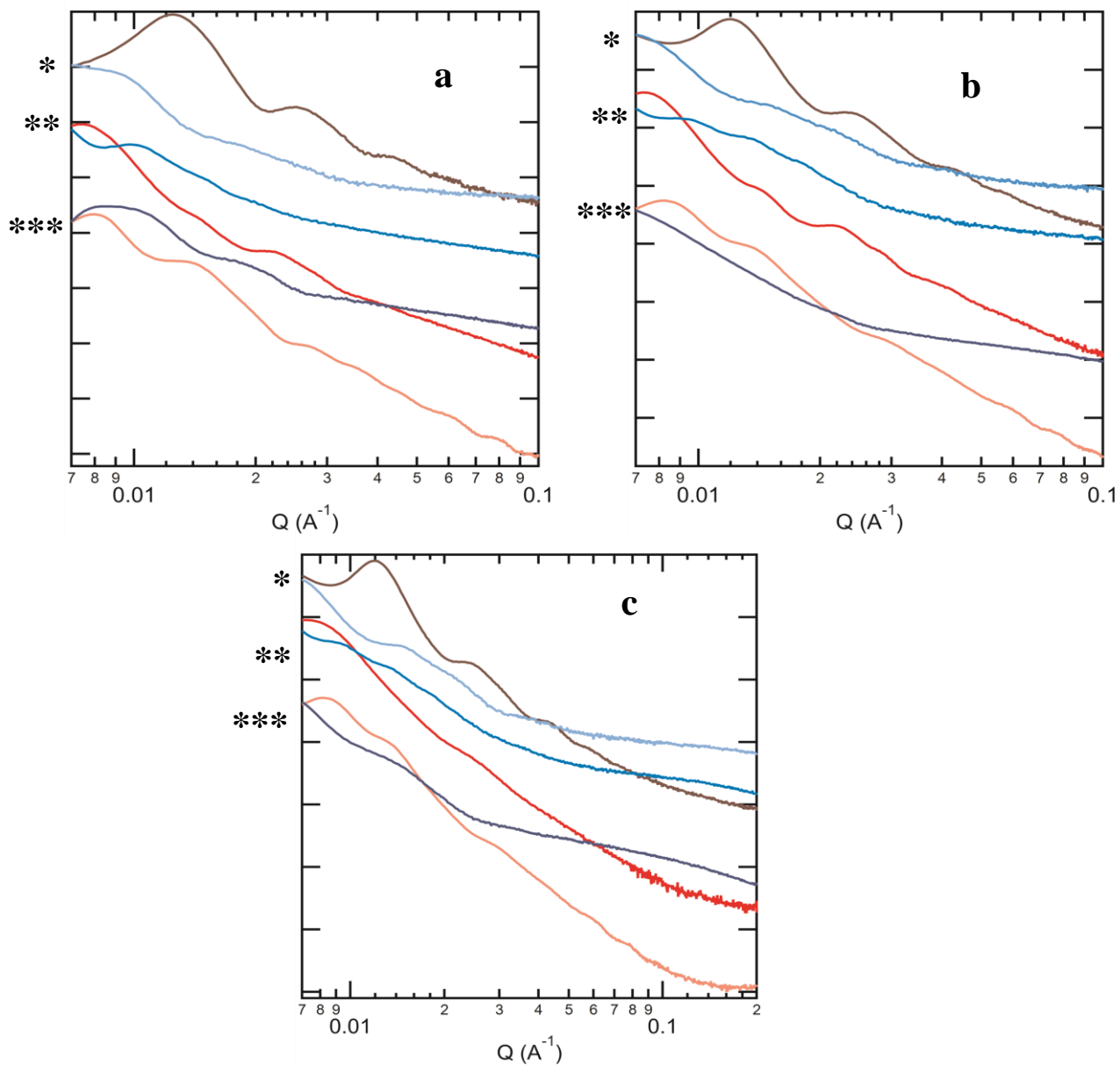


**Figure 3.7: Morphology study of block copolymer membrane with  $f=0.66$  by SAXS under controlled environment pretreated with a) pure DI water b) 0.5M NaCl aqueous solution c) 1.0M NaCl aqueous solution.**

\*0% zwitterion, \*\*50% zwitterion, \*\*\*100% zwitterion content

Red Trace : Oven dried sample under dry environment

Blue trace: Fully hydrated membrane under 95% relative humid condition

### 3.2.4 Study Via TEM

Real Space imaging of the photo crosslinked dry membranes were performed with the help of TEM imaging to compare the morphology with the reciprocal space morphology as obtained by SAXS. Morphology obtained via TEM matches with that of SAXS in terms of d-spacing and periodic arrangements. (Figure 3.8)

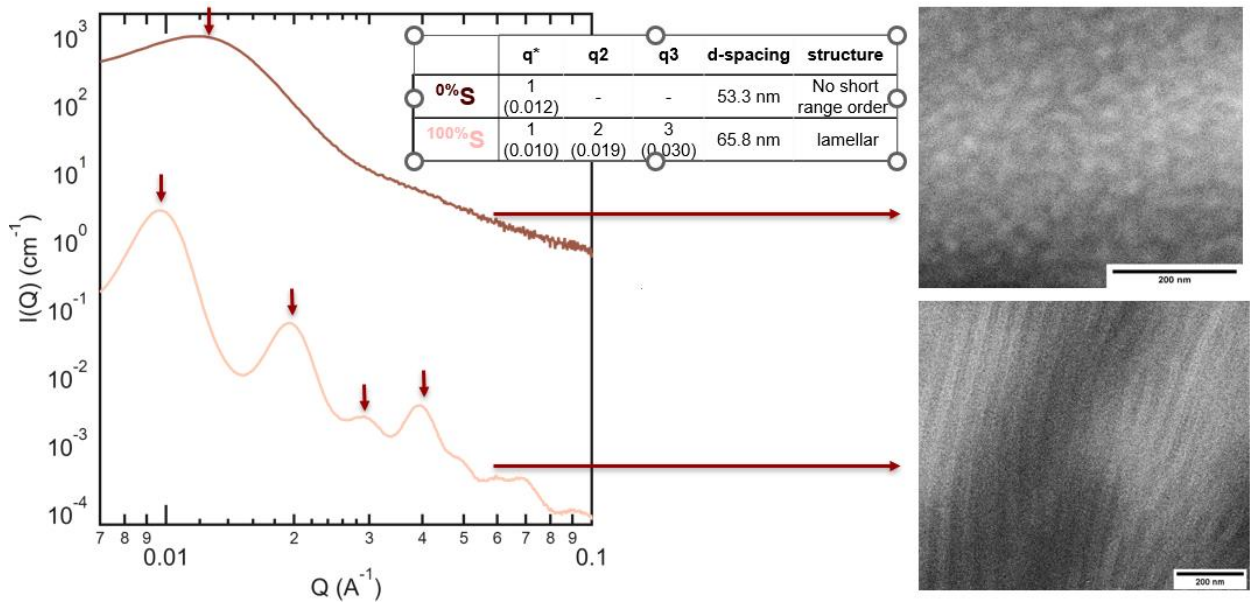


**Figure 3.8: TEM images of the parent block copolymer with  $f=0.10$  and its 100% zwitterionic form as compared to its SAXS images.**

### 3.3 Conclusions

In this chapter, a successful design of photo crosslinked robust membranes were synthesized from parent block copolymer and A-Z block copolymers. All the membranes are soaked in DI water to observe the retention of dimensional stability of the membrane. SAXS and TEM were performed to study the effect of coulombic interactions of the zwitterionic moieties on the polymer backbone on the self-assembled structure. It has been

observed that a noticeable shift in morphology was observed as the amount of zwitterion content increased from the parent block. The volume fraction of the hydrophilic block also played an important role on the morphology of the block copolymer.

In the future it would be interesting to observe the morphology of the A-Z block copolymer with different anionic groups. By changing the anionic group, the dipole moment of the zwitterion will shift, thereby influencing the morphology. Morphology studies could also be performed by reversing the dipole moment of the zwitterion as a way to help understand the effect of zwitterion dipole has on morphology. The real space imaging of the hydrated membrane will be interesting to observe under Cryo TEM preserving the native morphology in the hydrated state.



### 3.4 References

- (1) Bates, F. S.; Fredrickson, G. H. Block Copolymer Thermodynamics: Theory and Experiment. *Annu. Rev. Phys. Chem.* **1990**, *41* (1), 525–557. <https://doi.org/10.1146/annurev.pc.41.100190.002521>.
- (2) Matsen, M. W. The Standard Gaussian Model for Block Copolymer Melts. *J. Phys. Condens. Matter* **2002**, *14* (2). <https://doi.org/10.1088/0953-8984/14/2/201>.
- (3) Chan, E. P.; Frieberg, B. R.; Ito, K.; Tarver, J.; Tyagi, M.; Zhang, W.; Coughlin, E. B.; Stafford, C. M.; Roy, A.; Rosenberg, S.; Soles, C. L. Insights into the Water Transport Mechanism in Polymeric Membranes from Neutron Scattering. *Macromolecules* **2020**, *53* (4), 1443–1450. <https://doi.org/10.1021/acs.macromol.9b02195>.
- (4) Sing, C. E.; Zwanikken, J. W.; Olvera De La Cruz, M. Electrostatic Control of Block Copolymer Morphology. *Nat. Mater.* **2014**, *13* (7), 694–698. <https://doi.org/10.1038/nmat4001>.
- (5) Zwanikken, J. W.; Jha, P. K.; De La Cruz, M. O. A Practical Integral Equation for the Structure and Thermodynamics of Hard Sphere Coulomb Fluids. *J. Chem. Phys.* **2011**, *135* (6). <https://doi.org/10.1063/1.3624809>.
- (6) Sing, C. E.; Zwanikken, J. W.; de la Cruz, M. O. Interfacial Behavior in Polyelectrolyte Blends: Hybrid Liquid-State Integral Equation and Self-Consistent Field Theory Study. *Phys. Rev. Lett.* **2013**, *111* (16), 168303. <https://doi.org/10.1103/PhysRevLett.111.168303>.
- (7) Ertem, S. P.; Tsai, T. H.; Donahue, M. M.; Zhang, W.; Sarode, H.; Liu, Y.; Seifert, S.; Herring, A. M.; Coughlin, E. B. Photo-Cross-Linked Anion Exchange Membranes with Improved Water Management and Conductivity. *Macromolecules* **2016**, *49* (1), 153–161.

<https://doi.org/10.1021/acs.macromol.5b01784>.

(8) Tsai, T. H.; Ertem, S. P.; Maes, A. M.; Seifert, S.; Herring, A. M.; Coughlin, E. B. Thermally Cross-Linked Anion Exchange Membranes from Solvent Processable Isoprene Containing Ionomers. *Macromolecules* **2015**, *48* (3), 655–662.  
<https://doi.org/10.1021/ma502362a>.

(9) Ilčíková, M.; Tkáč, J.; Kasák, P. Switchable Materials Containing Polyzwitterion Moieties. *Polymers (Basel)*. **2015**, *7* (11), 2344–2370.  
<https://doi.org/10.3390/polym7111518>.

# **CHAPTER 4**

## **AMPHIPHILIC-ZWITTERIONIC POLYMER FOR WATER TRANSPORT AND SELECTIVE ION TRANSPORT MEMBRANE**

### **4.1 Background and Motivations**

With the growing demand for a stable supply of fresh water for agriculture, industrial, and community usage there is a need for developing advanced wastewater treatment technology. The focus has been on designing efficient technologies to produce clean and potable water from untreated agricultural runoff, industrial production of wastewater and inland brackish ground water. With this purpose in mind, this dissertation's objective was to design a membrane system using amphiphilic-zwitterionic polymers and to examine membranes prepared from these novel block copolymers for their feasibility for small-scale water treatment and desalination. Anticipated advantages of using amphiphilic-zwitterionic copolymers are their improved hydrophobicity, ion transport and antifouling nature. The challenge to identify a candidate membrane lies in designing amphiphilic-zwitterionic copolymers that show selective ion transport. Zwitterions have a high density of covalently bonded opposite charges, but overall charge neutrality, that shows potential characteristics of both charged and uncharged polymers. However, it is still unclear as to the fundamental mechanisms of water and ion transport in amphiphilic-zwitterionic copolymer membranes. This summary chapter will focus on the initial findings on the structure-property relationships discussed in the previous chapters on the effect of morphology of the amphiphilic-zwitterionic polymeric membrane on water and ion transport.

## 4.2 Water Uptake Experiments

### 4.2.1 Gravimetric Analysis

The weight percentage of the **Mass absorption** ( $w_w$ ) was calculated using the following equation:<sup>1</sup>

$$\text{Equation 4.1: Mass Absorbtion}$$
$$w_w = \frac{m_{wet} - m_{dry}}{m_{wet}} \times 100\%$$

Mass of the cast membrane was measured after drying under vacuum ( $m_{dry}$ ). The wet mass ( $m_{wet}$ ) was obtained by measuring the mass of the membrane after soaking it in DI water, 0.5 M and 1.0 M NaCl aqueous solution until equilibrium mass uptake has been reached. Surface water absorbed on the film was wiped off before taking the mass.

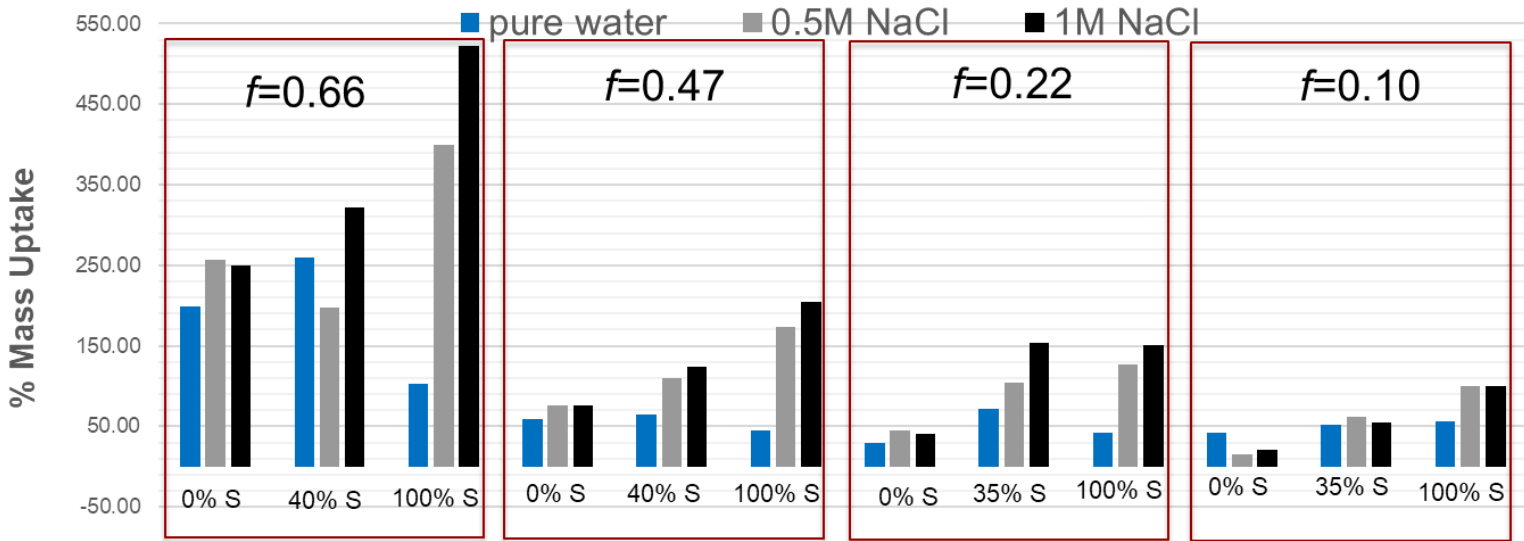


**Figure 4.1: Mass uptake of block copolymer system with different volume fraction of the hydrophilic block and different % of zwitterion content**

In the Figure 4.1 it was observed that the mass uptake for parent copolymer, 50% zwitterion content and 100% zwitterion content is reduced as the volume fraction of the hydrophilic block decreased. For pure water uptake, mass uptake was constant with an increase in

zwitterionic content. But for saltwater uptake, it was observed that the mass uptake is much higher in 100% zwitterion content than in the parent copolymer and the 50% zwitterion content. This can be attributed to the fact that due to coulombic interaction the zwitterion forms a core structure, with the hydrophobic section forming a shell around it. This reduces the water uptake even though the zwitterion is a better hydrophile than parent copolymer. But in presence of saltwater, the coulombic interactions between zwitterions is screened increasing the mass uptake of the zwitterionic block copolymer than its parent copolymer. Based on this study, in the future it will be possible to perform hydration number studies and the salt transportation capability of these A-Z block copolymers.

To determine water uptake, the hydration number ( $\lambda$ ) will be calculated to estimate the number of water molecules surrounding each zwitterionic entity. The calculations were based on a procedure from the literature.<sup>2,3</sup>

The amount of charge (c) present in each polymer chain could be determined by <sup>1</sup>H NMR.

The **hydration value** will be calculated using the following equations.

**Equation 4.2: Hydration Number**

$$\lambda = \frac{\left( \frac{m_{wet} - m_{dry}}{m_{dry}} \right) \times 1000}{MW_{water} \times C}$$

To determine the salt uptake capacity, **weight percent of the salt absorption (w<sub>s</sub>)** will be calculated by subtracting equilibrated mass of the fully hydrated membrane from the equilibrated mass of the membrane fully soaked in salt water.

The weight percent of the salt absorption will be calculated using the following equation.

**Equation 4.3: Weight Percent of Salt Absorbtion**

$$w_s = \frac{m_t - m_{wet}}{m_{wet}} \times 100\%$$

Where  $m_t$  is mass of the membrane soaked in saltwater solution and  $m_{wet}$  is the mass of the fully hydrated membrane

#### 4.2.2 Salt Transport Experiments

To study the salt selectivity and efficiency of salt transport in different sets of A-Z block copolymer, salt transport experiments could be conducted with various salts comprising different cations and anions. These experiments will be conducted using kinetic desorption techniques following published procedures.<sup>1,4</sup> In this procedure a disk of completely dry polymer membrane is cut out and equilibrated in salt solution of predetermined concentration. After drying any surface absorbed water, the membrane will be immersed in deionized water in a beaker. The beaker solution will be stirred thoroughly to maintain homogeneity and precautions will be taken to prevent any loss of liquid through evaporation. The conductivity of the liquid will be measured as a function of time. A calibration curve will correlate this conductivity value to salt concentration. Salt diffusion ( $D_s$ ) will be calculated using the following equation.

**Equation 4.4: Salt Diffusion**

$$D_s = \frac{\pi l^2}{16} \left[ \frac{d(M_t/M_\infty)}{d(t^{1/2})} \right]^2$$

$M_t$  is the salt mass desorbed at time  $t$  and  $M_\infty$  is the total mass of salt desorbed at equilibrium.

Salt permeability coefficient ( $P_s$ ) will be calculated in terms of measured diffusion salt sorption coefficients.

**Equation 4.5: Salt Permeability Coefficient**

$$P_S = D_S K_S$$

Salt sorption coefficient ( $K_s$ ) is the ratio of salt content in the fully hydrated polymer to the salt content in the solution used to equilibrate the polymer. It can also be explained as amount of salt desorbed by the polymer during the time needed to reach equilibrium ( $M_\infty$ ) under the assumption that the total amount of salt absorbed and desorbed to be similar.

**4.2.3 Water Flux Study**

The pure hydraulic water permeance ( $A_w$ ) in the A-Z block copolymer membranes was performed using dead-end filtration system, Figure 4.1.<sup>5</sup> After the polymer membrane is soaked in deionized water to equilibrium hydration, it will be put in a permeation cell where deionized water will be pressurized with nitrogen within the cell. Permeated water volume ( $\Delta V$ ) will be calculated in terms of time difference ( $\Delta t$ ) using following equation:

**Equation 4.6: Permeated Water Volume**

$$A_W = \frac{J_w}{l\Delta p} = \frac{\Delta V / \Delta t}{A_m l \Delta p}$$

Where  $J_w$  is the water flux,  $l$  is the polymer membrane thickness,  $\Delta p$  is cross-membrane pressure,  $A_m$  is the surface area available for transport.

Considering the solution-diffusion mechanism for water transport, a concentration gradient across the membrane thickness will drive the diffusion of water. Water diffusive

permeability ( $P_w$ ) will be calculated in terms of experimentally determined water permeability using the following equation:

*Equation 4.7: Water Permeability*

$$P_w = D_w K_W = A_W l \times \frac{R_g T}{V_W}$$

Where  $D_w$  is average water diffusion coefficient,  $T$  is temperature,  $R$  is ideal gas constant, and  $V_w$  is the molar volume of water.

For this study, a polymer solution was drop casted and photo crosslinked as described in Chapter 3, on a polyester backing. Then the membrane coated on the backing was cut into 1 inch diameter and dead-end filtration experiments are performed under 3 Bar pressure (Figure 4.2).<sup>6</sup>



**Figure 4.2: a) Schematic of working principle of dead end filtration system**

**b) the actual set up of Dead End Filtration instrument build by Dr. Kerianne**

**Dobosz. Image take from Ref. 5.**

Figure 4.3 shows there was water flux though the membranes. It was observed that the permeation reduces with the increases in the zwitterion content. There is also no proper correlation between the water uptake measurement with that of the volume fraction of the



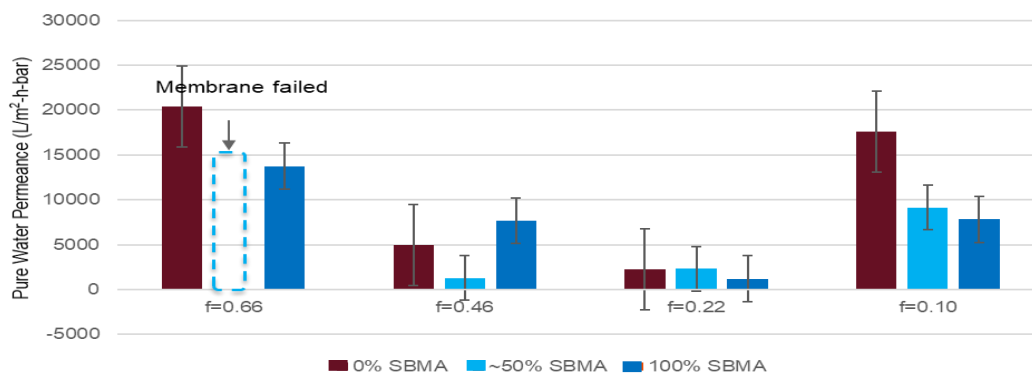


**Figure 4.3: Water permeability measurement of block copolymer with different volume fraction (f) of hydrophilic block and different % zwitterion content**

The water permeation was also observed under different pressure. After the previous study at 3 bar, the pressure was reduced to 1 bar. As expected, the water permeation reduced. But it stayed constant even with an increase in the pressure.

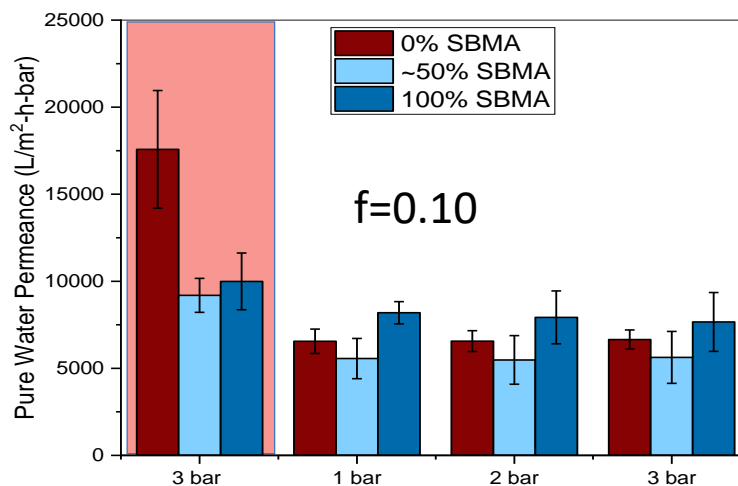


**Figure 4.4: Water permeability of block copolymer with hydrophilic f=0.10 and different % zwitterion under different pressure**

### **4.3 Conclusion**

The previous preliminary study shows that there is water and salt uptake observed by the A-Z block copolymer membranes. Gravimetric analysis shows the membranes have a tendency to uptake salt along hydrophilicity directly related to the hydrophilic block volume fraction and zwitterion content. Optimization of the membrane performance needs to be studied to get a better knowledge of the water permeation through the A-Z block copolymer membrane.

#### 4.4 References

- (1) Shah, S.; Liu, J.; Ng, S.; Luo, S.; Guo, R.; Cheng, C.; Lin, H. Transport Properties of Small Molecules in Zwitterionic Polymers. *J. Polym. Sci. Part B Polym. Phys.* **2016**, *54* (19), 1924–1934. <https://doi.org/10.1002/polb.24096>.
- (2) Tsai, T. H.; Ertem, S. P.; Maes, A. M.; Seifert, S.; Herring, A. M.; Coughlin, E. B. Thermally Cross-Linked Anion Exchange Membranes from Solvent Processable Isoprene Containing Ionomers. *Macromolecules* **2015**, *48* (3), 655–662. <https://doi.org/10.1021/ma502362a>.
- (3) Ertem, S. P.; Tsai, T. H.; Donahue, M. M.; Zhang, W.; Sarode, H.; Liu, Y.; Seifert, S.; Herring, A. M.; Coughlin, E. B. Photo-Cross-Linked Anion Exchange Membranes with Improved Water Management and Conductivity. *Macromolecules* **2016**, *49* (1), 153–161. <https://doi.org/10.1021/acs.macromol.5b01784>.
- (4) Ni, L.; Meng, J.; Geise, G. M.; Zhang, Y.; Zhou, J. Water and Salt Transport Properties of Zwitterionic Polymers Film. *J. Memb. Sci.* **2015**, *491*, 73–81. <https://doi.org/10.1016/j.memsci.2015.05.030>.
- (5) Dobosz, K. ScholarWorks @ UMass Amherst TUNING ELECTROSPUN NANOFIBERS AND CHEMISTRY TO ENHANCE THE FLUX AND FOULING RESISTANCE OF ULTRAFILTRATION Submitted to the Graduate School of The. **2019**, No. July.
- (6) Shah, R. M.; Cihanoğlu, A.; Hardcastle, J.; Howell, C.; Schiffman, J. D. Liquid-Infused Membranes Exhibit Stable Flux and Fouling Resistance. *ACS Appl. Mater. Interfaces* **2022**, *14* (4), 6148–6156. <https://doi.org/10.1021/acsami.1c20674>.

## **CHAPTER 5**

### **SUMMARY AND FUTURE PERSPECTIVE**

#### **5.1 Introduction**

In this final dissertation chapter, the tailoring of a novel amphiphilic-zwitterionic block copolymer to design a free-standing membrane by photo induced crosslinking will be summarized from the three studies presented in chapters 2, 3, and 4. The impact of these findings will be integrated into the current understanding of these complex systems. Based on these results, future directions will be proposed to expand upon this work to further the understanding of the structure-property relationship of A-Z block copolymer systems, specifically water transport membranes that utilize these copolymers.

#### **5.2 Summary of Conclusion**

In Chapter 2 the successful synthesis of block copolymer of amphiphilic zwitterionic block copolymer system has been reported. As a first step, a moderately polar polymer of poly (dimethyl amino ethyl methacrylate) (PDMAEMA) with different molecular weight were synthesized using the controlled radical polymerization RAFT. Block copolymers were then synthesized chain extension with several hydrophobic blocks were attempted. Finally, a successful synthesis of the parent block copolymer of poly (dimethyl amino ethyl methacrylate)-*b*-poly (n butyl acrylate-*ran*-allyl methacrylate) (PDMAEMA-*b*- P(nBA-*ran*-AMA)) were prepared, again using RAFT polymerization. The advantage of using this technique is the ability to synthesize a polymer chain with predetermined molecular weight and well-defined chemical composition while also maintaining a narrow dispersity. Variation of the zwitterionic groups; sulfobetaine,

carboxybetaine or cholinephosphate were investigated through post-polymerization modification of the PDMAEMA block using nucleophilic ring-opening reactions of 1,3-propane sultone,  $\beta$ -propiolactone or n-butyl substituted phospholane. Proton NMR spectroscopy and DMF-GPC data were analyzed to calculate degree of polymerization (DP) from the distinct peak of each repeating unit of pendent groups in parent neutral block copolymers and its modified amphiphilic-zwitterionic counterpart. These DP of the neutral block copolymer were then used to calculate the relative volume fraction of each block and aid the future calculation of post-polymerization modification on PDMAEMA block and crosslinking chemistry on the poly allyl methacrylate (PAMA) pendant group. Thermal stability of these zwitterionic systems was investigated by using thermogravimetric analysis (TGA) and differential scanning calorimetry (DSC)

In Chapter 3 mechanically robust free standing amphiphilic zwitterionic copolymer poly (n butyl acrylate-*ran*-allyl methacrylate)-*b*-polybetainemethacrylate membrane were tailored using thiol-ene click chemistry on the pendent double bond of the allyl methacrylate repeating unit with a dithiol crosslinking agent under UV irradiation. Success of the crosslinking was reported in terms of no loss in dimensional stability when these membranes were soaked in water for long periods of time. The analysis of the effect of composition on the resultant films morphologies was probed. The systematic variations in volume fractions of each block were targeted to generate different morphologies. The impact of the copolymer composition on the morphology were analyzed using small angle X-ray scattering (SAXS). Various relative humidity sweeps and temperature variation SAXS experiments were performed through collaboration with Argonne National Laboratory to investigate the effect of different environmental conditions of the

morphologies. For lower volume fraction of the hydrophilic block ( $f = 0.10$ ) there was a shift of morphology from short range arrangement to distinct hexagonal morphology as the composition shifted from 0% zwitterion content to 100% zwitterion content. This trend becomes opposite as the volume fraction of the hydrophilic block increases. For highest volume fraction ( $f = 0.67$ ) the morphology shifted from hexagonal to short range phase separated morphology from 0% zwitterion to 100% zwitterion content. Also, a prominent shift in morphology and phase separation was observed with the presence of water in the membrane. Transmission electron microscopy (TEM) was performed in addition to SAXS to study real space imaging of these structures. All the TEM images showed dimensions and morphologies similar to the SAXS data. With the results from these characterization methods, it was possible to perform an initial structure-property relationship study of these novel Amphiphilic- Zwitterionic block copolymers.

In chapter 4 preliminary studies have been done to study the potential application of these amphiphilic zwitterionic block copolymer system as water filtration membranes. Gravimetric analyses were done to show that these membranes are showing capacity to uptake salt along with hydrophilicity. This salt uptake and water uptake value was directly related to hydrophilic volume fraction and percent zwitterionic content. Finally dead end filtration was performed to study the water permeation through these membranes. All the membranes with different volume fractions showed water permeation at 3 bar pressure. The water permeation value showed a good correlation with the morphology of the membrane, hydrophilic block volume fraction and zwitterion content.

### 5.3 Future Perspective

The work presented in this dissertation provides detailed insight on the successful synthesis of A-Z block copolymer and role of zwitterion content and hydrophilic block volume fraction on the morphology of the polymer membrane. These membranes also showed potential application in the field of water filtration membranes. Building upon these results, several future investigations can be performed.

In the synthesis of the parent amphiphilic block copolymer other hydrophobic segments can be explored. Block copolymers with isoprene showed good flexibility in the membrane form, but due to difference in chemical compatibility between the blocks, processing into films was found to be very difficult after the quaternization step. Discovery of proper processing steps will further open the study of A-Z block copolymers with different hydrophobic identity. The route for making A-Z block copolymer using  $\beta$ -propiolactone or n-butyl substituted phospholane ring-opening for post polymerization modification needs to be further optimized. Proper reaction conditions need to be investigated to ideally achieve 100% quaternization using these ring structures. Other chemistry can be explored for achieving new types of zwitterionic identity from the same parent block copolymer. These will open pathways for applying one basic framework of parent copolymer toward different applications just by changing the post polymerization step. Using RAFT also open pathway to develop block copolymer with significant architecture (branched, multi arm, *etc.*). These will also open further the scope of study the self-assembled property of these A-Z block copolymer with distinct architectures.

SAXS study of the A-Z block copolymer can be done to see the effect of chemical identity (zwitterion identity and hydrophobic identity) on the morphology. Different

zwitterions will have different dipole moments which will presumably show some effect on the morphology. Same with the case of different hydrophobic identity. Because different  $T_g$  will show different self-assembly in dry state versus in the presence of water. Cryo-TEM study of the hydrated membrane would be a good way to investigate the real space imaging of the morphology of the hydrated membranes.

Dead-end filtration study and gravimetric analysis shows that these membranes have potential in the field of water filtration. But more study needs to be done to understand how morphology plays a role during the water flux. Morphology analysis before and after water flux at high pressure will give a better idea how morphology shifts during water flux experiments. For application more studies need to be done to optimize the membrane. Salt absorption and desorption studies need to be performed to study the salt screening property of these membranes. Different cations and anions can be used to see which salt can permeate through these membranes and which salt can be screened. This will open a broad field of application of salt filtration.

All the studies that have been reported are experimental. Previously several computational studies have been reported to theoretically predict the self-assembled structure of conventional block copolymer systems<sup>1-3</sup> and polyelectrolytic block copolymer systems.<sup>4,5</sup> The work presented in this dissertation also opens the possibility for studies to see if any computational theoretical models can be developed that can predict the self-assembled behavior of the A-Z block copolymers.



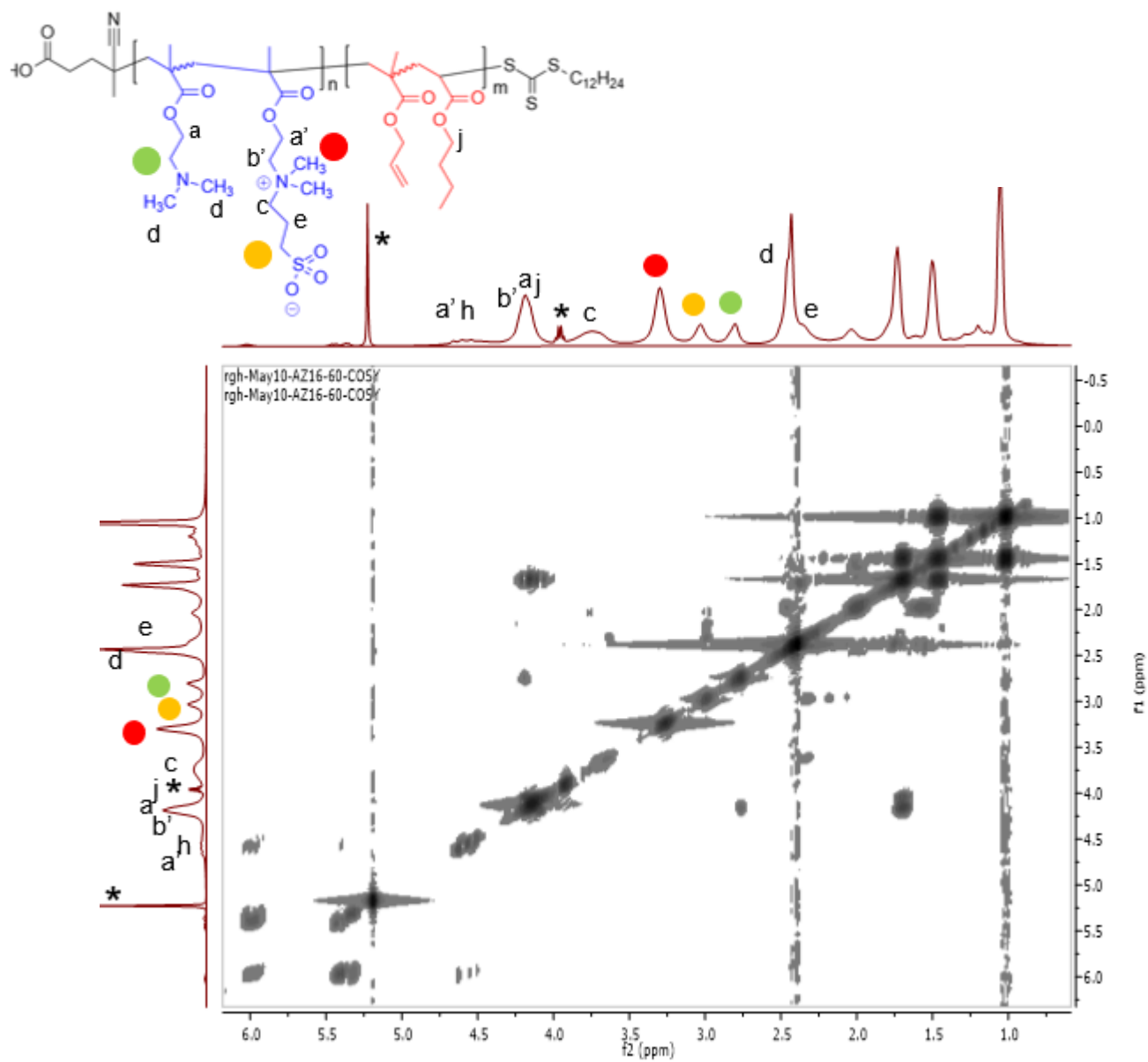
## 5.4 Outlook

With the wealth of knowledge available for these ionomers systems, much work can still be done in this field. Particularly, this work should be extended and developed for different advanced applications. Much of the current work on these applications is limited by the availability of the copolymers. With the development of these A-Z block copolymers, these novel copolymers can have a significant impact in various fields. Some possible applications to explore could include antifouling membranes, self-healing materials, and smart materials.

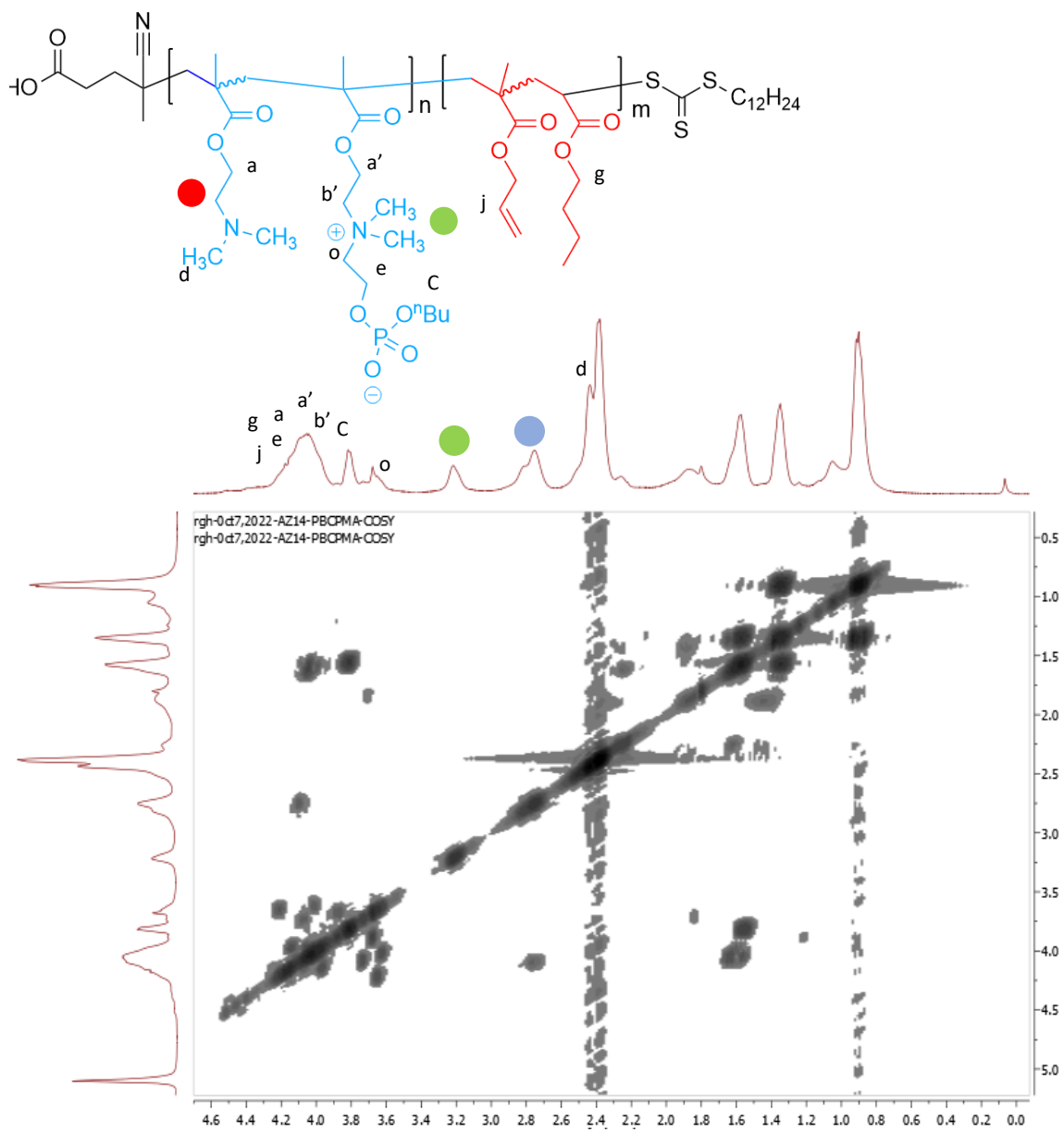
## 5.5 References

- (1) Mai, Y.; Eisenberg, A. Self-Assembly of Block Copolymers. *Chem. Soc. Rev.* **2012**, *41* (18), 5969–5985. <https://doi.org/10.1039/c2cs35115c>.
- (2) Cochran, E. W.; Garcia-Cervera, C. J.; Fredrickson, G. H. Stability of the Gyroid Phase in Diblock Copolymers at Strong Segregation. *Macromolecules* **2006**, *39* (7), 2449–2451. <https://doi.org/10.1021/ma0527707>.
- (3) Tang, J.; Jiang, Y.; Zhang, X.; Yan, D.; Chen, J. Z. Y. Phase Diagram of Rod-Coil Diblock Copolymer Melts. *Macromolecules* **2015**, *48* (24), 9060–9070. <https://doi.org/10.1021/acs.macromol.5b02235>.
- (4) Sing, C. E.; Zwanikken, J. W.; de la Cruz, M. O. Interfacial Behavior in Polyelectrolyte Blends: Hybrid Liquid-State Integral Equation and Self-Consistent Field Theory Study. *Phys. Rev. Lett.* **2013**, *111* (16), 168303. <https://doi.org/10.1103/PhysRevLett.111.168303>.
- (5) Sing, C. E.; Zwanikken, J. W.; Olvera De La Cruz, M. Electrostatic Control of Block Copolymer Morphology. *Nat. Mater.* **2014**, *13* (7), 694–698. <https://doi.org/10.1038/nmat4001>.

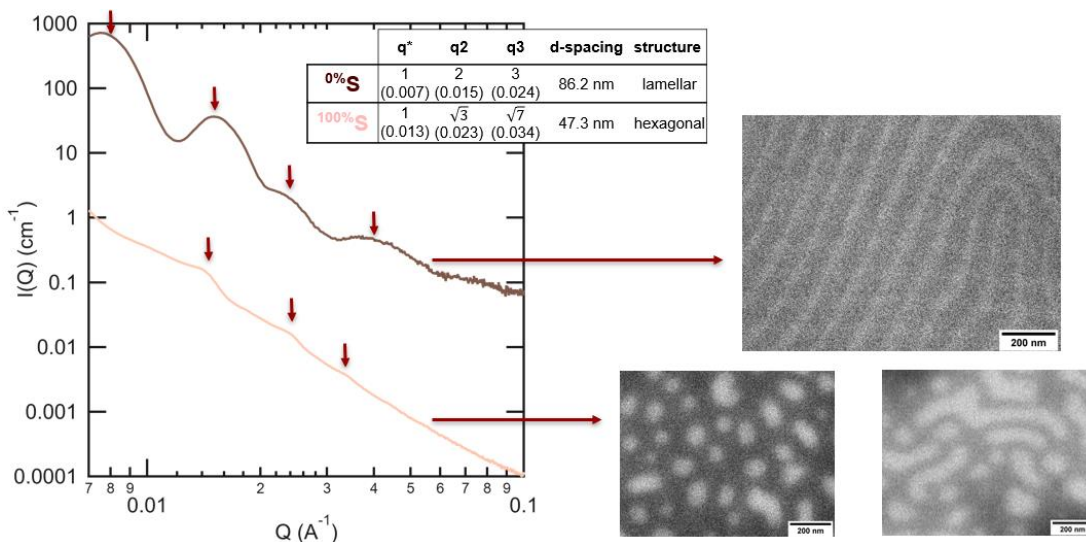
## APPENDIX SUPPLEMENTAL FIGURES



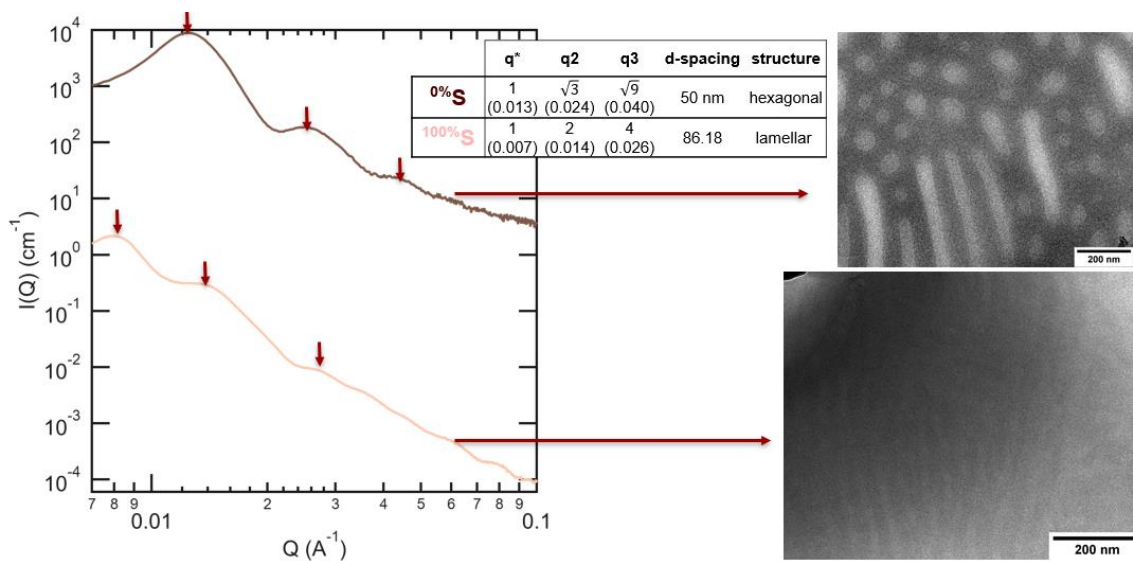
**A 1: COSY-NMR of A-Z block copolymer, 50% quaternized with 1,3-propane sultone**



**A 2: COSY-NMR of A-Z block copolymer, 50% quaternized with n-butyl substituted phospholane ring**



**A 3: TEM images of the parent block copolymer with  $f=0.46$  and its 100% zwitterionic form as compared to its SAXS images.**



**A 4: TEM images of the parent block copolymer with  $f=0.67$  and its 100% zwitterionic form as compared to its SAXS images.**

## BIBLIOGRAPHY

Annaka, M.; Morishita, K.; Okabe, S. Electrostatic Self-Assembly of Neutral and Polyelectrolyte Block Copolymers and Oppositely Charged Surfactant. *J. Phys. Chem. B* 2007. <https://doi.org/10.1021/jp074404q>.

Asai, Y.; Yamada, K.; Yamada, M.; Takano, A.; Matsushita, Y. Formation of Tetragonally-Packed Rectangular Cylinders from ABC Block Terpolymer Blends. *ACS Macro Lett.* 2014, 3 (2), 166–169. <https://doi.org/10.1021/mz400647v>.

Astafieva, I.; Khougaz, K.; Eisenberg, A. Micellization in Block Polyelectrolyte Solutions. 2. Fluorescence Study of the Critical Micelle Concentration as a Function of Soluble Block Length and Salt Concentration. *Macromolecules* 1995, 28 (21), 7127–7134. <https://doi.org/10.1021/ma00125a015>.

Astafieva, I.; Zhong, X. F.; Eisenberg, A. Critical Micellization Phenomena in Block Polyelectrolyte Solutions. *Macromolecules* 1993, 26 (26), 7339–7352. <https://doi.org/10.1021/ma00078a034>.

Banerjee, S. L.; Bhattacharya, K.; Samanta, S.; Singha, N. K. Self-Healable Antifouling Zwitterionic Hydrogel Based on Synergistic Phototriggered Dynamic Disulfide Metathesis Reaction and Ionic Interaction. *ACS Appl. Mater. Interfaces* 2018, 10 (32), 27391–27406. <https://doi.org/10.1021/acsami.8b10446>.

Bates, F. S.; Fredrickson, G. H. Block Copolymer Thermodynamics: Theory and Experiment. *Annu. Rev. Phys. Chem.* 1990, 41 (1), 525–557. <https://doi.org/10.1146/annurev.pc.41.100190.002521>.

Bielawski, C. W.; Grubbs, R. H. Living Ring-Opening Metathesis Polymerization. *Progress in Polymer Science* (Oxford). 2007. <https://doi.org/10.1016/j.progpolymsci.2006.08.006>.

Binder, H.; Zschörnig, O. The Effect of Metal Cations on the Phase Behavior and Hydration Characteristics of Phospholipid Membranes. *Chem. Phys. Lipids* 2002. [https://doi.org/10.1016/S0009-3084\(02\)00005-1](https://doi.org/10.1016/S0009-3084(02)00005-1).

Blackman, L. D.; Gunatillake, P. A.; Cass, P.; Locock, K. E. S. An Introduction to Zwitterionic Polymer Behavior and Applications in Solution and at Surfaces. *Chem. Soc. Rev.* 2019, 48 (3), 757–770. <https://doi.org/10.1039/c8cs00508g>.

Blasco, E.; Sims, M. B.; Goldmann, A. S.; Sumerlin, B. S.; Barner-Kowollik, C. 50th Anniversary Perspective: Polymer Functionalization. *Macromolecules* 2017, 50 (14), 5215–5252. <https://doi.org/10.1021/acs.macromol.7b00465>.

Cao, B.; Li, L.; Tang, Q.; Cheng, G. The Impact of Structure on Elasticity, Switchability, Stability and Functionality of an All-in-One Carboxybetaine Elastomer. *Biomaterials* 2013. <https://doi.org/10.1016/j.biomaterials.2013.06.063>.

Cao, B.; Tang, Q.; Li, L.; Humble, J.; Wu, H.; Liu, L.; Cheng, G. Switchable Antimicrobial and Antifouling Hydrogels with Enhanced Mechanical Properties. *Adv. Healthc. Mater.* 2013. <https://doi.org/10.1002/adhm.201200359>.

Chan, E. P.; Frieberg, B. R.; Ito, K.; Tarver, J.; Tyagi, M.; Zhang, W.; Coughlin, E. B.; Stafford, C. M.; Roy, A.; Rosenberg, S.; Soles, C. L. Insights into the Water Transport Mechanism in Polymeric Membranes from Neutron Scattering. *Macromolecules* 2020, 53 (4), 1443–1450. <https://doi.org/10.1021/acs.macromol.9b02195>.

Chang, Y.; Liao, S. C.; Higuchi, A.; Ruan, R. C.; Chu, C. W.; Chen, W. Y. A Highly Stable Nonbiofouling Surface with Well-Packed Grafted Zwitterionic Polysulfobetaine for Plasma Protein Repulsion. *Langmuir* 2008. <https://doi.org/10.1021/la800228c>.

Chelushkin, P. S.; Lysenko, E. A.; Bronich, T. K.; Eisenberg, A.; Kabanov, V. A.; Kabanov, A. V. Polyion Complex Nanomaterials from Block Polyelectrolyte Micelles and Linear Polyelectrolytes of Opposite Charge. 2. Dynamic Properties. *J. Phys. Chem. B* 2008, 112 (26), 7732–7738. <https://doi.org/10.1021/jp8012877>.

Cheng, X. Q.; Liu, Y.; Guo, Z.; Shao, L. Nanofiltration Membrane Achieving Dual Resistance to Fouling and Chlorine for “Green” Separation of Antibiotics. *J. Memb. Sci.* 2015. <https://doi.org/10.1016/j.memsci.2015.06.048>.

Cheryan, M.; Rajagopalan, N. Membrane Processing of Oily Streams. *Wastewater Treatment and Waste Reduction. J. Memb. Sci.* 1998, 151 (1), 13–28. [https://doi.org/10.1016/S0376-7388\(98\)00190-2](https://doi.org/10.1016/S0376-7388(98)00190-2).

Ciferri, a.; Kudaibergenov, S. Natural and Synthetic Polyampholytes, 2, Functions and Applications. *Macromol. Rapid Commun.* 2007. <https://doi.org/10.1002/marc.200700162>.

Cochran, E. W.; Garcia-Cervera, C. J.; Fredrickson, G. H. Stability of the Gyroid Phase in Diblock Copolymers at Strong Segregation. *Macromolecules* 2006, 39 (7), 2449–2451. <https://doi.org/10.1021/ma0527707>.

Discher, D. E.; Ahmed, F. POLYMERSOMES. *Annu. Rev. Biomed. Eng.* 2006, 8 (1), 323–341. <https://doi.org/10.1146/annurev.bioeng.8.061505.095838>.

Dobosz, K. ScholarWorks @ UMass Amherst TUNING ELECTROSPUN NANOFIBERS AND CHEMISTRY TO ENHANCE THE FLUX AND FOULING RESISTANCE OF ULTRAFILTRATION Submitted to the Graduate School of The. 2019, No. July.

Eisenberg, A. Block Copolymers: Synthetic Strategies, Physical Properties, and Applications By Nikos Hadjichristidis and Stergios Pispas (University of Athens) and George Floudas (University of Ioannina). John Wiley and Sons, Inc.: Hoboken, NJ. 2003. Xx + 420 Pp. \$12. *J. Am. Chem. Soc.* 2003. <https://doi.org/10.1021/ja025357c>.

Ertem, S. P.; Tsai, T. H.; Donahue, M. M.; Zhang, W.; Sarode, H.; Liu, Y.; Seifert, S.; Herring, A. M.; Coughlin, E. B. Photo-Cross-Linked Anion Exchange Membranes with Improved Water Management and Conductivity. *Macromolecules* 2016, 49 (1), 153–161. <https://doi.org/10.1021/acs.macromol.5b01784>.

Ertem, S. P.; Tsai, T. H.; Donahue, M. M.; Zhang, W.; Sarode, H.; Liu, Y.; Seifert, S.; Herring, A. M.; Coughlin, E. B. Photo-Cross-Linked Anion Exchange Membranes with Improved Water Management and Conductivity. *Macromolecules* 2016, 49 (1), 153–161. <https://doi.org/10.1021/acs.macromol.5b01784>.

Förster, S. Amphiphilic Block Copolymers for Templating Applications BT - Colloid Chemistry I; Antonietti, M., Ed.; Springer Berlin Heidelberg: Berlin, Heidelberg, 2003; pp 1–28. [https://doi.org/10.1007/3-540-36408-0\\_1](https://doi.org/10.1007/3-540-36408-0_1).

Geise, G. M.; Falcon, L. P.; Freeman, B. D.; Paul, D. R. Sodium Chloride Sorption in Sulfonated Polymers for Membrane Applications. *J. Memb. Sci.* 2012. <https://doi.org/10.1016/j.memsci.2012.08.014>.

Geise, G. M.; Freeman, B. D.; Paul, D. R. Characterization of a Sulfonated Pentablock Copolymer for Desalination Applications. *Polymer (Guildf)*. 2010, 51 (24), 5815–5822. <https://doi.org/10.1016/j.polymer.2010.09.072>.

Geise, G. M.; Freeman, B. D.; Paul, D. R. Sodium Chloride Diffusion in Sulfonated Polymers for Membrane Applications. *J. Memb. Sci.* 2013. <https://doi.org/10.1016/j.memsci.2012.09.029>.

Geise, G. M.; Lee, H. S.; Miller, D. J.; Freeman, B. D.; McGrath, J. E.; Paul, D. R. Water Purification by Membranes: The Role of Polymer Science. *J. Polym. Sci. Part B Polym. Phys.* 2010. <https://doi.org/10.1002/polb.22037>.

Geise, G. M.; Paul, D. R.; Freeman, B. D. Fundamental Water and Salt Transport Properties of Polymeric Materials. *Progress in Polymer Science*. 2014. <https://doi.org/10.1016/j.progpolymsci.2013.07.001>.

Grady, B. P. Review and Critical Analysis of the Morphology of Random Lonomers across Many Length Scales. *Polymer Engineering and Science*. 2008. <https://doi.org/10.1002/pen.21024>.

Greenlee, L. F.; Lawler, D. F.; Freeman, B. D.; Marrot, B.; Moulin, P. Reverse Osmosis Desalination: Water Sources, Technology, and Today's Challenges. *Water Research*. 2009. <https://doi.org/10.1016/j.watres.2009.03.010>.

Hadjichristidis, N.; Pispas, S.; Iatrou, H.; Pitsikalis, M. Linking Chemistry and Anionic Polymerization. *Curr. Org. Chem.* 2005. <https://doi.org/10.2174/1385272023374463>.



Hammond, M. R.; Li, C.; Tsitsilianis, C.; Mezzenga, R. Hierarchical Self-Organization in Polyelectrolyte-Surfactant Complexes Based on Heteroarm Star Block Copolyampholytes. *Soft Matter* 2009. <https://doi.org/10.1039/b817219f>.

Harada, A.; Kataoka, K. Chain Length Recognition: Core-Shell Supramolecular Assembly from Oppositely Charged Block Copolymers. *Science* (80-. ). 1999. <https://doi.org/10.1126/science.283.5398.65>.

Hickner, M. A.; Ghassemi, H.; Kim, Y. S.; Einsla, B. R.; McGrath, J. E. Alternative Polymer Systems for Proton Exchange Membranes (PEMs). *Chem. Rev.* 2004, 104 (10), 4587–4611. <https://doi.org/10.1021/cr020711a>.

Hickner, M. A.; Herring, A. M.; Coughlin, E. B. Anion Exchange Membranes: Current Status and Moving Forward. *Journal of Polymer Science, Part B: Polymer Physics*. 2013. <https://doi.org/10.1002/polb.23395>.

Hildebrand, V.; Laschewsky, A.; Päch, M.; Müller-Buschbaum, P.; Papadakis, C. M. Effect of the Zwitterion Structure on the Thermo-Responsive Behaviour of Poly(Sulfobetaine Methacrylates). *Polym. Chem.* 2017, 8 (1), 310–322. <https://doi.org/10.1039/c6py01220e>.

Hoffman, A. S. Hydrogels for Biomedical Applications. *Advanced Drug Delivery Reviews*. 2012. <https://doi.org/10.1016/j.addr.2012.09.010>.

Hu, G.; Parelkar, S. S.; Emrick, T. A Facile Approach to Hydrophilic, Reverse Zwitterionic, Choline Phosphate Polymers. *Polym. Chem.* 2015, 6 (4), 525–530. <https://doi.org/10.1039/c4py01292e>.

Ihsan, A. Bin; Sun, T. L.; Kurokawa, T.; Karobi, S. N.; Nakajima, T.; Nonoyama, T.; Roy, C. K.; Luo, F.; Gong, J. P. Self-Healing Behaviors of Tough Polyampholyte Hydrogels. *Macromolecules* 2016. <https://doi.org/10.1021/acs.macromol.6b00437>.

Ilčíková, M.; Tkáč, J.; Kasák, P. Switchable Materials Containing Polyzwitterion Moieties. *Polymers* (Basel). 2015, 7 (11), 2344–2370. <https://doi.org/10.3390/polym7111518>.

Ji, Y. L.; An, Q. F.; Zhao, Q.; Sun, W. D.; Lee, K. R.; Chen, H. L.; Gao, C. J. Novel Composite Nanofiltration Membranes Containing Zwitterions with High Permeate Flux and Improved Anti-Fouling Performance. *J. Memb. Sci.* 2012. <https://doi.org/10.1016/j.memsci.2011.11.047>.

Jiang, S.; Cao, Z. Ultralow-Fouling, Functionalizable, and Hydrolyzable Zwitterionic Materials and Their Derivatives for Biological Applications. *Adv. Mater.* 2010, 22 (9), 920–932. <https://doi.org/10.1002/adma.200901407>.

Johnston, D. S.; Sanghera, S.; Pons, M.; Chapman, D. Phospholipid Polymers—Synthesis and Spectral Characteristics. *Biochim. Biophys. Acta - Biomembr.* 1980. [https://doi.org/10.1016/0005-2736\(80\)90289-8](https://doi.org/10.1016/0005-2736(80)90289-8).

Jones, M. N. The Surface Properties of Phospholipid Liposome Systems and Their Characterisation. *Advances in Colloid and Interface Science*. 1995. [https://doi.org/10.1016/0001-8686\(94\)00223-Y](https://doi.org/10.1016/0001-8686(94)00223-Y).

Ju, H.; McCloskey, B. D.; Sagle, A. C.; Kusuma, V. A.; Freeman, B. D. Preparation and Characterization of Crosslinked Poly(Ethylene Glycol) Diacrylate Hydrogels as Fouling-Resistant Membrane Coating Materials. *J. Memb. Sci.* 2009. <https://doi.org/10.1016/j.memsci.2008.12.054>.

Kaditi, E.; Mountrichas, G.; Pispas, S. Amphiphilic Block Copolymers by a Combination of Anionic Polymerization and Selective Post-Polymerization Functionalization. *Eur. Polym. J.* 2011, 47 (4), 415–434. <https://doi.org/10.1016/j.eurpolymj.2010.09.012>.

Kim, Y.; Binauld, S.; Stenzel, M. H. Zwitterionic Guanidine-Based Oligomers Mimicking Cell-Penetrating Peptides as a Nontoxic Alternative to Cationic Polymers to Enhance the Cellular Uptake of Micelles. *Biomacromolecules* 2012. <https://doi.org/10.1021/bm301351e>.

Koga, Y.; Morii, H. Biosynthesis of Ether-Type Polar Lipids in Archaea and Evolutionary Considerations. *Microbiol. Mol. Biol. Rev.* 2007. <https://doi.org/10.1128/membr.00033-06>.

Koutalas, G.; Pispas, S.; Hadjichristidis, N. Micelles of Poly(Isoprene-*b*-2-Vinylpyridine-*b*-Ethylene Oxide) Terpolymers in Aqueous Media and Their Interaction with Surfactants. *Eur. Phys. J. E* 2004. <https://doi.org/10.1140/epje/i2004-10075-3>.

Laschewsky, A. Structures and Synthesis of Zwitterionic Polymers. *Polymers (Basel)*. 2014, 6 (5), 1544–1601. <https://doi.org/10.3390/polym6051544>.

Lazzari, M.; Liu, G.; Lecommandoux, S. Block Copolymers in Nanoscience; 2008. <https://doi.org/10.1002/9783527610570>.

Leng, C.; Sun, S.; Zhang, K.; Jiang, S.; Chen, Z. Molecular Level Studies on Interfacial Hydration of Zwitterionic and Other Antifouling Polymers in Situ. *Acta Biomaterialia*. 2016. <https://doi.org/10.1016/j.actbio.2016.02.030>.

Lindquist, G. M.; Stratton, R. A. The Role of Polyelectrolyte Charge Density and Molecular Weight on the Adsorption and Flocculation of Colloidal Silica with Polyethylenimine. *J. Colloid Interface Sci.* 1976, 55 (1), 45–59. [https://doi.org/10.1016/0021-9797\(76\)90007-2](https://doi.org/10.1016/0021-9797(76)90007-2).

Lonsdale, H. K.; Merten, U.; Riley, R. L. Transport Properties of Cellulose Acetate Osmotic Membranes. *J. Appl. Polym. Sci.* 1965. <https://doi.org/10.1002/app.1965.070090413>.

Lowe, A. B.; McCormick, C. L. Synthesis and Solution Properties of Zwitterionic Polymers. *Chem. Rev.* 2002, 102 (11), 4177–4189. <https://doi.org/10.1021/cr020371t>.

Mai, Y.; Eisenberg, A. Self-Assembly of Block Copolymers. *Chem. Soc. Rev.* 2012, 41 (18), 5969–5985. <https://doi.org/10.1039/c2cs35115c>.

Matsen, M. W. Effect of Architecture on the Phase Behavior of AB-Type Block Copolymer Melts. *Macromolecules* 2012, 45 (4), 2161–2165. <https://doi.org/10.1021/ma202782s>.

Matsen, M. W. The Standard Gaussian Model for Block Copolymer Melts. *J. Phys. Condens. Matter* 2002, 14 (2). <https://doi.org/10.1088/0953-8984/14/2/201>.

Matyjaszewski, K. Atom Transfer Radical Polymerization (ATRP): Current Status and Future Perspectives. *Macromolecules* 2012, 45 (10), 4015–4039. <https://doi.org/10.1021/ma3001719>.

Miller, D. J.; Huang, X.; Li, H.; Kasemset, S.; Lee, A.; Agnihotri, D.; Hayes, T.; Paul, D. R.; Freeman, B. D. Fouling-Resistant Membranes for the Treatment of Flowback Water from Hydraulic Shale Fracturing: A Pilot Study. *J. Memb. Sci.* 2013. <https://doi.org/10.1016/j.memsci.2013.03.019>.

Mitchell, D. E.; Cameron, N. R.; Gibson, M. I. Rational, yet Simple, Design and Synthesis of an Antifreeze-Protein Inspired Polymer for Cellular Cryopreservation. *Chem. Commun.* 2015. <https://doi.org/10.1039/c5cc04647e>.

Muthukumar, M. 50th Anniversary Perspective: A Perspective on Polyelectrolyte Solutions. *Macromolecules* 2017, 50 (24), 9528–9560. <https://doi.org/10.1021/acs.macromol.7b01929>.

Nakamura, I.; Balsara, N. P.; Wang, Z.-G. Thermodynamics of Ion-Containing Polymer Blends and Block Copolymers. *Phys. Rev. Lett.* 2011, 107 (19), 198301. <https://doi.org/10.1103/PhysRevLett.107.198301>.

Narayanan Nair, A. K.; Martinez Jimenez, A.; Sun, S. Complexation Behavior of Polyelectrolytes and Polyampholytes. *J. Phys. Chem. B* 2017, 121 (33), 7987–7998. <https://doi.org/10.1021/acs.jpcc.7b04582>.

Narayanan Nair, A. K.; Uyaver, S.; Sun, S. Conformational Transitions of a Weak Polyampholyte. *J. Chem. Phys.* 2014. <https://doi.org/10.1063/1.4897161>.

Neuse, E. W.; Perlwitz, A. G. As Drug Carriers Polyamides. 1991, 394–404.

Ni, L.; Meng, J.; Geise, G. M.; Zhang, Y.; Zhou, J. Water and Salt Transport Properties of Zwitterionic Polymers Film. *J. Memb. Sci.* 2015, 491, 73–81. <https://doi.org/10.1016/j.memsci.2015.05.030>.

Peng, S.; Bhushan, B. Smart Polymer Brushes and Their Emerging Applications. *RSC Adv.* 2012. <https://doi.org/10.1039/c2ra20451g>.

Priftis, D.; Laugel, N.; Tirrell, M. Thermodynamic Characterization of Polypeptide Complex Coacervation. *Langmuir* 2012. <https://doi.org/10.1021/la302729r>.

Pummerer, R. Die Hochmolekularen Organischen Verbindungen Kautschuk Und Cellulose. Von Dr. Phil. Hermann Staudinger, o. Prof., Direktor Des Chemischen Laboratoriums Der Universität Freiburg i. Br. 540 Seiten in Großoktav, 113 Abbildungen, Ein Ausführliches Sachverzeic. Angew. Chemie 1932. <https://doi.org/10.1002/ange.19320455113>.

Ramachandran, G. N.; Ramakrishnan, C.; Sasisekharan, V. Stereochemistry of Polypeptide Chain Configurations. *Journal of Molecular Biology*. 1963. [https://doi.org/10.1016/S0022-2836\(63\)80023-6](https://doi.org/10.1016/S0022-2836(63)80023-6).

Rodriguez, A. K.; Ayyavu, C.; Iyengar, S. R.; Bazzi, H. S.; Masad, E.; Little, D.; Hanley, H. J. M. Polyampholyte Polymer as a Stabiliser for Subgrade Soil. *Int. J. Pavement Eng.* 2018. <https://doi.org/10.1080/10298436.2016.1175561>.

Roosjen, A.; Van Der Mei, H. C.; Busscher, H. J.; Norde, W. Microbial Adhesion to Poly(Ethylene Oxide) Brushes: Influence of Polymer Chain Length and Temperature. *Langmuir* 2004. <https://doi.org/10.1021/la048469l>.

Sagle, A. C.; Sharma, M. M.; Freeman, B. D. Structure-Property Relationships in PEG-Based Hydrogels for Potential Hydrophilic Membrane Coating Materials. *PMSE Prepr.* 2007.

Schanze, K. S.; Shelton, A. H. Functional Polyelectrolytes. *Langmuir* 2009, 25 (24), 13698–13702. <https://doi.org/10.1021/la903785g>.

Schönemann, E.; Laschewsky, A.; Wischerhoff, E.; Koc, J.; Rosenhahn, A. Surface Modification by Polyzwitterions of the Sulfobetaine-Type, and Their Resistance to Biofouling. *Polymers (Basel)*. 2019, 11 (6), 1–34. <https://doi.org/10.3390/polym11061014>.

Schulz, D. N.; Peiffer, D. G.; Agarwal, P. K.; Larabee, J.; Kaladas, J. J.; Soni, L.; Handwerker, B.; Garner, R. T. Phase Behaviour and Solution Properties of Sulphobetaine Polymers. *Polymer (Guildf)*. 1986. [https://doi.org/10.1016/0032-3861\(86\)90269-7](https://doi.org/10.1016/0032-3861(86)90269-7).

Shah, R. M.; Cihanoğlu, A.; Hardcastle, J.; Howell, C.; Schiffman, J. D. Liquid-Infused Membranes Exhibit Stable Flux and Fouling Resistance. *ACS Appl. Mater. Interfaces* 2022, 14 (4), 6148–6156. <https://doi.org/10.1021/acsami.1c20674>.

Shah, S.; Liu, J.; Ng, S.; Luo, S.; Guo, R.; Cheng, C.; Lin, H. Transport Properties of Small Molecules in Zwitterionic Polymers. *J. Polym. Sci. Part B Polym. Phys.* 2016, 54 (19), 1924–1934. <https://doi.org/10.1002/polb.24096>.

Shen, H.; Akagi, T.; Akashi, M. Polyampholyte Nanoparticles Prepared by Self-Complexation of Cationized Poly( $\gamma$ -Glutamic Acid) for Protein Carriers. *Macromol. Biosci.* 2012. <https://doi.org/10.1002/mabi.201200062>.

Shi, W.; Lynd, N. A.; Montarnal, D.; Luo, Y.; Fredrickson, G. H.; Kramer, E. J.; Ntaras, C.; Avgeropoulos, A.; Hexemer, A. Toward Strong Thermoplastic Elastomers with

Asymmetric Miktoarm Block Copolymer Architectures. *Macromolecules* 2014, 47 (6), 2037–2043. <https://doi.org/10.1021/ma402566g>.

Sing, C. E.; Zwanikken, J. W.; de la Cruz, M. O. Interfacial Behavior in Polyelectrolyte Blends: Hybrid Liquid-State Integral Equation and Self-Consistent Field Theory Study. *Phys. Rev. Lett.* 2013, 111 (16), 168303. <https://doi.org/10.1103/PhysRevLett.111.168303>.

Sing, C. E.; Zwanikken, J. W.; Olvera De La Cruz, M. Electrostatic Control of Block Copolymer Morphology. *Nat. Mater.* 2014, 13 (7), 694–698. <https://doi.org/10.1038/nmat4001>.

Sujanani, R.; Landsman, M. R.; Jiao, S.; Moon, J. D.; Shell, M. S.; Lawler, D. F.; Katz, L. E.; Freeman, B. D. Designing Solute-Tailored Selectivity in Membranes: Perspectives for Water Reuse and Resource Recovery. *ACS Macro Lett.* 2020, 9 (11), 1709–1717. <https://doi.org/10.1021/acsmacrolett.0c00710>.

Sun, T. L.; Kurokawa, T.; Kuroda, S.; Ihsan, A. Bin; Akasaki, T.; Sato, K.; Haque, M. A.; Nakajima, T.; Gong, J. P. Physical Hydrogels Composed of Polyampholytes Demonstrate High Toughness and Viscoelasticity. *Nat. Mater.* 2013. <https://doi.org/10.1038/nmat3713>.

Tang, J.; Jiang, Y.; Zhang, X.; Yan, D.; Chen, J. Z. Y. Phase Diagram of Rod-Coil Diblock Copolymer Melts. *Macromolecules* 2015, 48 (24), 9060–9070. <https://doi.org/10.1021/acs.macromol.5b02235>.

Tarannum, N.; Singh, M. Advances in Synthesis and Applications of Sulfo and Carbo Analogues of Polybetaines: A Review. *Rev. Adv. Sci. Eng.* 2013. <https://doi.org/10.1166/rase.2013.1036>.

Tsai, T. H.; Ertem, S. P.; Maes, A. M.; Seifert, S.; Herring, A. M.; Coughlin, E. B. Thermally Cross-Linked Anion Exchange Membranes from Solvent Processable Isoprene Containing Ionomers. *Macromolecules* 2015, 48 (3), 655–662. <https://doi.org/10.1021/ma502362a>.

Vaisocherová, H.; Yang, W.; Zhang, Z.; Cao, Z.; Cheng, G.; Piliarik, M.; Homola, J.; Jiang, S. Ultralow Fouling and Functionalizable Surface Chemistry Based on a Zwitterionic Polymer Enabling Sensitive and Specific Protein Detection in Undiluted Blood Plasma. *Anal. Chem.* 2008. <https://doi.org/10.1021/ac8015888>.

Vaisocherová, H.; Zhang, Z.; Yang, W.; Cao, Z.; Cheng, G.; Taylor, A. D.; Piliarik, M.; Homola, J.; Jiang, S. Functionalizable Surface Platform with Reduced Nonspecific Protein Adsorption from Full Blood Plasma-Material Selection and Protein Immobilization Optimization. *Biosens. Bioelectron.* 2009. <https://doi.org/10.1016/j.bios.2008.09.035>.

Vavasour, J. D.; Whitmore, M. D. Self-Consistent Field Theory of Block Copolymers with Conformational Asymmetry. *Macromolecules* 1993, 26 (25), 7070–7075. <https://doi.org/10.1021/ma00077a054>.

Wanakule, N. S.; Virgili, J. M.; Teran, A. A.; Wang, Z. G.; Balsara, N. P. Thermodynamic Properties of Block Copolymer Electrolytes Containing Imidazolium and Lithium Salts. *Macromolecules* 2010, 43 (19), 8282–8289. <https://doi.org/10.1021/ma1013786>.

Wang, Z.-G. Effects of Ion Solvation on the Miscibility of Binary Polymer Blends. *J. Phys. Chem. B* 2008, 112 (50), 16205–16213. <https://doi.org/10.1021/jp806897t>.

Ward, T. C.; Tobolsky, A. V. Viscoelastic Study of Ionomers. *J. Appl. Polym. Sci.* 1967, 11 (12), 2403–2415. <https://doi.org/10.1002/app.1967.070111201>.

Wever, D. A. Z.; Picchioni, F.; Broekhuis, A. A. Polymers for Enhanced Oil Recovery: A Paradigm for Structure-Property Relationship in Aqueous Solution. *Progress in Polymer Science (Oxford)*. 2011. <https://doi.org/10.1016/j.progpolymsci.2011.05.006>.

Wischerhoff, E.; Badi, N.; Laschewsky, A.; Lutz, J. F. Smart Polymer Surfaces: Concepts and Applications in Biosciences. *Adv. Polym. Sci.* 2010. [https://doi.org/10.1007/12\\_2010\\_88](https://doi.org/10.1007/12_2010_88).

Wu, Y. H.; Park, H. B.; Kai, T.; Freeman, B. D.; Kalika, D. S. Water Uptake, Transport and Structure Characterization in Poly(Ethylene Glycol) Diacrylate Hydrogels. *J. Memb. Sci.* 2010. <https://doi.org/10.1016/j.memsci.2009.10.025>.

Yethiraj, A. Liquid State Theory of Polyelectrolyte Solutions. *J. Phys. Chem. B* 2009, 113 (6), 1539–1551. <https://doi.org/10.1021/jp8069964>.

Zhang, Z.; Chen, S.; Jiang, S. Dual-Functional Biomimetic Materials: Nonfouling Poly(Carboxybetaine) with Active Functional Groups for Protein Immobilization. *Biomacromolecules* 2006. <https://doi.org/10.1021/bm060750m>.

Zhang, Z.; Vaisocherová, H.; Cheng, G.; Yang, W.; Xue, H.; Jiang, S. Nonfouling Behavior of Polycarboxybetaine-Grafted Surfaces: Structural and Environmental Effects. *Biomacromolecules* 2008. <https://doi.org/10.1021/bm800407r>.

Zhao, L.; Li, N.; Wang, K.; Shi, C.; Zhang, L.; Luan, Y. A Review of Polypeptide-Based Polymersomes. *Biomaterials*. 2014. <https://doi.org/10.1016/j.biomaterials.2013.10.063>.

Zhu, J.; Lennox, R. B.; Eisenberg, A. Interfacial Behavior of Block Polyelectrolytes. 4. Polymorphism of (Quasi) Two-Dimensional Micelles. *J. Phys. Chem.* 1992, 96 (12), 4727–4730. <https://doi.org/10.1021/j100191a002>.

Zhu, Y.; Noy, J. M.; Lowe, A. B.; Roth, P. J. The Synthesis and Aqueous Solution Properties of Sulfoethylbetaine (Co)Polymers: Comparison of Synthetic Routes and Tuneable Upper Critical Solution Temperatures. *Polym. Chem.* 2015, 6 (31), 5705–5718. <https://doi.org/10.1039/c5py00160a>.

Zwanikken, J. W.; Jha, P. K.; De La Cruz, M. O. A Practical Integral Equation for the Structure and Thermodynamics of Hard Sphere Coulomb Fluids. *J. Chem. Phys.* 2011, 135 (6). <https://doi.org/10.1063/1.3624809>.